

https://dspace.org/

The use of geographic information systems (GIS) and remote sensing on the matchless amphibolite belt (MAB), gorob-hope area, Namibia

Kaasheka, Elina K

2018

https://hdl.handle.net/10539/27068

Kaasheka, Elina Kaushiwetu, (2018) The use of geographic information systems (GIS) and remote sensing on the matchless amphimbolite belt (MAB), Gorob-Hope area, Namibia, University of the Witwatersrand, Johannesburg, https://hdl.handle.net/10539/27068.

Downloaded from a DSpace repository. https://dspace.org/



Faculty of Science

School of Geosciences

THE USE OF GEOGRAPHIC INFORMATION SYSTEMS (GIS) AND REMOTE SENSING ON THE MATCHLESS AMPHIBOLITE BELT (MAB), GOROB-HOPE AREA, NAMIBIA

Thesis submitted to the Faculty of Science, University of Witwatersrand in partial fulfilment of the requirements for the Master of Science degree in Economic Geology

BY

Elina K Kaasheka (1535831)

Email:emuzanima@gmail.com

October 2018

Supervisor: Prof Paul Nex

Co-Supervisor: Prof Judith Kinnaird

Declaration

I, Elina Kaushiwetu Kaasheka hereby declare that the work presented in this thesis is my own original work and that I have not previously in its entirety or in part submitted it at any other university for a degree.

Signature… 

Date: 05/10/2018

Abstract

The Matchless Amphibolite Belt (MAB) is a linear geological feature up to 3 kilometers wide and at least 350 kilometers long within the Damara Orogen of Namibia (Miller, 1983). The exact length of the belt is not well known due to the superficial cover of Kalahari sand, especially east of Windhoek, towards the border with Botswana. The Matchless amphibolite belt is associated with Neoproterozoic massive sulphide Cu-Au-(Zn-Ag) deposits (Breitkopf & Maiden, 1988; and Killick, 2000).

Conventional geological and mineral exploration practices need enormous investments, a long time period plus intensive human labour especially in areas that are not easily accessible or with complex geological features such as the Gorob-Hope area. This study focused on the occurrence of mineralization in the Gorob-Hope area of the Matchless Amphibolite Belt and involved gathering, processing and interpretation of historic geological and remote sensing data using ENVI and ArcGIS software. These techniques were applied with a view to establish how the ore deposits are associated with the presence of the MAB and to establish the relationship between lithological units, the structures and the ore body localization.

Application of ENVI and GIS techniques proved that it stands for an efficient and cost effective option of outlining mafic units, metasedimentary units, structures and ore body localization based on the available historical geological, and remote sensing data. The study also established that ore deposits found in the study area are controlled by structural features and are associated with MAB.

Acknowledgement

I would like to thank the Almighty for the strength and blessings bestowed upon me throughout this research. I would also like to thank a number of individuals and institutions, who generously contributed to its success. I would like to express my gratitude to the Namibia Students Financial Assistance Fund (NSFAF) for the financial support that enabled me to carry out my studies. Furthermore, I would like to thank the University of Witwatersrand in general, and the school of geosciences in particular for the opportunity offered to me to study at this university, as well as the necessary tools, equipment and facilities used.

I am deeply indebted to my supervisor, Professor Paul Nex and co-supervisor Professor Judith Kinnaird who supported and guided me from the initial stages of my research, to the point that I am today able to produce this report. I will be amiss if I do not acknowledge the assistance from the Geological Survey of Namibia (GSN) in general and Ms. Paulina Pokolo of the GSN in particular through the provision of data. Lastly, I offer my regards and blessings to my husband Jonathan, my two sons Given and Divine for their unconditional love and support, motivation, understanding, consideration and encouragement in every way possible throughout the process of this report and beyond.

Table of Contents

Declaration i

Abstract ii

Acknowledgement iii

List of Figures vi

List of Tables vii

List of Abbreviations viii

Chapter 1: 1

1. Introduction 1

1.1 Research background 1

1.2 Research problem definition 1

1.3 Research aim and objectives 2

Chapter 2: 4

2. Remote Sensing (RS) and Geographic Information Systems (GIS) 4

2.1 Remote sensing (RS) 4

2.2 Applications of Remote Sensing in Geology 4

2.3 Geographic Information Systems (GIS) 5

2.4 Application of GIS in Geology 6

Chapter 3: 7

3. Description of the study Area 7

3.1 Overview of the Namibia Geology 7

3.2 The Damara Orogeny 7

3.3 The Matchless Amphibolite Belt (MAB) 11

3.4 Local geology of the study area 15

Chapter 4: 21

4. Research Methodology 21

4.1 Introduction 21

4.2 Data collection and software 21

4.3 Geological field observation 21

4.4 Data Processing and Integration 26

Chapter 5: 52
5. Data interpretation 52
5.1. Geological Data 52
5.2 Remote sensing Data 56
Chapter 6: 59
6. Discussion and Conclusion 59
6.1 Discussion 59
6.2 Conclusion 62
References 63
Appendices 66

List of Figures

Figure 1.1: The location Map showing Exclusive Prospecting Licence (EPL) 5796 which incorporates the study area (data source: Geological Survey of Namibia). 3

Figure 3.1: The location map of the Damara Orogen showing the 350 km long MAB in the southern zone (modified after Killick, 2000).....7

Figure 3.2: A simplified geological map showing the distribution of the main tectonostratigraphic zones of the Damara orogeny (modified after Miller, 1983). 9

Figure 3.3: A geological map of the Gorob-Hope area showing folded MAB at the western end (Miller, 2008). 12

Figure 3.4: A map showing main copper deposits associated with the MAB (modified after Killick 2000).....14

Figure 3.5: A geological map of Gorob-hope area showing the Hope synform and the Gorob, Vendome, Luigi, Bruna as well as Hope lenses (Haussinger et al., 1993)).....16

Figure 3.6: A stratigraphic section of Hope lens showing two parallel quartzitic horizons (After Cowey, 1981). 17

Figure 3.7: A geological map of Gorob-hope area, showing different lithologies (after Preussinger 1990). 1- calcrete and gravel, 2- amphibolite, 3- metagabbros, 4- talc schist and related rocks, 5- metasediments, 6- zones of pre-metamorphic hydrothermal alteration, 7- magnetite-quartzite, 8- graphitic schist, 9- F_1 axial plane trace, 10- F_2 axial plane trace, 11- S_2 foliation, 12- F_2 axial plane and plunge, 13- L_2 intersection lineation, 14-S_o bedding form line.....18

Figure 4.1: A Photograph showing staurolite schist at the Gorob Lens 22

Figure 4.2: Garnet-mica schist from the country rocks surrounding the Hope Lens with garnet porphyroblasts 23

Figure 4.3:A photograph showing folding of magnetite-quartzite and quartz-biotitie schist at Hope Lens. 24

Figure 4.4: A photograph showing magnetite-quartzite at Vendome Lens....25

Figure 4.5: A Screen shot showing one of the geological maps that have been utilized for lithological units discrimination (source: Gold fields prospecting company, 1987).....27

Figure 4.6: A screen shot showing one of the geological maps that have been utilized for rock units discrimination (source: Gold fields prospecting company, 1976).....28

Figure 4.7: A screen shot showing the layer stacking process of colour composite (RGB) 321....31

Figure 4.8: A screen shot of a Landsat 7 ETM+ showing the process of true colour composite (RGB) 321 32

Figure 4.9: A map of Gorob-Hope area that was produced from a true colour composite image (RGB) 321.....33

Figure 4.10: A screen shot of a Landsat 7 ETM+ showing the process of false colour composite (RGB) 457 34

Figure 4.11: A map of Gorob-Hope area that was produced from a false colour composite 457 showing the MAB in blueish, sand and soils in yellow-whitish and Kuiseb schist in greyish colour. 35

Figure 4.12: A screen shot of a Landsat 7 ETM+ showing the process of false colour composite (RGB) 751 36

Figure 4.13: A map of Gorob-Hope area that was produced from false colour composite 751 showing linear structures of the MAB. 37

Figure 4.14: Showing the comparison of spectral Bands between ASTER and Landsat (% ref is reflectance percentage) (Williams, 2009). 38

Figure 4.15: A screen shot of the ASTER_2314_2316 (RGB) 321 band combination process....40

Figure 4.16: A screen shot of ASTER_2314_2316 image showing the process of true colour composite (RGB) 321....41

Figure 4.17: A screen shot of ASTER_2314_2316 image showing the process of true colour composite (RGB) 321.....42

Figure 4.18: A screen shot of the ASTER_2314_2316 (RGB) 468 band combination.....43

Figure 4.19: A screen shot of ASTER_2314_2316 image showing the process of false colour composite (RGB) 468.....44

Figure 4.20: A screen shot of ASTER_2314_2316 image showing the process of false colour composite (RGB) 468....45

Figure 4.21: A map of Gorob-Hope area that was produced from ASTER_2314_2316 False colour composite (RGB) 468 46
Figure 4.22: A graph showing the characteristic spectra of iron and clay minerals (after Williams, 2009) 47
Figure 4.23: A screen shot of the ASTER_2314_2316 showing Band ratios 4/6, 5/6, and 5/8 process 48
Figure 4.24: A screen shot of the ASTER_2314_2316 showing the process of band ratios of 4/6, 5/6, and 5/8.....49
Figure 4.25: showing the output of ASTER band ratio of 4/6, 5/6, and 5/8 50
Figure 4.26: A map of Gorob-Hope area that was produced from band ratios of 4/6, 5/6, and 5/8 51
Figure 5.1: A lithological map of Gorob-Hope produced from historic geological data (Table 4.1) 53
Figure 5.2: A lithological map of the Gorob-hope area produced from historical data (Table 4.1) showing the dip and strike of the staurolite schist outcrop that was found during the traverse (Fig 4.2)......54
Figure 5.3: A lithological map of the Gorob-Hope produced from historic geological data (Table 4.1)showing the dip and strike of the sillimanite-muscovite-quartz-biotite schist outcrop that was found during the traverse (Fig 4.3) 55
Figure 5.4: A Structural map of Gorob-Hope produced from Landsat 7 ETM+ image, Historic geolo5gical maps and field visit structural measurements. 56
Figure 5.5: A geological map of Gorob-Hope area showing hydrothermal alterations that was produced from ASTER_2314_2316 image. 58
Figure 6.1: A Geological map of Gorob-Hope area with main lithologies, structures alterations and the mineralisation based on historic geological maps and remote sensing data 61

List of Tables

Table 3.1: The 4 major stratigraphic units of the Damara sequence (after Miller, 1983). 10
Table 3.2: The stratigraphy of the southern part of the northeast-trending branch of the Damara sequence showing the position of the MAB (modified after Miller, 2008) 11
Table 4.1: A list of historic geological maps and the UTM zone that was used. 26
Table 4.2: the type of the image and the georeference system used 29
Table 4.3: Landsat 7 ETM+ characteristics 30
Table 4.4: showing band characteristics (after Williams, 2009). 30
table 4.5: showing the characteristics of the 3 aster sensor systems (after williams, 2009).....*38*

List of Abbreviations

MAB – Matchless Amphibolite Belt
EPL – Exclusive Prospecting License
MORB – Mid Oceanic Ridge Basalts
ENVI - Environment for Visualizing Images
GIS – Geographic Information System
RS – Remote Sensing
ASTER – Advanced Spaceborne Thermal Emission and Reflection Radiometer
Landsat (ETM+) - Landsat Enhanced Thematic mapper plus
Landsat (TM) - Thematic Mapper
GSN – Geological Survey of Namibia
UTM – Universal Transverse Mercator
NP - Northern Platform
CZ - Central Zone
NCZ- Northern Central Zone
SCZ- Southern Central Zone
OLZ - Okahandja Lineament Zone
SZ - Southern Zone
SMZ - Southern Margin Zone
SF - Southern Foreland
SP - Southern Platform
NIR- Near Infrared
SWNIR – Short Wave Near Infrared
TIR-Thermal Infrared
VMS-Volcanogenic Massive Sulphide

Chapter 1:

1. Introduction

1.1 Research background

To sustain development especially in developing countries, further resource generation and make full use of mineral deposits, particularly deposits that are metalliferous is vital. Metals like copper, zinc and lead are essential in aiding and conserving the rapid growing industrial expansion (Amera, 2007). It is therefore essential not only to discover new mineral deposits but also to have a better understanding of the existing deposits for developing countries like Namibia, to ensure their economy prospers.

According to Amera (2007), geo-information given in a consistent manner in the form of Mineral and geological prospecting maps is essential for resource generation and mineral resources development. In addition, geophysical techniques such as remote sensing, and magnetic data as well as the use of GIS applications are considered to be low-cost ways and means in geological and mineral exploration.

Remote sensing is important for prospective investors in terms of mineral resource generation as well as for geological surveys in developing countries. Hence, the utilisation of remote sensing may assist by minimizing the risk level when investing in the mining sector (Drury, 2001).Much more mineral exploration activities may be simplified by understanding further the ore deposits and their mineral zonation pattern. Thus, the main drive of this study is to assist field exploration by making geo-information available to geological as well as mineral prospecting mapping by analysing and integrating spatial information from collected of remote sensing data.

1.2 Research problem definition

Traditional geological and mineral resource generation practices need enormous investments, a long time period plus intensive human labour especially in areas that are not easily reachable or with complex geological features such as Gorob-Hope area. To effectively localise exploration targets and reduce costs as well as time spent during exploration field work doing geological, geochemical and geophysical studies of an area, we should use remote sensing data as well as GIS applications (Rokos et al., 2000).

It is against this background that this study focused mainly on the utilisation of remote sensing data and GIS applications so as to gain an appreciation of the spatial distribution and controls of base metal mineralisation in the Gorob-Hope area of the Matchless Amphibolite Belt (MAB). This study may contribute to an understanding of how the mineralisation occurs and it may be of valuable assistance to explorers in their quest to discover new mineral deposits in the MAB, since it may add new useful information to the package of exploration techniques that are available so far.

Several massive sulphide deposits of Cu-Zn (Ag-Au) are found alongside the 350 kilometers strike length of the late Proterozoic era (MAB) in the Damara orogenic belt at the central part of Namibia (Breitkopf and Maiden, 1988). The belt is associated with amphibolites and metasedimentary rocks that were subjected to three episodes of deformation where the primary rocks (basalts and sediments) have been

metamorphosed and hydrothermally altered (Miller, 1983). Hence, by merging, assessing and integrating remote sensing data from the Gorob-Hope area, we may gain an appreciation of the spatial distribution and controls at base metal mineralisation within or around the Gorob-Hope area of the MAB.

1.3 Research aim and objectives

1.3.1 Aim

To use remote sensed data and GIS techniques to gain an appreciation of the spatial distribution and controls of the base metal mineralisation in the Gorob-Hope area of the MAB. This is done to understand how the ore deposits are related to the MAB member as well as to establish the relationship between structures and orebody localisation.

1.3.2 Research Objectives

A particular objective is to understand how the ore deposits are interrelated to the presence of quartz-magnetite bodies, and to conclude if structural features apply a dominant control on ore body localization using ASTER images. The study also aimed to gain an appreciation on how the alteration is spatially distributed in the interior of the schist that surround the base metal ore bodies, and to determine if remote sensing images can be utilised to delineate them.

The main questions of the study are as follow:

Magnetite orebodies

1. What exactly is the spatial relationship between the quartzite-hosted orebodies and the mafic volcanic rocks along the MAB? Can this be quantified?
2. Are there any particular magnetic features of note associated with the orebodies- or not? Are these systematic?

Structures

1. Are there any recognizable structural features related to deposits?
2. To what extent can these be recognized as possible guides to ore?

Alteration

The Schists surrounding the deposits of the MAB are variably altered to quartz-muscovite-pyrite schist and chlorite-ankerite-amphibolite schist.

1. How widely distributed around the deposits are these alteration zones?
2. Can they be recognized from remote sensing imagery?

1.3.3 Previous work on the use of remote sensing datasets

As in the past, a lot of work continues to be carried out with regard to the geology of the MAB due to the occurrence of ore mineralisation of several massive sulphide deposits along the belt. Geological, geochemical as well as geophysical techniques have been applied during exploration for base metals along the belt. However, several studies show how important is remote sensing and geo-information in the utilisation of mineral exploration. Sabins (1999) pointed out that usually there are two methods for

the utilisation of remote sensing applications during mineral exploration. Firstly, to map out all the lithologies as well as fractures that contain ore deposits, and secondly, to recognise the rocks that are altered hydrothermally by their spectral signatures.

Sabins (1999) further described that multispectral and hyperspectral imagery is used in the identification of hydrothermal alteration. Satellite images such as Landsat Enhanced Thematic Mapper Plus (ETM+) are very useful during the interpretation of geology and structures. ASTER (Advanced Space borne Thermal Emission and Reflection Radiometer) imagery is suitable during the interpretation of lithological units, structural features, as well as zones of hydrothermal alteration. On the other hand, to obtain detailed mineralogical data we must process and analyse hyperspectral raw information. Hyperspectral information acquired from Short Wave Infrared (SWIR) in the wavelength region of 2.0-2.5 µm is convenient for the mapping of minerals in the hydrothermal systems (Van der Meer and Bakker, 1998). They deduced that for the mapping of VMS discharge zones as well as to target potential base metal occurrences, one has to use information from hyperspectral VNIR-SWIR data.

1.3.4 Location of the study area

The Gorob-Hope study area (Fig 1.1) is hosted along the MAB. The area is located in the Namib Naukluft Park, about 225 Km southwest of the capital city of Namibia, Windhoek. It is located between latitudes 23° 31' S and 23˚31' S and longitudes 15° 11'E and 15° 29' E. It is in arid environment with well-exposed rocks.

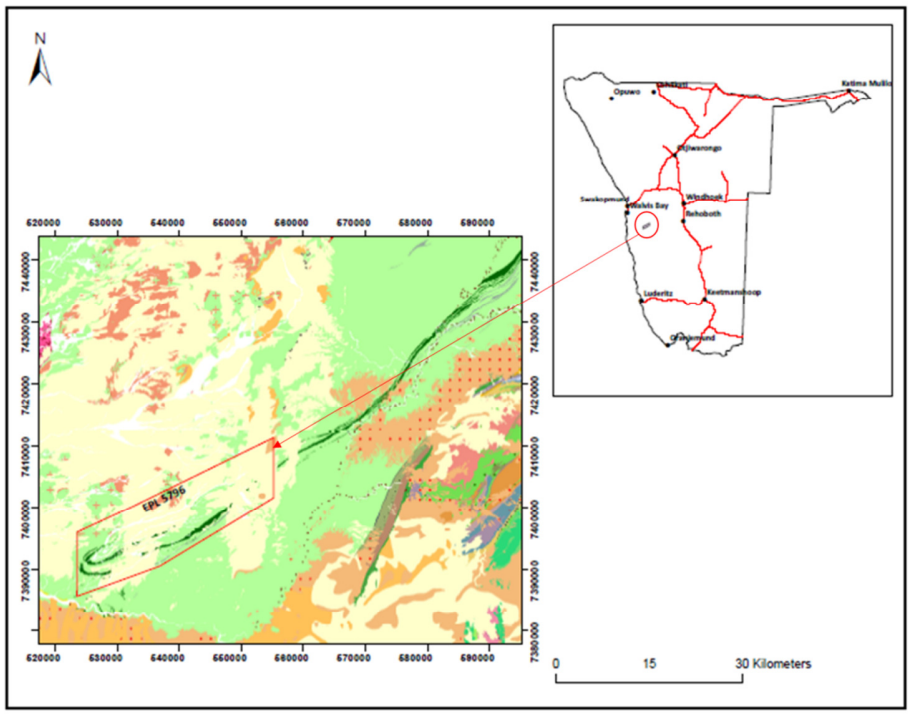

Figure 1.1: The location Map showing Exclusive Prospecting Licence (EPL) 5796 which incorporates the study area (data source: Geological Survey of Namibia).

Chapter 2:

2. Remote Sensing (RS) and Geographic Information Systems (GIS)

2.1 Remote sensing (RS)

The photographs and observations models had been the widely used means of viewing the Earth using visible light up until the late 1950s. The use of aircraft and telescopes made it possible for the attainment of distant viewing. However, present day scientific advancement in the form of remote sensing ushered in tools that observe our Earth at wavelengths different from those of visible light. These tools are mainly mounted on satellites and aircraft to capture and transmit images of the Earth to the Earth-based stations, where such images would be digitally analysed using computers to generate information on a variety of topics, including geology (Rees, 1990).

The original form of remote sensing known as aerial photography remains the furthermost used method and the interpretations of these photographs have resulted into the discovery of numerous mineral as well as oil deposits. The achievements of using the visible part of the electromagnetic spectrum suggested that more finds are possible through the use of other wavelengths (Vane et al.,1993). In the 1960s, a more advanced technological approach was employed as to acquire images in the infrared (IR) and microwave regions, which substantially enlarged the scope and application of RS. The dawn of the 1960s ushered in the development and use of controlled and uncontrolled earth satellites and offered an orbital vantage point for obtaining the Earth images. Apart from aerial photographs, most RS data are now obtained digitally and processed through the use of computers in order to generate images for interpretation (Rees, 1990).

Remote sensing is defined as the branch of knowledge that obtains process and interprets images, and associated data, secured from satellites as well as aircraft which captured the interaction happening between electromagnetic radiation and matter. Obtaining imagery denotes the tools used, such as an electro-optical scanning system. Processing allude to the strategies that change the unprocessed data into imagery. Interpreting the image is to transform an image into meaningful and valuable information for extensive variety of usages (Rees, 1990).

2.2 Applications of Remote Sensing in Geology

According to Farina et al. (2005), RS techniques ushered in a new era in lithological mapping. Traditionally, geological maps have always been prepared from ground surveys according to observations in the field. They had been sketched on the topographic base along the lines of traverse and then ultimate maps are created by means of the details extrapolation. In this process certain mistakes are unescapable and usually cause imprecisions in final maps. Ever since the advent of RS development tools, the mapping techniques have experienced tremendous variation. Nowadays RS techniques play a significant role in mapping programs.

There has always been a challenge in the mapping of lithology and alteration zones especially in hard to reach places like mountains and forest terrains. Disagreements often existed regarding the accurateness in the boundaries of the lithological units and details on structures in these maps. Sometimes the vastness of a given area to be surveyed provided an access challenge due to its remoteness, thereby obstructing every outcrop's physical investigation. This is the reason the prospective of RS is appreciated by many in today's world.

The uppermost benefit derived from RS is the provision of synoptic view which has regional as well as an integrated viewpoint of cross-cutting relations between different land features. Multi-spectral images and data of high resolution, as well as the progressive capabilities of digital image processing methods, are available to generate enhanced and easy to interpret images. Such images further broaden the potential of RS during the delineation of lithological units contacts and geological structural features in more details and with improved precision (Drury, 1987).

According to Crippen and Blom (2001), multi spectral satellite systems in effect are intended to explore natural resources with a greater emphasis on the exposure of vegetation, lithological units, as well as mineral exploration. The extensive area presentation of the data in connection with their long-term availability permits the spatial dynamics analysis with large areas. Most of the applications of RS in geology include the delineation of structures, differentiation of rock units and soil types and resources exploration. After the Landsat Thematic Mapper (TM) was launched in 1982, in comparison with the multi spectral scanner (MSS) that had been used for in-depth geological studies, geologists have since then expanded access to better spatial (30m) and spectral resolution (Abrams, 1984).

Several geological studies have used Landsat TM and ETM+ data to differentiate various lithological units, lineaments and minerals by use of hyper-spectral laboratory (Abrams, 1984). In areas such as Gorob-Hope where bed rock is exposed, multi-spectral images of RS are very useful for lithological mapping and zones of alterations.

2.3 Geographic Information Systems (GIS)

The more we get to understand the functionality of the Earth with its intricate system with a large number of cross-cutting mechanisms, the indispensable need for a revolutionary approach towards studying and understanding such mechanisms becomes more evident. The sophisticated character of the earth sciences poses significant challenges for geologists in understanding the nature and dynamic mechanisms of the functioning of the Earth. This implies that we have to apply GIS techniques as a way of utilising the opportunity presented by the constantly increasing observations number and huge data sets, and utilise such tools proficiently in pursuit of geological studies intended to solve Earth science complications.

Major challenges facing geologists include assimilation, dissemination as well as management of the exceedingly increasing volume of digital data. The availability of all relevant data enhances the potential of improving the quality of scientific research. One of the solutions to these challenging problems is to change the manner in which earth data, information as well as knowledge are preserved, utilised and disseminated. The geosciences community needs proper systems that provide digital data and the important tools that are user friendly in manipulation, questioning, choosing and cross-referencing each

section of the data sets with the requisite effectiveness and pace. One obvious system available for use by geoscientists is GIS.

GIS is a structured assemblage of hardware, software and data aimed at storing, manipulating, analysing, querying and displaying data for decision-making and error-free analysis of any kind of spatial data. GIS is widely misunderstood to be just a map-making tool. The fact is that this system has many more functions than just producing maps. For example the system allows users to analyse, enquiry, explore and do databases selections for a particular purpose. For instance, in seismotectonic studies, one can display active faults within a region, and measure the magnitude of seismic events. In the same vein, a user can choose a geological unit; find its area, the topography, as well as the faults within such unit. With GIS these trivial tasks can be accomplished within seconds. Thus GIS provides a convenient approach in expanding human capabilities to carry out improved research effectively and efficiently in order to bring about multidisciplinary methods for scientific studies, in that it allows ways to cross-reference multiple data sets. One of the advantages of using GIS software is that it allows the data to be stored in a spatially registered structure as well as providing for the cross-referencing of heterogeneous, multidisciplinary data sets.

GIS also allows for improved management of datasets as information layers. Geographical features such as lakes and rivers or geological features like sample locations, faults and lithological units are all illustrations of layers of information. Although every layer is free of the others, they all have mutual geographic registration and therefore can be interconnected to each other by the use of specific identification labels. This makes it easily possible to select the required data from the database and make it readily available for advance analysis and decision-making.

2.4 Application of GIS in Geology

Recently, several studies have been carried out using GIS to deliver an integrated geological data collection method to provide for a more accurate data interpretation. Aiken et al. (1997) have used GIS in mapping and interpreting and magnetic field and the gravity in Mexico. Similarly, Orange et al. (1999) utilised GIS in the prediction and identification of geological-hazard areas in California, USA. Furthermore, GIS had been utilised in studying the evolution of geology of Syria (Brew et al., 2000). The vital part of GIS in the exploration of oil had been recognised in a research paper by Pawlowski (2000).

Furthermore, a study by Sebel et al., (2000) revealed different GIS applications in the geology of the Middle East. Equally, GIS had been utilised broadly during mapping exercise in 2-dimension and 3-dimension in the case studies carried out by Kirkham et al. (2003) and Belt et al. (2005). GIS has also been used in environmental geology to determine the impact on the environment in the mining of heavy metals like Cu, Zn and Fe in Turkey (Akcay, 2004). GIS was also applied in engineering geology during a study on how to overcome geo-environmental difficulties in town developments (Aly et al., 2005).

GIS is a crucial application in tectonic mapping and structural interpretation. As alluded to earlier on, manipulating, visualising, integrating and interpreting of data had been a time consuming and vigorous process, but the advent of GIS made this process very user friendly, in that it allows for faster and accurate analysis, as well better quality and easily accessible end products.

Chapter 3:

3. Description of the study Area

3.1 The overview of the Namibia Geology

The history of geology as well as rock units of Namibia varies from the Achaean to the Phanerozoic, blanketing over 2600 Ma of history of the earth. Almost 50% of the country's exterior extent is bedrock coverage, whereas the rest is enclosed by younger surficial deposits of the Namib and Kalahari Deserts (Geological Survey of Namibia, 2005).

3.2 The Damara Orogeny

According to Downing and Coward (1981), the Damara Orogenic Belt, that strikes east-northeast across the Central and the Northern Namibia, is a portion of the late Precambrian to early Palaeozoic network of Pan-African mobile belts (Fig 3.1).

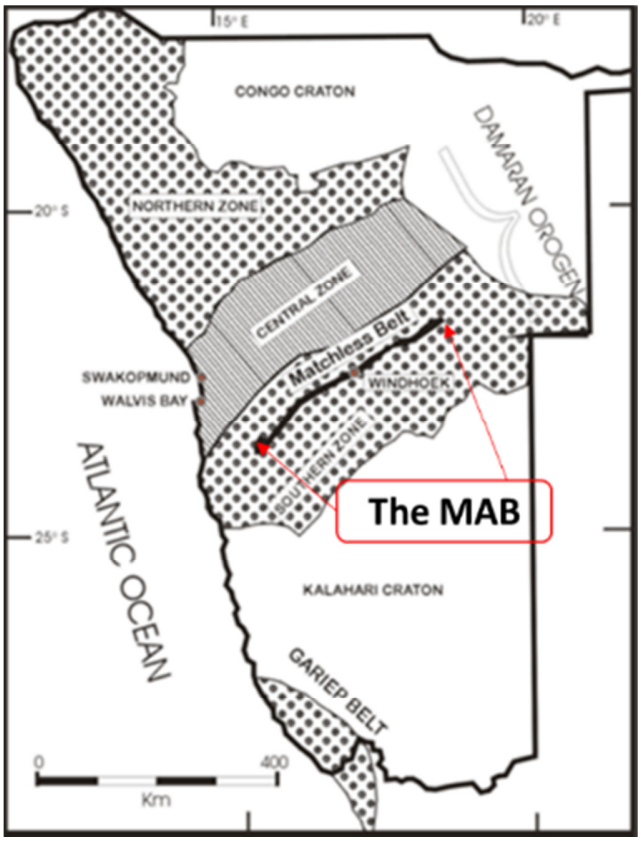

Figure 3.1: The location map of the Damara Orogen showing the 350 km long MAB in the southern zone (modified after Killick, 2000).

The Damara Orogen is formed between the Kalahari and the Congo Cratons (Poli and Oliver, 2001). The depositional, the metamorphism, as well as the deformational evolution of the Central Damara orogen is described as a complex sequence of extensional-rifting-spreading and compressional-convergence-

collision phases (Miller, 1983). The orogeny is associated with widespread depositional flysch facies as well as the crustal thinning which is believed to have taken place at about 700 Ma ago and this might have been escorted by some degree of seafloor spreading that is believed to have caused the formation of a 3 km wide, 350 km long linear feature known as Matchless Amphibolite Belt (Jung and Mezger, 2003).

The Damara Orogeny is partitioned into several number of tectonostratigraphic regions founded on the metamorphism grade, stratigraphy, plutonic rocks, structures, geochronology as well as their aeromagnetic expression (Fig 3.2). From north to south across the orogeny, the zones are known as the Northern Platform (NP) that includes the folded edge or foreland of the area, the Northern Zone (NZ), Central Zone (CZ), Okahandja Lineament Zone (OLZ), Southern Zone (SZ), Southern Margin Zone (SMZ) and the Southern Foreland (SF), as well as the Southern Platform (SP) (Miller, 1983).

The NP consists of a thick succession of shelf-type carbonates of the Otavi Group overlain by mainly siliciclastic molasse-type deposits of the Mulden Group. Deformation is characterized by open folding that decreases in intensity towards the north and east (Miller, 1983). The NZ is transitional between the NP and CZ, containing large basement inliers. Folds and thrusts are commonly verging towards the NP (Miller, 1983).

The CZ partitioned further into the northern and southern Central Zone (nCZ and sCZ), distinguished by different lithofacies and levels of exposure, the SCZ exposes lower parts of the Damara Supergroup and numerous basement windows. Characteristic are the high-Temperature, low-Pressure metamorphism, the huge amount of pre-tectonic, syn-tectonic, late- and post-tectonic granites (Badenhorst.1992). The CZ is referred to as the magmatic axis of the orogen with regional-scale NE-trending dome features that form the regional structural grain of the belt. Folds and thrusts commonly verge to the NW, onto the northern foreland (NZ and NP) in the lower-grade (lower amphibolite facies) parts, with local back folding and thrusting. In the higher-grade sections (upper amphibolite-facies) of the SCZ, vergence is to the SW, parallel to the orogen, indicating the orogen-parallel, oblique extrusion of the mid-crustal levels (Badenhorst, 1992).

The OLZ is thought to represent a major suture within the Damara orogeny, being situated between the CZ, located on the Congo Craton and the SZ, having formed above the Kalahari Plate. It is a long-lived major crustal structure in the Damara Belt that has controlled early sedimentation and volcanism of the Nosib Group, late- to post collisional differential uplift between the CZ and SZ and even later faulting during Karoo times. The OLZ (and parts of the SZ) are intruded by the large, post-tectonic Donkerhoek Granite (Kroner et al, 1991).

The SZ is made up of a several thousand meter thick sequence of metaturbidites. The MAB represents a thin, but over 300km long sliver of amphibolite, with MORB characteristics, tectonically imbricated with the metaturbidites. Folds and thrust verge to the SE and towards the southern foreland. The SZ is characterized by a medium- to high-pressure and low-to medium-temperature metamorphism (P: 6-8kbar, T: ca. 400-600°C). The SZ is interpreted to represent the remnants of an accretionary prism, forming above the NW- dipping subduction zone of the Kalahari plate below the Congo plate (Hoffmann, 1983).

The SMZ is a SE verging fold and thrust belt, also involving basement slivers. Metamorphic grades decrease to lower greenschist. The SF is the southern foreland basin of the Damara orogeny filled by the

mainly lower Phanerozoic sediments of the Nama Group deposited on the Kalahari Craton. The margins of the Nama basin are deformed by the propagating fold and thrust belt of both the Damara and the Gariep orogenic belts (Hoffmann, 1983).

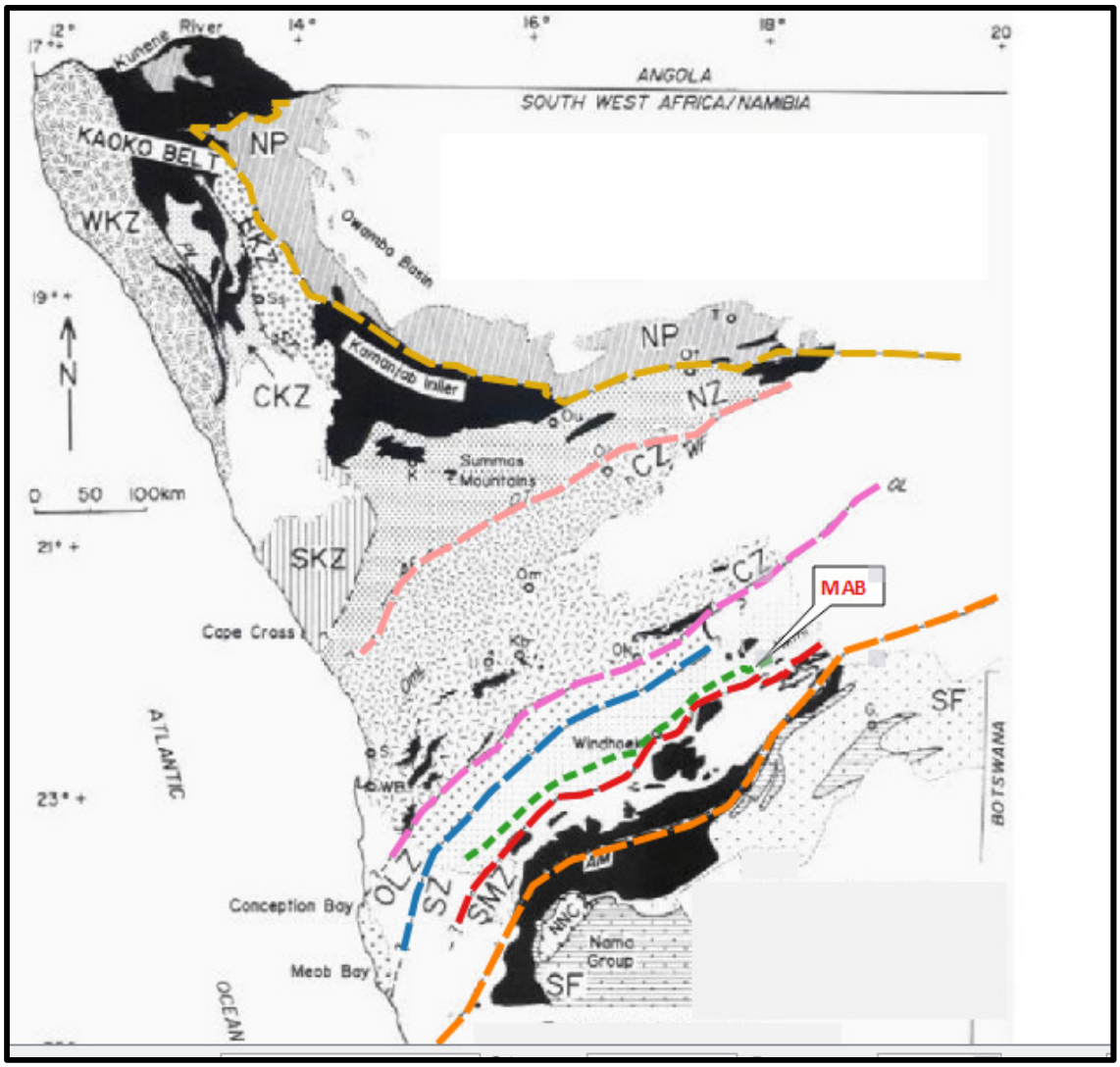

Figure 3.2: A simplified geological map showing the distribution of the main tectonostratigraphic zones of the Damara orogeny (modified after Miller, 1983).

The OLZ and SZ comprise of only one lithostratigraphic unit which is the schistose Kuiseb Formation. The region is underlain by rocks belonging to the Kuiseb Formation in the interior of the Khomas Subgroup of the Swakop Group of the Damara Sequence and is structurally situated near the southern limit of the Khomas trough, a north-east trending flysch deposit of late Neoproterozoic age (Miller, 2008). The Kuiseb Formation consists mainly of quartz-biotite schists with minor calc-silicate rocks, quartzites and carbonaceous schists, and is regarded as a metapelitic sequence by Adamson and Teichmann (1986).

The structures appear vertical in the OLZ and south-eastward verging in the SZ and they have increased in intensity southwards for culmination of a single schistosity (Miller et al 1983). The 350 kilometers

long, two-mica Donkerhoek granite batholith, which is post-tectonic, garnetiferous, is confined to the OLZ and a minor portion of the SZ. According to Finnermore (1978), a linear belt of amphibolite 350 kilometers long and 1 to 3 kilometers wide with the composition of mid-ocean ridge basalt, the MAB found in the southern third of the SZ.

The volcanic rocks occur in NZ and SZ, but appear to be more abundant in the high-pressure zone. The mafic rocks are all pre-tectonics (Kroner, 1977), and have the condition of mid ocean ridge (Finnermore, 1978). They have been considered to be either obducted oceanic crust (Bruke et al., 1977) or synsedimentary rocks emplaced above and into sediments casing a submerged mid-ocean ridge (Miller, 1983).

The Damara Sequence comprises 4 major stratigraphic units (table 3.1) which from the base upwards are the Nosib Group, a basal Arkosic arenite with local alkaline volcanics and evaporates. Nosib Group is overlain by the Otavi Group and lower Swakop Group, a middle carbonate sequence with variable amounts of associated clastics that include an extensive marker Mixtite, upper Swakop group, is an upper pelitic to semipelitic succession that includes the MAB and a younger syntectonic fore-arc sequence in the OLZ and SZ, superimposed by Mulden Group, an older northern molasse and Fish River subgroup of the Nama Group, a younger southern molasse (Miller, 1983).

Table 3.1: The four major stratigraphic units of the Damara sequence (after Miller, 1983).

<table>
<tr><th>Ma</th><th colspan="2">Group</th><th colspan="2">Subgroup</th><th>Formation</th></tr>
<tr><td>535</td><td colspan="2">Nama

Mulden</td><td colspan="2"></td><td></td></tr>
<tr><td>650</td><td rowspan="3">Swakop</td><td rowspan="3">Otavi</td><td rowspan="2">Khomas</td><td rowspan="3">Tsumeb</td><td rowspan="3">Kuiseb

Karibib

Auas

Chuos</td></tr>
<tr><td>700</td></tr>
<tr><td>730</td><td>Ugab

Kudis</td></tr>
<tr><td>820</td><td colspan="2">Nosib</td><td colspan="2"></td><td></td></tr>
</table>

The Swakop Group is further divided into the Khomas and Kudis Subgroups. The rocks that form the

Khomas Subgroups appear in a coastal arm of the NZ and CZ. The Kuiseb Formation which is the uppermost unit is the only unit present in the OLZ and SZ. The Kuiseb Formation is a thick succession of interlayered metapelites and metagreywackes (feldspar-rich quartz-mica schists) that forms the uppermost unit of the Swakop Group and is 10 km thick in the NZ (Miller 1983). The MAB is the most prominent unit in the Kuiseb Formation and is confined to the high-pressure SZ; it is a linear belt of amphibolite of up to 3 kilometers wide and 350 kilometers long. The mafic rocks are generally concentrated in two zones about 200-500 m apart where they form lenses and layers interbedded in the Kuiseb schist.

Even though the MAB experienced intense deformation and medium grade of metamorphism, the size and shape of grains are largely preserved. Tuffs, lavas, pillow lavas, differentiated and undifferentiated metagabbros and metabasite dykes are also recorded (Miller 1983). Miller and Hoffmann (1981) noted that deformation has rendered all schist-amphibolite contacts pseudoconformable with bedding in the schist, but the chilled contacts of the dykes and of many metagabbros and chlorite-rich bases of the differentiated metagabbros clearly demonstrate their intrusive nature.

3.3 The Matchless Amphibolite Belt (MAB)

The Matchless Amphibolite Belt (MAB) is a protruding linear geological feature up to 3 kilometers wide and at least 350 kilometers long within the Damara orogeny of Namibia (Miller, 1983). The exact length of the belt is not well known due to the superficial cover of Kalahari sands, especially east of Windhoek, towards the border with Botswana (Fig 3.1). The MAB which consists of amphibolites that form lenses and layers occurs conformably interbedded within the sequence of semi-pelitic to pelitic metasedimentary rocks of the Kuiseb Formation in the Damaran Southern Zone (Table 3.2). The amphibolites of the MAB have a mid-oceanic ridge basalts (MORB) signature, and therefore have been interpreted by Breitkopf (1989) as metamorphosed tholeiitic basaltic rocks that are formed in an extensional tectonic setting.

Table 3.2: The stratigraphy of the southern part of the northeast-trending branch of the Damara sequence showing the position of the MAB (modified after Miller, 2008)

Group	Subgroup	Formation	Lithology
Swakop	***Khomas***	***Kuiseb***	**Quartz-mica schist with minor intercalations of carbonaceous schist and amphibolite (*MAB*)**
		Auas	**Quartzite, schist, dolomite, and amphibolite**
		Chuos	**Mixtite, schist, amphibolite and itabirite**
	Kudis		**Dolomite, mica schist, carbonaceous schist and quartzite**
Nosib			**Quartzite, phyllite and conglomerate**

The MAB shows evidence of folding at its western end and it disappears beneath the Kalahari sand cover to the east (Fig 3.3). In the lower half of the Kuiseb Formation, the MAB occurs as numerous layers,

lenses and bands of medium to fine-grained amphibolite and chlorite-amphibole schist enveloped in the metasediments, and is often accompanied, along strike, by lenses of sericitic quartzite, all lying within isoclinally folded Khomas schist of the Damara sequence (Miller, 2008 and Kanehira & Tatsumi, 1970).

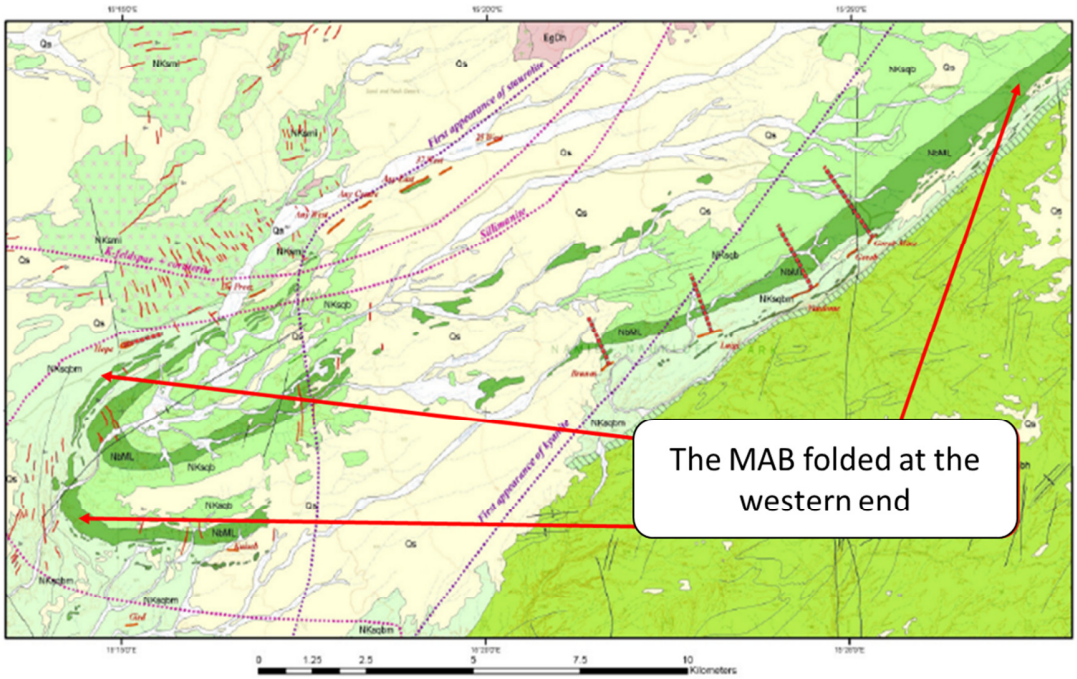

Figure 3.3: A geological map of the Gorob-Hope area showing folded MAB at the western end (Miller, 2008).

The MAB is associated with Neoproterozoic massive sulphide Cu-Au-(Zn-Ag) deposits that are similar to Besshi-type Cu-pyrite deposits (Kanehira and Tatsumi, 1970). These authors further stated that both the Besshi and Matchless type deposits are conformable with the surrounding crystalline, isoclinally-folded, schists of mafic and pelitic origin and are accompanied by quartzitic rocks. In addition, the deposits are tabular in form and are associated with metamorphosed mafic volcanic rocks. The sulphide deposits of the MAB are classified into three types: compact ore, banded ore and Cu-rich ore (Breitkopf and Maiden, 1988). The compact ore consists mainly of pyrite, chalcopyrite, sphalerite and small amount of gangue minerals. The banded ore is a mixture of sulphides and silicates and Cu-rich ore is essentially a mixture of chalcopyrite and chalcocite (Breitkopf and Maiden, 1988).

The main Cu deposits associated with the MAB are at Otjihase mine, 20 km northeast of Windhoek, the Matchless mine, 30 km southwest of Windhoek and the Gorob-Hope mines in the Namib desert park, about 225 km southwest of Windhoek (Fig 3.3). The Cu-pyrite deposits found along the belt vary in size but are essentially similar to one another in their mode of occurrence, shape, mineralogy and ore texture and have the following common characteristics: the deposits occur in the hangingwall or footwall of units of the MAB, the mineralisation is associated with tabular masses of siliceous, cherty and /or quartzitic rock (Klemd et al., 1987).

The ore bodies are lenticular in form and lie conformably within crystalline, isoclinally-folded, semi-pelitic and mafic schists. In addition, they are composed mainly of massive compact ore, consisting of pyrite with chalcopyrite, some sphalerite and pyrrhotite (Kanehira and Tatsumi, 1970).

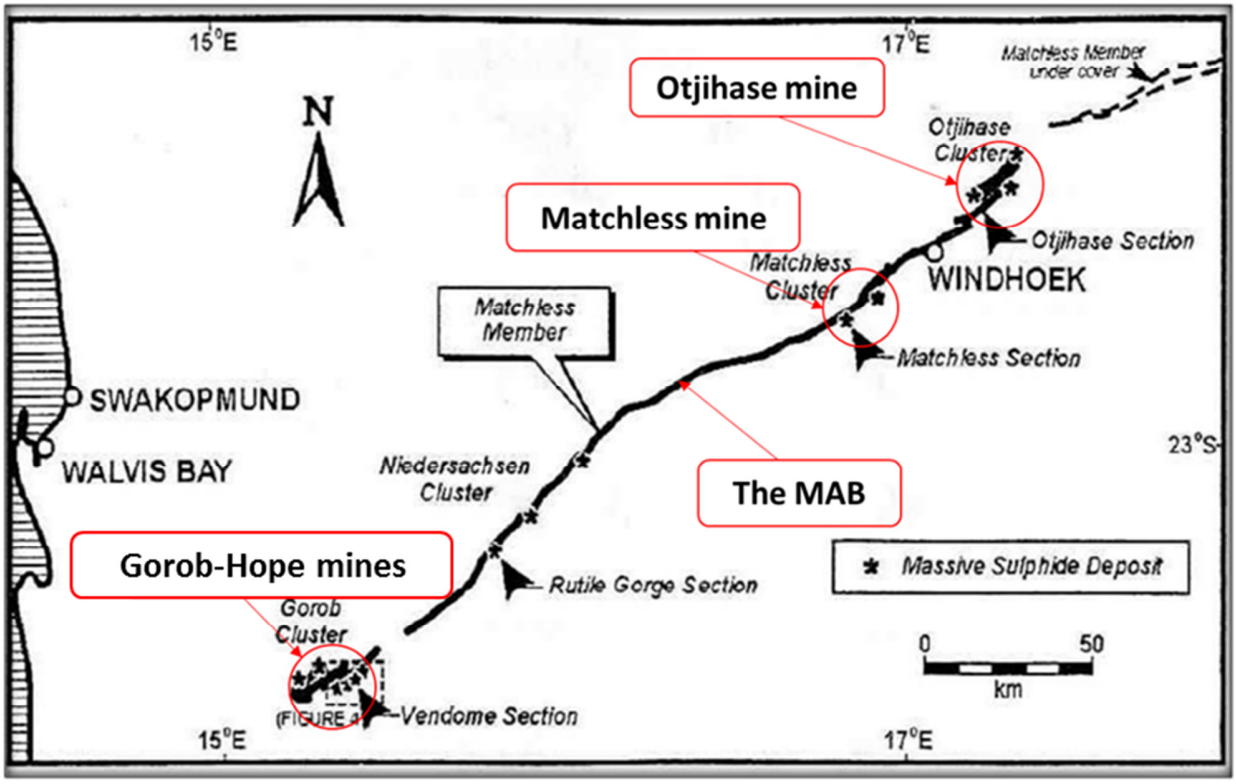

Figure 3.4: A map showing main copper deposits associated with the MAB (modified after Killick 2000).

3.3.1 Deformation and Metamorphism

All units of the MAB have undergone three phases of deformation (Miller et al., 1983). In the southern zone of the Damara orogeny, the deformation intensity increases toward the southern part of the zone. The Kuiseb schist displays three phases of deformation with D1 and D2 phases forming isoclinal to recumbent folds while D3 is characterized by north-trending S3 crenulation cleavage dipping to the west (Miller et al., 1983).

Major porphyroblastic mineral growth occurred subsequent to second deformation at amphibolite facies metamorphic grade of 550 – 625 ^{o}C and 6-8 Kbar (Klemd et al., 1989). Massive sulphide mineralisation was subjected to processes of boudinage, brecciation, plastic flow, pressure solution and recrystalisation during deformation and metamorphism (Klemd et al., 1987). These processes caused differences in texture in a range of sulphide-rich rock types including sulphide-bearing schist, sulphide-bearing magnetite quartzite, pyritic quartzite and a pyrite-quartz-muscovite unit, banded to massive sulphide unit, foliated sulphide ore, sulphide-matrix breccia ore and quartz-sulphide veins (Cook et al., 1994).

3.3.2 Alteration and Structures

Considering the model of volcanic-hosted massive sulphide deposit formation, the massive sulphides are believed to have formed as an exhalation on the sea floor and were simultaneous with sedimentation. The underlying disseminated epigenetic mineralisation is understood to have been initiated below the sea floor and accompanied by hydrothermal alteration of what may have been still partially

unconsolidated sediments (Killick, 1982).

In the Gorob-Hope area, the sedimentary layers are over turned and metamorphosed regionally at staurolite-kyanite-sillimanite grade. In the stratigraphic footwall of the sulphide lenses, pre-metamorphic alteration zones can be recognised as they appear discordant to the lithostratigraphy. Hydrothermal alteration of the original sediments is associated with exhalative ore-forming processes of the submarine environment, that led to overall enrichment of Mg, Fe, Mn, Cu, Zn, Ba and P and depletion of Ca, Na, K, Rb, Sr and Ce (Haussinger et al., 1993).

Mica-rich schists occur close to the sulphide mineralisation and range from quartz-mica-schists (containing both muscovite and biotite), through to quartz-muscovite schists and sericitic quartzites to magnetite quartzite at the stratigraphic top of the deposits (Klemd et al., 1987). Klemd et al. (1987) further noted that all four of the above rock types may include garnet. The sericitic quartzites appear to be in between the hydrothermally altered sediment (quartz-mica schist) and the exhalative magnetite quartzite.

Klemd et al. (1989) concluded that the unusual presence of the chlorite schist in the hangingwall of the orebody indicates that either the chlorite schist was originally basalt or basaltic pyroclastic materials which have been altered due to tectonism during collision or the chlorite schist could be altered sedimentary rocks or mixed sedimentary-pyroclastic rocks which are hydrothermally altered. The structures within the MAB area developed southeast verging and isoclinal folds superimposed all the older structures. Bedding-parallel foliation as well as northwest dipping structures can be recognized (Miller, 2008).

3.4 Local geology of the study area

In the Gorob-Hope area, the MAB consists of two main bands of amphibole-bearing schists, metagabbros, and intercalated metapelitic rocks, striking east- north-east through the area, and to the west it has been deformed into major asymmetrical syncline, known as Hope Synform and it is over folded towards the southeast (Fig 3.4). Two distinct amphibolite layers of the southern limb appear to amalgamate on the northern limb, where they locally reach a combined thickness of 500 m (Cowey, 1981).

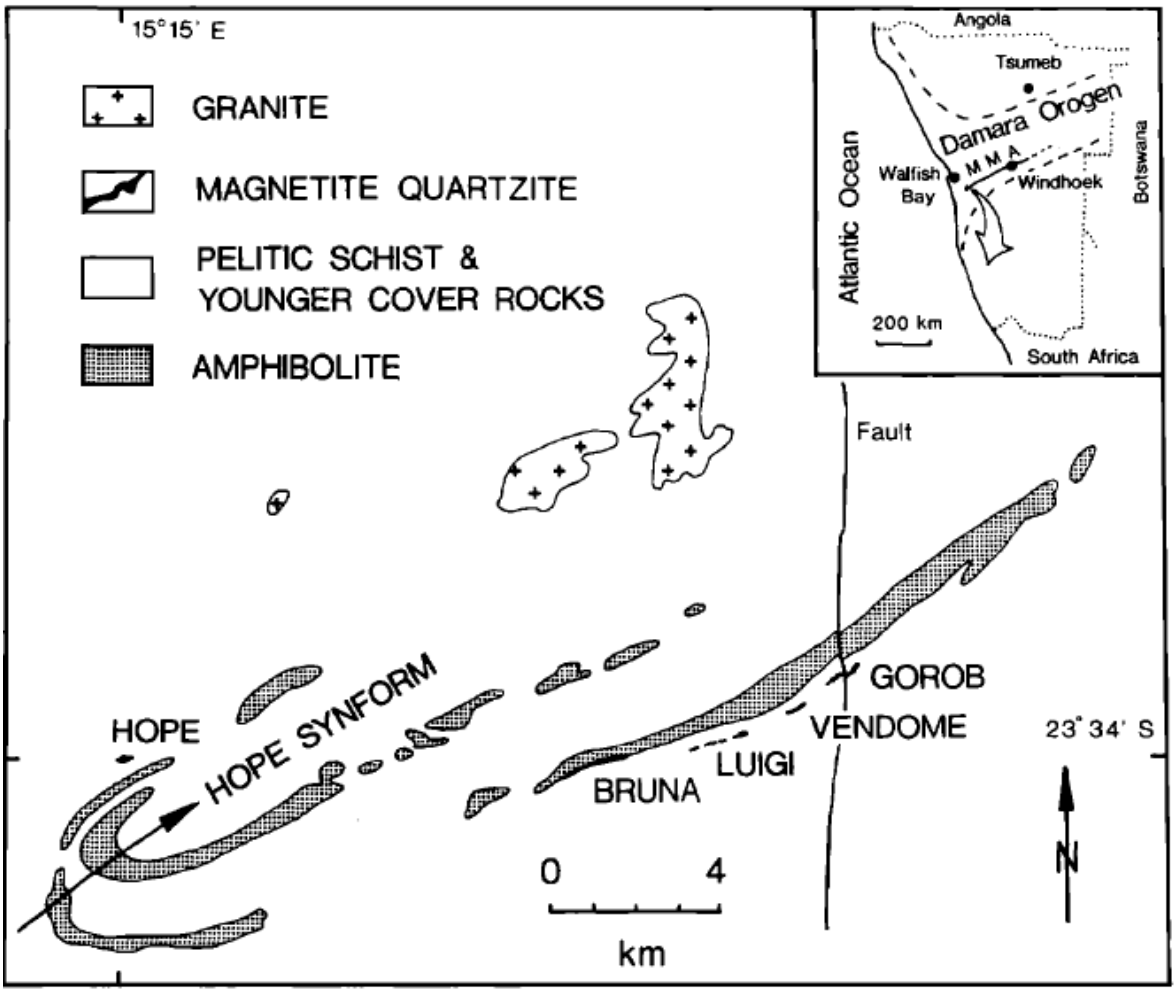

Figure 3.5: A geological map of Gorob-hope area showing the Hope synform and the Gorob, Vendome, Luigi, Bruna as well as Hope lenses (Haussinger et al., 1993)).

The two limbs of the synform differ considerably in mineral facies and texture owing to a higher grade of metamorphism and more intense deformation on the northern limb. The foliation has a moderate north-north-westerly dip on the southern part of the fold closure, and rapidly steepening to near vertical or overturned along the northern limb (Cowey, 1981).

The Gorob-Hope cluster is made up of eight cupreous pyrite lenses which occur in two main stratigraphic positions (Fig 3.5). The Gorob, Vendome, Luigi and Hope lenses occur in the amphibolite units, whereas the Bruna and Anomaly lenses are in contact between the quartzites and the amphibolite units (Cowey, 1981).

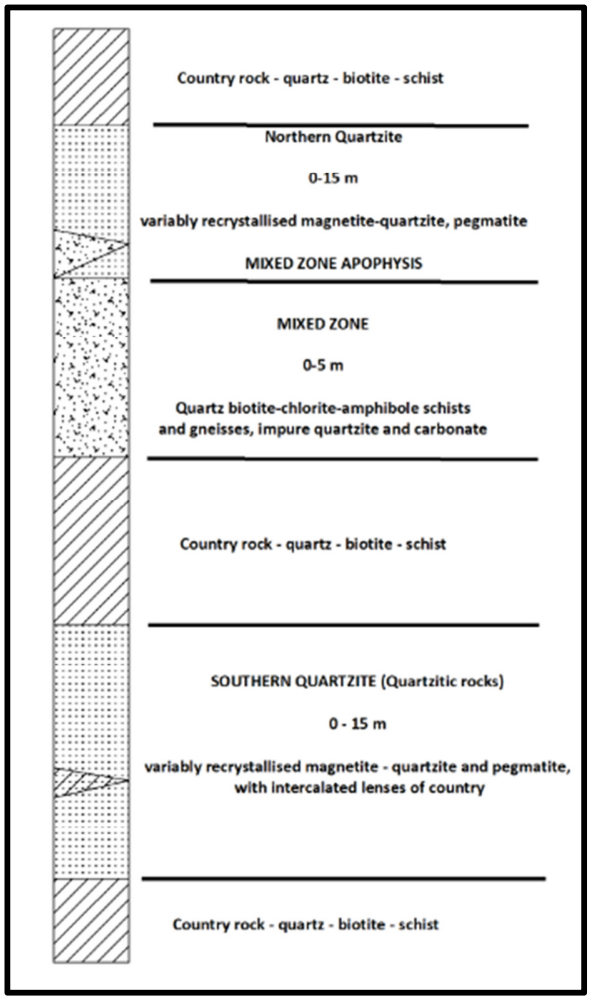

Figure 3.6: A stratigraphic section of Hope lens showing two parallel quartzitic horizons (After Cowey, 1981).

The expression of the Hope lens takes the form of a small hill about 300 m north of the MAB. Two parallel quartzitic horizons consisting of variably-recrystallised magnetite-quartzite with accessory garnet, ferromagnesian minerals and sulphides, outcrop for a strike distance of 490 m, and continue in the subsurface to the east (Cowey, 1981). Associated with the southern quartzite, located along its northern side, is the principal host to the mineralisation, a “mixed zone” of mafic schistose and gneissic rocks. The mixed zone is heterogeneous, and includes hornblende, actinolite and biotite-bearing quartzitic schists, impure quartzites and carbonate rocks.

The southern quartzite zone is heterogeneous as well, and it consists mostly of quartz and magnetite with secondary and variable biotite, garnet, amphibole and chlorite. The magnetite content varies from evenly disseminated to laminated. There are occasions where pure quartz veins and pegmatitic materials occur. Some of the pegmatites contain magnetite and appear to be intensely recrystallised quartzite, whereas others may be of metasomatic origin and interrelated to the intrusion of the Donkerhoek granite (Cowey, 1981).

The attitude and thickness of the strata comprising the Hope lens vary considerably due to folding and

boudinage. Dips are generally steep to the south to vertical, except at the western end of the outcrop where exposure is apparently terminated by a fault. Here, the northern quartzite forms a shallow easterly-plunging partial synformally closure, but appears to terminate independently of the southern quartzite (Cowey, 1981). Based on mapping and surface diamond-drilling, two contrasting structural models for the Hope lens, were proposed. Cowey (1981) favoured two independent synformally folded quartzitic horizons, whereas Comline (1986) proposed a single isoclinally-folded antiformal quartzite duplicated by a strike-parallel thrust.

3.4.1 Lithological units

The lithologies of the Gorob-Hope area are shown in Figure 3.6 below.

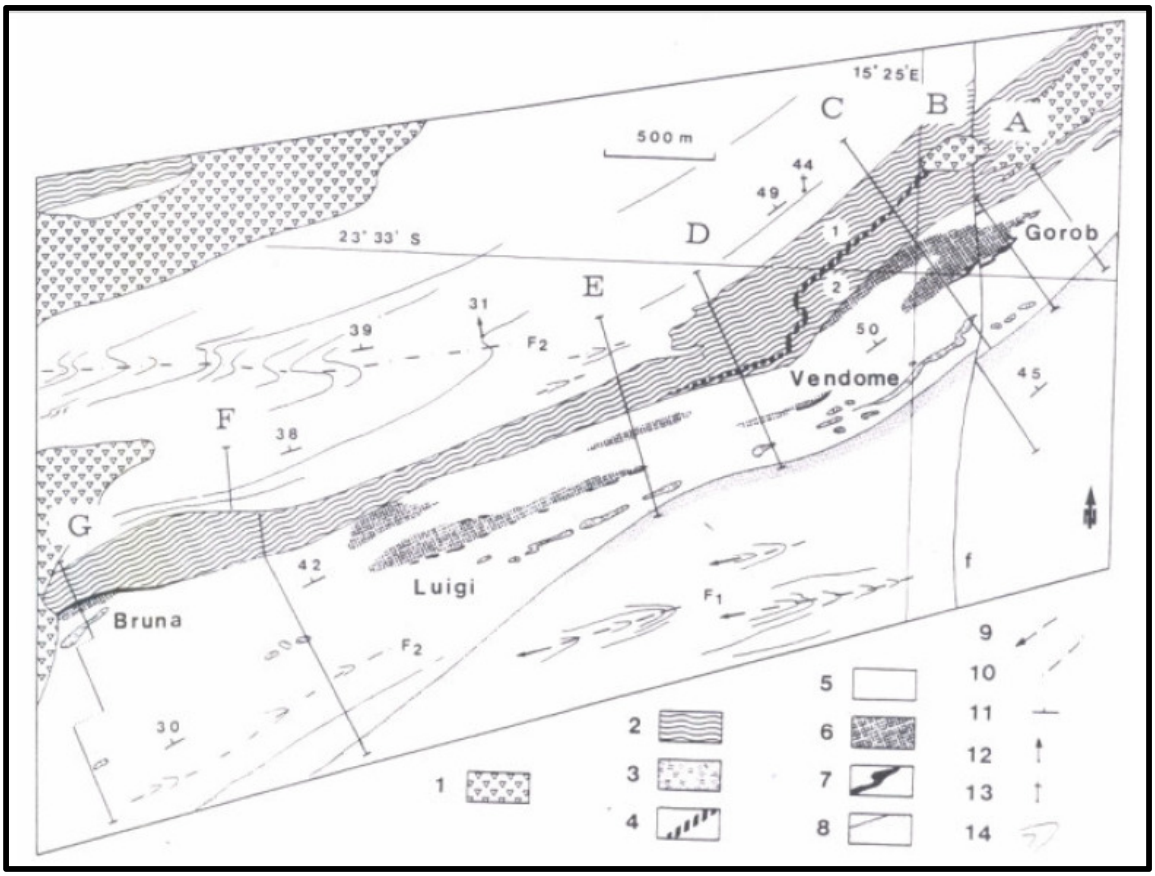

Figure 3.7: A geological map of Gorob-hope area, showing different lithologies (after Preussinger 1990). 1- calcrete and gravel, 2- amphibolite, 3- metagabbros, 4- talc schist and related rocks, 5- metasediments, 6- zones of pre-metamorphic hydrothermal alteration, 7- magnetite-quartzite, 8- graphitic schist, 9- F_1 axial plane trace, 10- F_2 axial plane trace, 11- S_2 foliation, 12- F_2 axial plane and plunge, 13- L_2 intersection lineation, 14-S_o bedding form line.

The area consists of two units of amphibolites, each with an extreme width of 400m (Preussinger, 1990). The two units are the footwall wall and the hanging wall amphibolite that are developed best at the centre and in the southern limb of the Hope synform, respectively. These two prominent layers of amphibolite seem to amalgamate on the northern limb. There are pillow-structures that are widespread

within the MAB. In addition, there are a number of boudinaged, sill-like and thin amphibolite layers in the structural foot wall of the Gorob area, that are interpreted as intrusions metamorphosed gabbroic units (Preussinger, 1990).

There are two main types of metasedimentary rocks known as graded units and psammitic intercalations. Graded units that are thought to have initially resulted from the deposition of turbidity currents appear with a continuous high lateral (Preussinger, 1990). The layers and boundins of calc-silicate rocks such as hornblende-garnet gneiss are common within the graded cycles and they are understood by Preussinger (1990) to be original contents of detrital carbonates. Unlike the graded units, psammitic intercalations appear discontinuous laterally however, they appear homogeneous in composition and they don't preserved sedimentary features. The rock types are altered from psammitic quartz-biotite-plagioclase schists to pelitic staurolite-muscovite-plagioclase schists. Preussinger (1990) further understood the psammitic turbidite beds north of the amphibolites at Gorob as a numeral of thickening and coarsening upward cycles.

According to Haussinger et al. (1993), pre-metamorphic alteration zones boundaries appear gradual. Structures like graded bedding can be observed at the outer edges, however they are totally destroyed in the centres of the zones. They further noted that the same turbiditic origin should hence be presumed for these rocks, but they are intensely overprinted by pre-metamorphic hydrothermal alteration.

Haussinger et al. (1993) emphasised that the fact that calc-silicate rocks are absent and the chlorite schists are present implies conspicuous features of the alteration zones. Kyanite occurs abundant in comparison to the surrounding metapelites and sillimanite occurs as an additional mineral. They further noted that there is a trend to smaller number of phases in individual rocks where muscovite and plagioclase become less abundant and disappear locally, while the amount of staurolite increases, which suggests that Na_2O, CaO, and K_2O are depleted and FeO and MgO are, enriched in the alteration zones.

There are three main types of rocks that are recognised such as *aluminous schists* that consist at least of one of the Al-rich silicates, such as staurolite, kyanite or sillimanite, as well as biotite and quartz. Other minerals such as muscovite, plagioclase and garnet may exist but are fewer amounts than in staurolite schists within metaturbidite sequences outside the zones of pre-metamorphic alteration (Haussinger et al., 1993).

Chlorite schists are characterized by chlorite content of more than 5 vol % in addition to quartz, biotite and varying amounts of staurolite, garnet, muscovite, plagioclase and rare fibrolitic sillimanite. *Mica-rich schists* are fewer and they are characterised by major volumes of randomly recrystallised muscovite and biotite and by the absence of staurolite, kyanite, sillimanite and chlorite, and have only been formed close to the main ore bodies (Haussinger et al., 1993). Apart from the Bruna lens, the pre-metamorphic alteration zones around Gorob are between the hanging wall and the amphibolites. The pre-metamorphic hydrothermal alteration zones at Bruna are found in the footwall of the ore bodies (Preussinger, 1990).

Magnetite quartzites are known to be equal to the ferruginous cherts which precipitated chemically due

to exhaled hydrothermal fluids that mixed with the sea water (Haussinger, 1990). Magnetite quartzites were then quickly deposited on the seafloor capping the massive sulphide lenses (Breitkopf and Maiden, 1988). The term magnetite quartzite is introduced regionally for a group of rocks that ranges from almost pure quartzites to almost pure magnetite ores (Haussinger et al., 1993).

In Gorob area, the magnetite-quartzite as well as quartzite-muscovite schists are found in the lowest parts of the mineralised units and these units escort the lenses of ore in the area. According to Pirajno and Jacob (1991) the magnetite-quartzites are the metamorphosed equivalents of Fe-and Si-rich exhalites. The mineralisation in these units is mostly stratiform. Preussinger (1990) noted that in the footwall the amount of sulphides reduces as the magnetite content rises.

3.4.2 Mineralisation

In the Gorob area the mineralisation appears as cuspate structures and lenses of different size enclosed by quartz-muscovite schist and magnetite-quartzite. The quartz-muscovite schists are fine-grained in the hanging wall and exhibit a strong planar fabric that mostly described by the orientation of muscovite. Layers of chalcopyrite, pyrrhotite, and pyrite appear thin and arranged conformably to the fabric. The ore body and hydrothermal zones appear in an elongated shape in the direction of northeast-southwest that is believed to be a result of simple shear. All mineralised zones appear elongated towards the west due deformation (Preussinger, 1990).

The mineralisation in the area is considered to be of a typical proximal volcanogenic sulphide deposits that forms at the site of sea-floor thinning out. Preussinger (1990) clarified that massive sulphide deposits in the Gorob-Hope area are hosted in psammitic and pelitic schists of the Kuiseb Formation and are associated with the MAB. Moreover, he put forward that the main ore-forming processes are the convection of hydrothermal and metal-rich fluids that expelled on the seafloor. The magnetite-quartzites at Gorob-hope area are understood as ferruginous cherts of exhalative source that are metamorphosed and that migration path ways for the hydrothermal fluids are provided by synsedimentary faults in the area.

Eight different sulphide-mineralised lenses are found in the Gorob-hope area including Gorob, Vendome, Luigi, Bruna and Hope. Pirajno and Jacob (1991) noted that the sulphide ore bodies in the schists appear not only as lenses but as disseminated zones as well and they are associated with magnetite-quartzite. Vesignieite, a secondary copper mineral, was discovered in the gossan zone of Gorob, Vendome, Bruna and Hope lenses (Schneider and Lauenstein, 1992). The gossan lenses are controlled by tectonics and appear to be concentrated at the boundaries of the magnetite-quartzites and the quartz-muscovite schists.

Chapter 4:

4. Research Methodology

4.1 Introduction

The main objective of this chapter is to report on magnetite orebodies, structures and alteration in order to identify the spatial relationship between the quartz-magnetite bodies and mafic rocks and to see if they can be measured. It is also important to consider if there are any particular magnetic features of note associated with the orebodies and if it is possible to set up a buffer around the magnetic features. In addition, the identification of any recognisable structures related to the deposits and to what extent these can be recognised as possible ore guides is necessary. The distribution and width of alteration zones are considered and if they can be recognised from remote sensing images.

A desktop study of the existing published literature and maps was conducted and the study area was visited for four days for the familiarization of the geology of the area. Data collection, processing, interpretation and integration which involve remote sensing data, geological maps, and geochemical data were completed.

4.2 Data collection and software

The ASTER and Landsat 7 Enhanced Thematic Mapper Plus (ETM+) imagery, as well as historic geological maps have been utilized. All of these data sets have been obtained from the Geological Survey of Namibia. These data sets were utilized for rock type discrimination, the relationship between magnetite quartzite bodies and mafic volcanic rocks as well as structures and rock alteration features of rock units. Environment for Visualizing Images (ENVI) software application was used for processing remote sensing images, whereas ArcGIS (ArcMap 10.2) software was used for georeferencing, editing, creating maps, and handling of different datasets by comparing them with each other and finally integrate these datasets into final images that highlighted the features of interest.

4.3 Geological field observation

Geological field observations were conducted on the 10 -13/03/2017 at the Gorob, the Vendome, the Luigi, the Bruna and the Hope lenses within EPL 5796. The area is relatively rocky and largely covered by outcrops.

4.3.1 The Gorob Lens

This lens outcrops over a strike length of about 700 meters and dips at 41° to the north. The quartzites are tightly folded at several places, with folds arranged in an en-echelon manner. This repeated drag folding and stretching resulted in thickening and thinning of the quartzites along the outcrop.

The host rocks to the mineralisation are sericite-quartzites and magnetite quartzites. In the hanging wall they are surrounded by an envelope of impure sericitic schists containing staurolite, kyanite, biotite, chlorite and garnet. Further up into the hanging wall, porphyroblastic staurolite-kyanite-quartz-biotite

schists and medium- to fine-grained staurolite-garnet schists occur as far as the footwall contact of the MAB.

An outcrop (approximate 20 m in length) located at 542789mE, 7395678mN was found traversing north wards and identified as a staurolite schist (Fig 4.1) striking NE and dipping 41°N (Fig 5.2) with garnet porphyroblasts, biotite, and chlorite. The outcrop is of a psammitic composition enveloped magnetite quartzite.

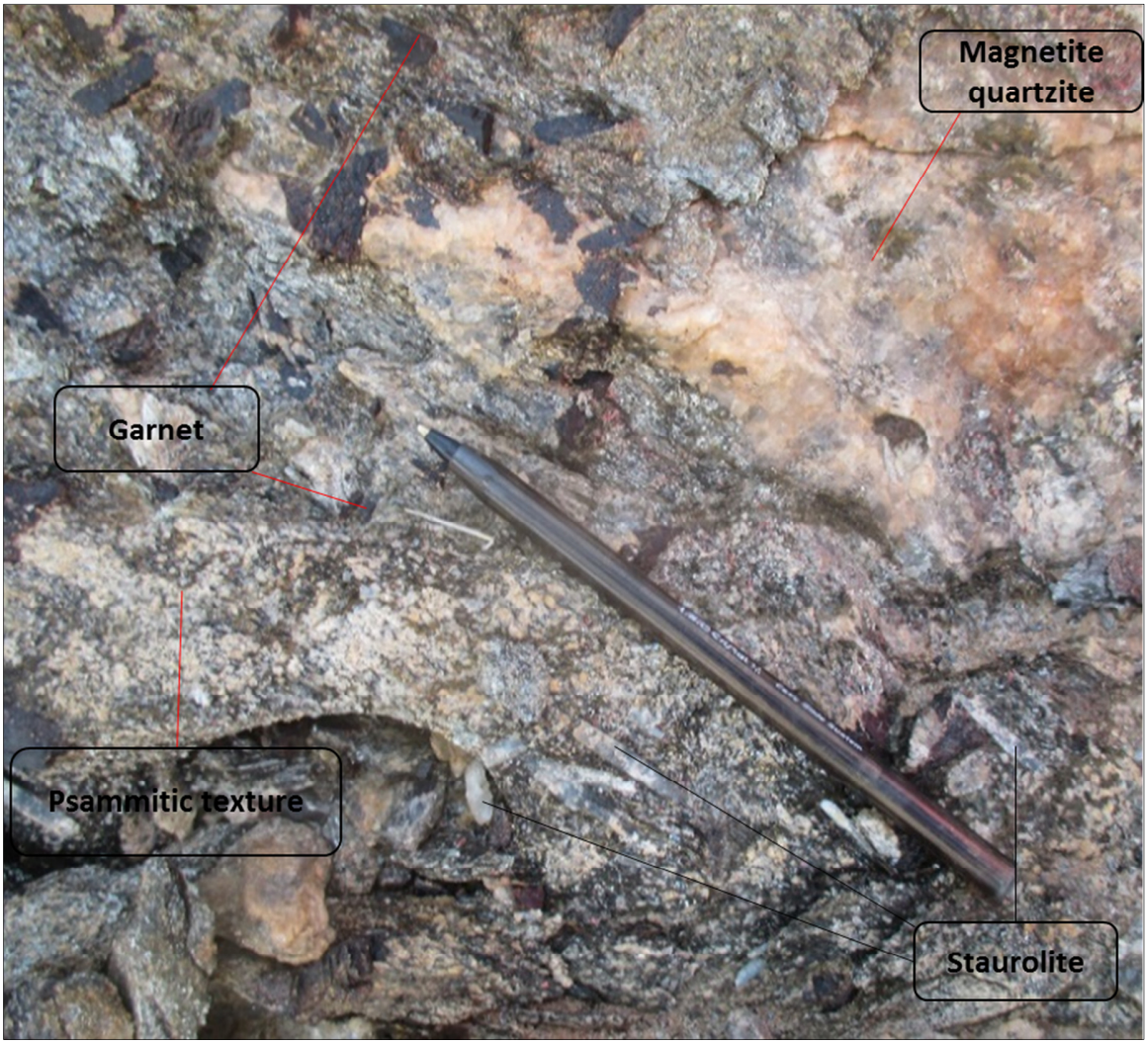

Figure 4.1: A Photograph showing staurolite schist at the Gorob Lens

4.3.2 The Hope Lens

The Hope Lens takes the shape of a very complex tightly folded, flattened and overturned synform plunging at about 12° to the east (Fig 5.4). The closure of the fold in the west is terminated by a fault and forms a small hill. At surface, the lens outcrops for a distance of about 400 m along the plunge and attains a maximum width of 60 m at the fold nose. The vertical dimension of the fold is only a few meters at the nose where it has been eroded, but increases with depth to about 100 m from closure to

the end of the limb.

The country rocks surrounding the Hope Lens consists of undifferentiated sillimanite-muscovite-quartz-biotite gneisses and schists with development of minor kyanite and garnet. Quartz boundins and small pegmatite veins are abundant and a few large discordant pegmatites comprising of quartz, feldspar and muscovite with minor tourmaline, garnet and beryl occur occasionally.

The Hope Lens consists of the following lithologies: a thick and massive magnetite quartzite varying in composition and structure from well laminated and strongly disseminated magnetite to poorly laminated and weakly disseminated magnetite. The magnetites occur as large blebs or in massive bands, and layers rich in garnet porphyroblasts are found sporadically.

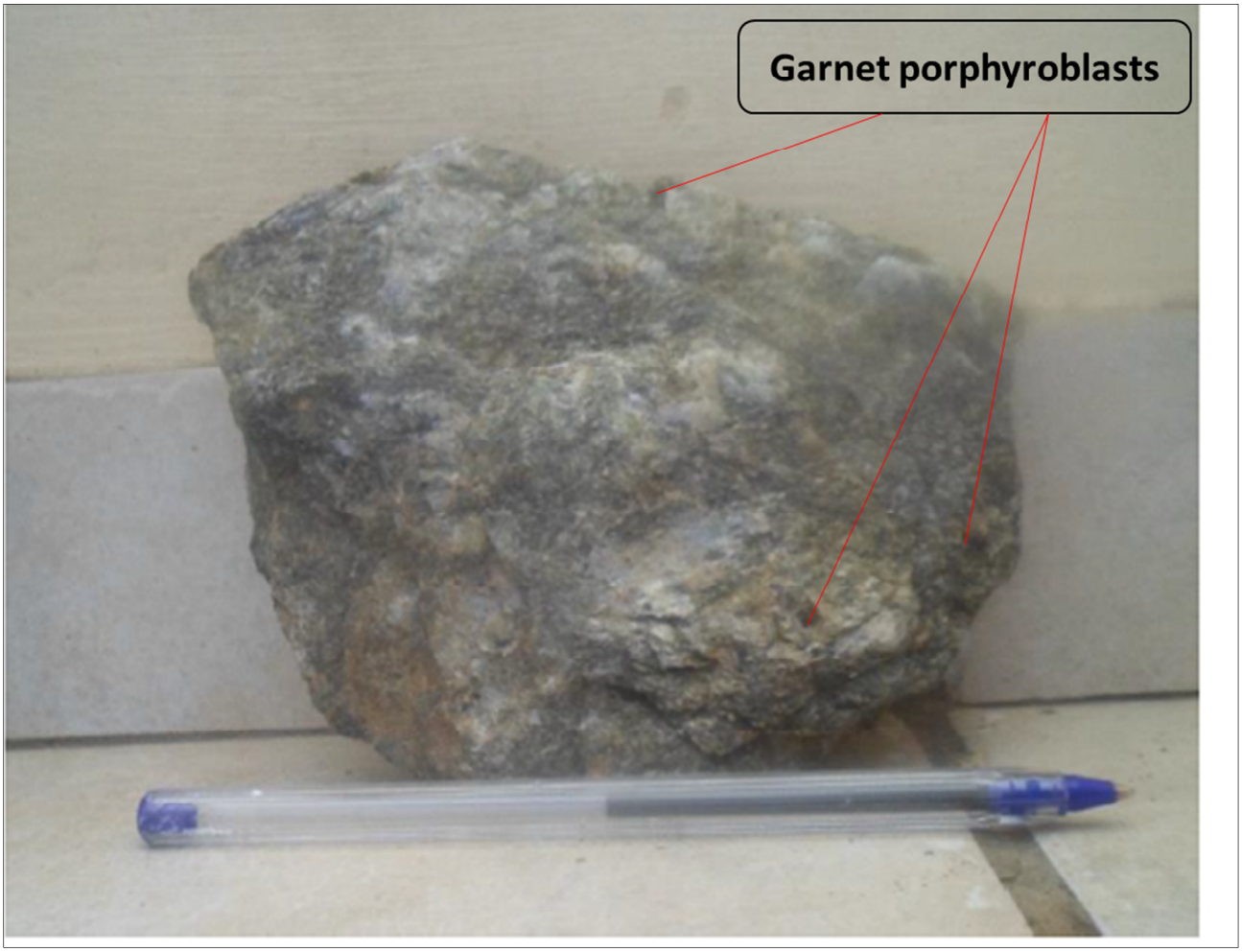

Figure 4.2: Garnet-mica schist from the country rocks surrounding the Hope Lens with garnet porphyroblasts

An outcrop (approximate 15 m in width) located at 525662mE; 7393107mN was found and identified as sillimanite-muscovite-quartz-biotite schist (Fig 4.3) striking NE and dipping 41°N (Fig 5.3). The outcrop is of a psammitic composition that is folded, as well as magnetite quartzite that is also folded.

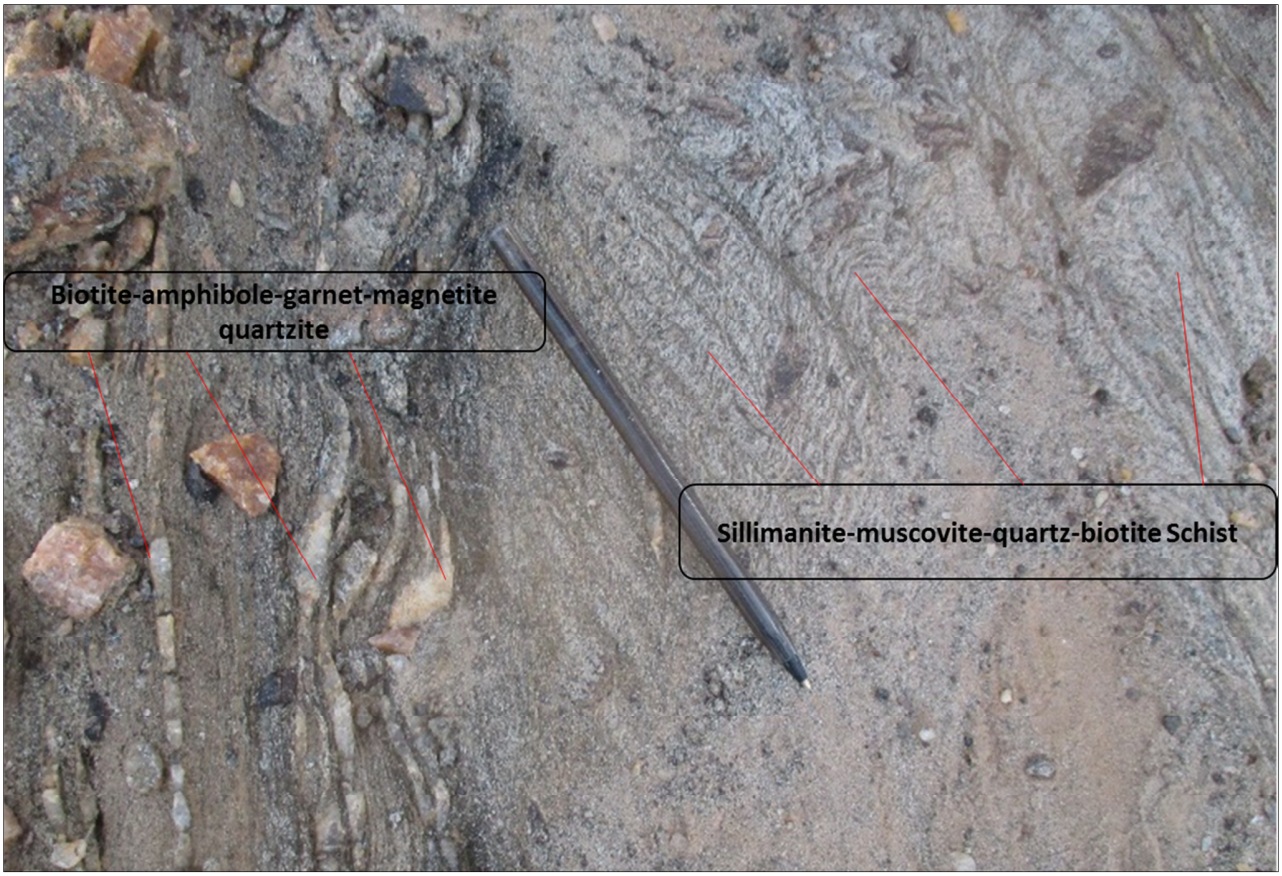

Figure 4.3: A photograph showing folding of magnetite-quartzite and quartz-biotitie schist at Hope Lens.

4.3.3. The Vendome Lens

The magnetite quartzite of the Vendome Lens crops out as a ridge over a strike length of about 250m. The Vendome Lens is lithologically identical to the Gorob Lens, except that the sulphide mineralisation transgresses from magnetite-quartzite as host rocks through sericitic-quartzite and into the schist.

An outcrop of about 5m in diameter was located at 540309mE, 7394035mN which was found traversing south ward and identified a as magnetite quartzite unit (fig 4.4)with some loose quartz pebbles, sub rounded ranging from 3 cm to 40 cm in size.



Figure 4.4: A photograph showing magnetite-quartzite at Vendome Lens

4.3.4. Luigi Lens

Geologically the Luigi Lens is very similar to the Gorob and the Vendome lenses. A magnetite-quartzite horizon is visible over a strike length of nearly 1 km but sericite-quartzite is confined to a tight drag fold in the west. The sericite-quartzite occurs over a strike distance of about 40 meters and attains a width of up to 4 m. The sericite quartzite is overlain by a sequence of coarse-grained schist containing kyanite, chlorite, garnet and abundant large (up to 20 cm long) euhedral staurolite porphyroblasts.

4.3.5. Bruna Lens

The Bruna Lens consist of about 1.5 km strike length of magnetite-quartzite, sericite-quartzite and

quartz-biotite-chlorite garnet schist. This lens is situated on the footwall contact of the amphibolite belt. The (fig 5.1) quartzites dip at 30° to the north and attain a maximum thickness of about 4 m.

4.4 Data Processing and Integration

4.4.1. Geological Data

Historic geological maps were combined in ArcGIS which involved georeferencing and digitizing rocks units and geological structures. The final maps showing the features of interest that have aided in answering the study questions were produced. Historic geological maps (Fig. 4.5 & 4.6) are some of the maps that were utilized to digitize the outcrops of rock units of interest that are found within the area of study. The maps were firstly georeferenced in UTM, and then used as base maps to digitize the features of interest. Shapefiles were created and used to produce new geological maps.

Table 4.1: A list of historic geological maps and the UTM zone that was used.

Geological Map Name	**Map Date**	**UTM zone of georeferenced**
3281_EPL226_Geol_Map6_GO-B_1	24/04/1987	33S
2887_EPL507_GLG_MAP_Area	Not recorded	33S
2887_EPL507_GLG_PLAN_MAP	27/04/1970	33S
2931_EPL507_Geology_GOR_83	04/10/1976	33S

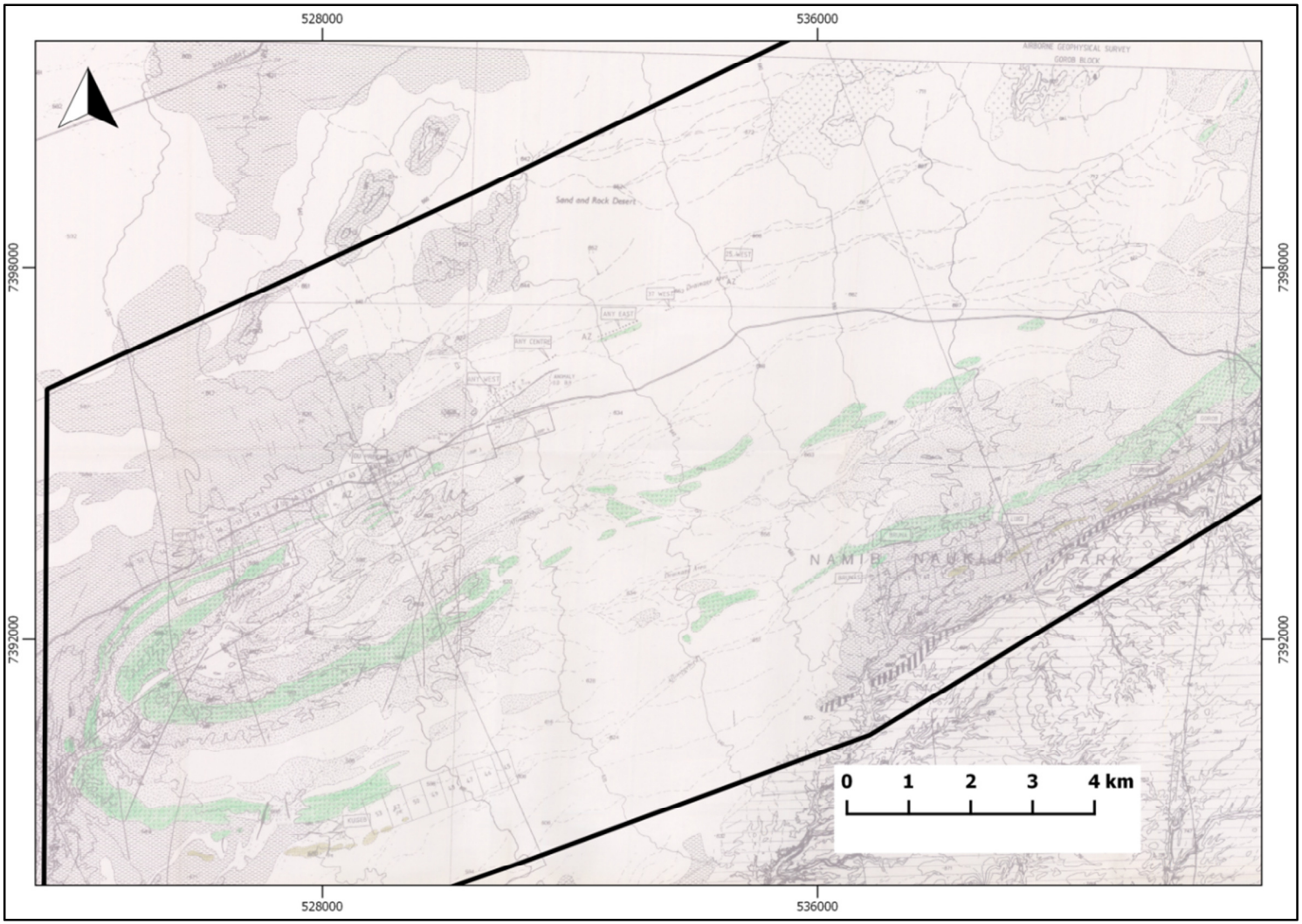

Figure 4.5: A Screen shot showing one of the geological maps that have been utilized for lithological units discrimination (source: Gold fields prospecting company, 1987).

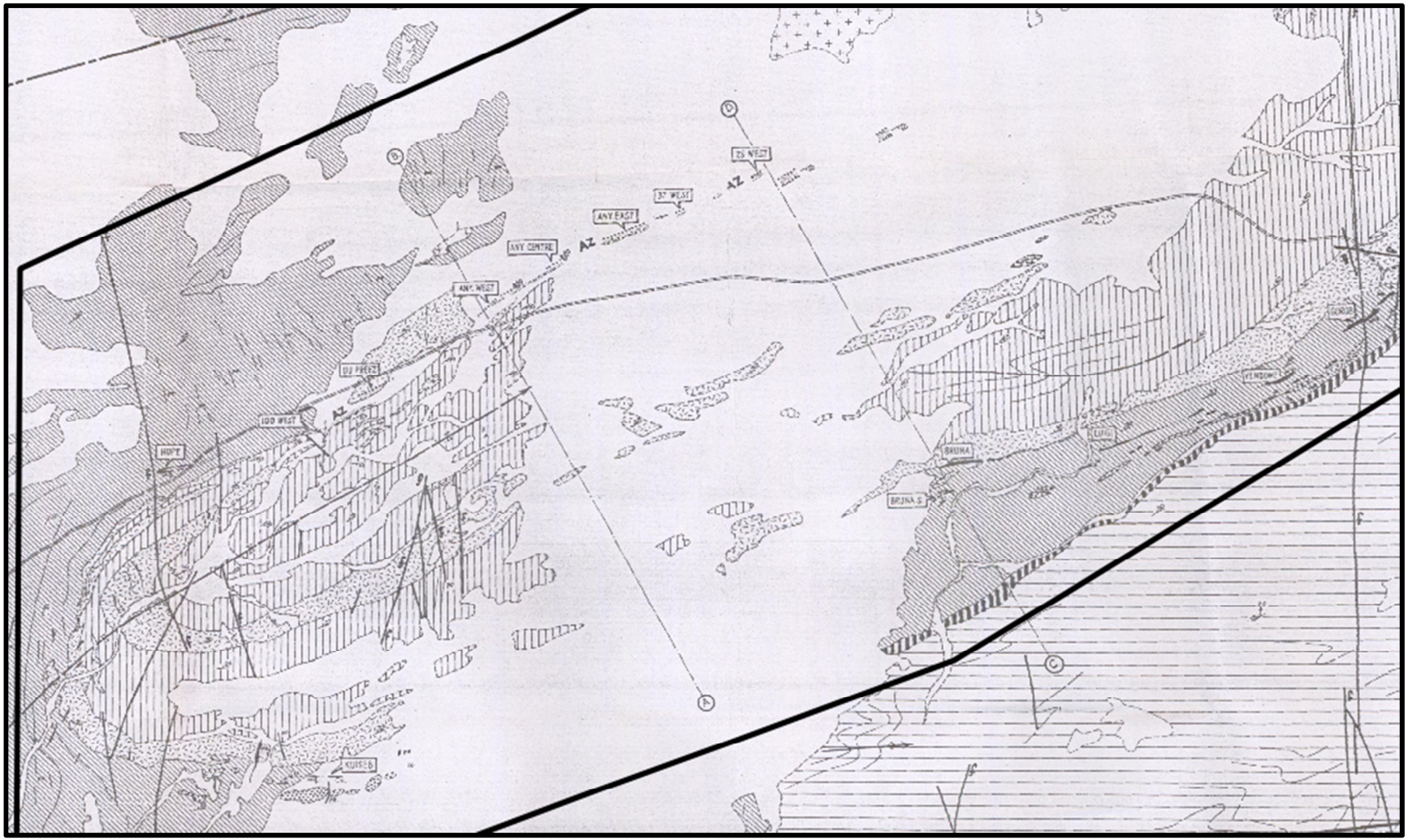

Figure 4.6: A screen shot showing one of the geological maps that have been utilized for rock units discrimination (source: Gold fields prospecting company, 1976).

4.4.2. Remote sensing Data

Different remote sensing images were used in the application of image processing methods during mineral explorations. The spectral information interrelated to minerals of interest signifies a very small portion of the total amount of information in these remote sensing imagery. Hence, the information of interest within the huge quantity of information in spectral remote sensing image is generally not distinguishable or its extraction is challenging if the data is not well processed.

According to Drury (2001), the majority of the images are presented in grey scales. Conversely, the human eye is able to discriminate about 30 grey levels in the black to white range and a lot more different sensitive colours to recognise the patterns of the colours. Hence, different false colour combinations of Landsat ETM+ and ASTER images were used to recognize lithological units and linear structural features as well as zones of hydrothermal alteration.

Landsat 7 ETM+

The Landsat ETM+ image that was acquired at Gorob-Hope area was obtained from the Geological Survey of Namibia within the Ministry of Mines and Energy. This image was processed using ENVI so that it can be geologically interpreted. This was done using band combination to extract and enhance spectral information such as lithological units, structures, and hydrothermal alteration within the study area.

Table 4.2: the type of the image and the georeference system used

Landsat 7	**Date image acquired**	**UTM zone**
P179r010	6/04/2000	33S
P179r020	6/04/2000	33S
P179r030	6/04/2000	33S
P179r040	6/04/2000	33S
P179r050	6/04/2000	33S
P179r070	6/04/2000	33S

The characteristics of Landsat 7 ETM+

The Landsat 7 was launched on the 06 of April 2000 and is equipped with a multispectral sensor known as the Enhanced Thematic Mapper Plus (ETM+). Table 4.3 and 4.4 are showing a summary of Landsat 7 and band features as established on the NASA website in the Landsat 7 science data and uses. This study only utilized band 1, 2, 3, 4, 5 and 7 for image processing and classification since they have the same resolution, rows and columns.

Table 4.3: Landsat 7 ETM+ characteristics

Altitude	705 Km (nominal)
Inclination	98.2°
Quantization	Best 8 of 9 bits
Swath width	185 km
Period of revolution	98.9 minutes
Repeat coverage interval	16 day (233 orbits)

Table 4.4: showing band characteristics (after Williams, 2009).

Band Number and spectral response	Spectral range (Microns)	Ground	Uses
1 (Blue)	0.45 – 0.515	30	Coastal water mapping, soil/vegetation discrimination, forest classification, manmade feature identification.
2 (green)	0.525 – 0.605	30	Spanning the region between the blue and red chlorophyll absorption bands, this band shows the green reflectance of healthy vegetation. It is useful for differentiating between types of plants, determining the health of plants, and identifying manmade objects.
3 (Red)	0.63 – 0.69	30	The visible red band is one of the most important bands for discriminating among different kinds of vegetation. It is also useful for mapping soil type boundaries and geological formation boundaries.
4 (Near infrared)	0.75 – 0.90	30	This band is especially responsive to the amount of vegetation biomass present in a scene. It is useful for crop identification, for distinguishing between crops and soil, and for seeing the boundaries of bodies of water (biomass).
5 (Mid-infrared)	1.55 – 1.75	30	This band is sensitive to turgidity- the amount of water in plants. Turgidity is useful in drought studies and plant vigor studies. In addition, this band can be used to discriminate between clouds, snow and ice.
6 (Thermal infrared)	10.4 – 12.5	60	Measures the amount of infrared radiant flux (heat) emitted from surfaces, and helps to locate geothermal activity, classify vegetation, analyses vegetation stress, and measure soil moisture.
7 (Mid-infrared)	2.09 – 2.35	30	Helpful for discriminating among types of rock formations (lithology) and hydrothermal mapping.
8 (PAN)	0.52 – 0.90	15	

Landsat 7 ETM+ Processing

Layer stacking

Layer stacking (fig 4.7) which is a process of combining several bands into a single image was done in ENVI. In order to achieve this, the images need have the equal number of rows and equal number of columns, meaning that bands with different spatial resolution are resampled to get the target

resolution. This means that all bands are expected to have same spatial resolution to be able to carry out layer stacking.

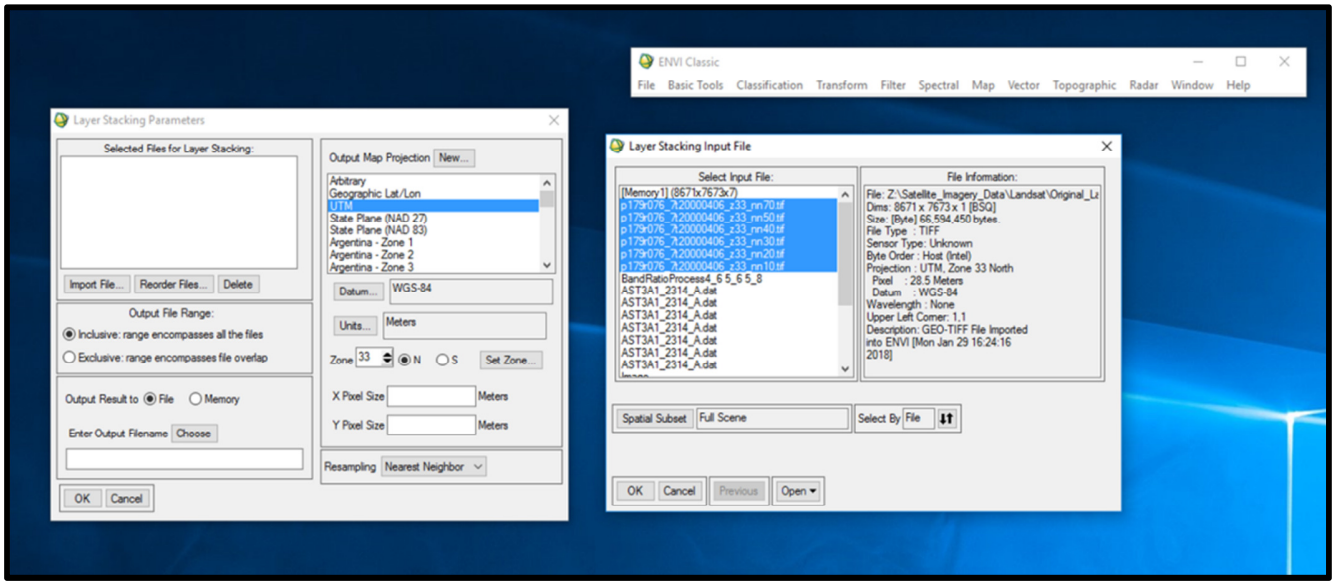

Figure 4.7: A screen shot showing the layer stacking process of colour composite (RGB) 321

Landsat 7 ETM+ Combination of Bands

The following Landsat image bands of p179r070, p179r050, p179r040, p179r030, p179r020 and p179r010 were used for band combinations. The selection of RGB colour combination images using Landsat data were mainly done based on the reflectance spectra of main rock types. The original image bands were shown in an RGB colour composite in order to distinguish the best combination that shows more information of geological features of the study area. The band combination 321 (RGB) were displayed for true colour visual analysis of geological features.

Landsat True colour composite (RGB) 321

In a True Colour composite, the visible bands are carefully chosen and allocated to their corresponding colours to attain an image that approximates true colour. The visible bands estimate the range of vision for the human eye, and therefore they seem to be close by to what we would imagine to see in a normal photograph. True colour tends to appear flat and have low contrast due to the Electromagnetic (EM) radiation in the blue visible region being more susceptible to atmospheric scattering.

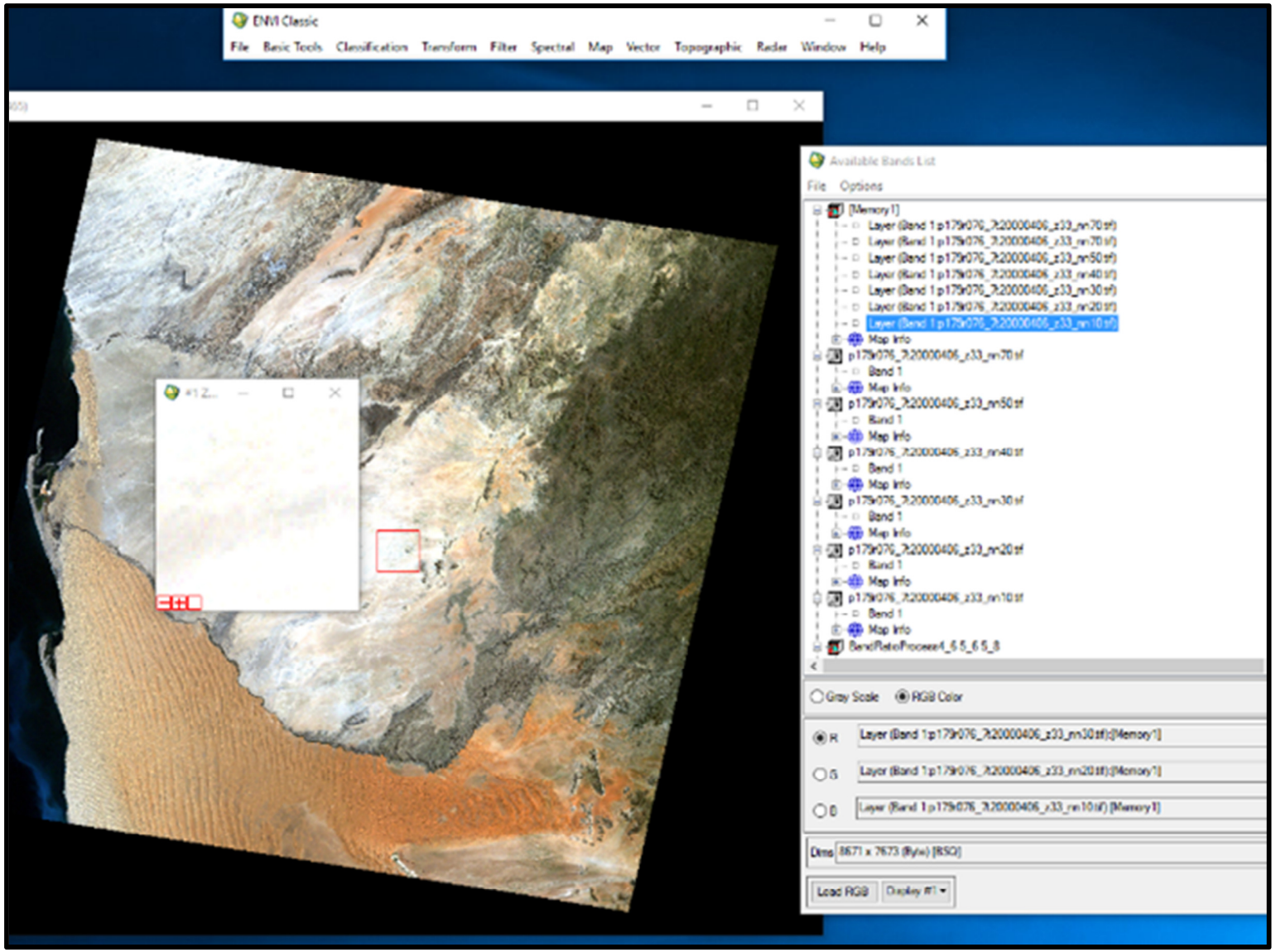

Figure 4.8: A screen shot of a Landsat 7 ETM+ showing the process of true colour composite (RGB) 321

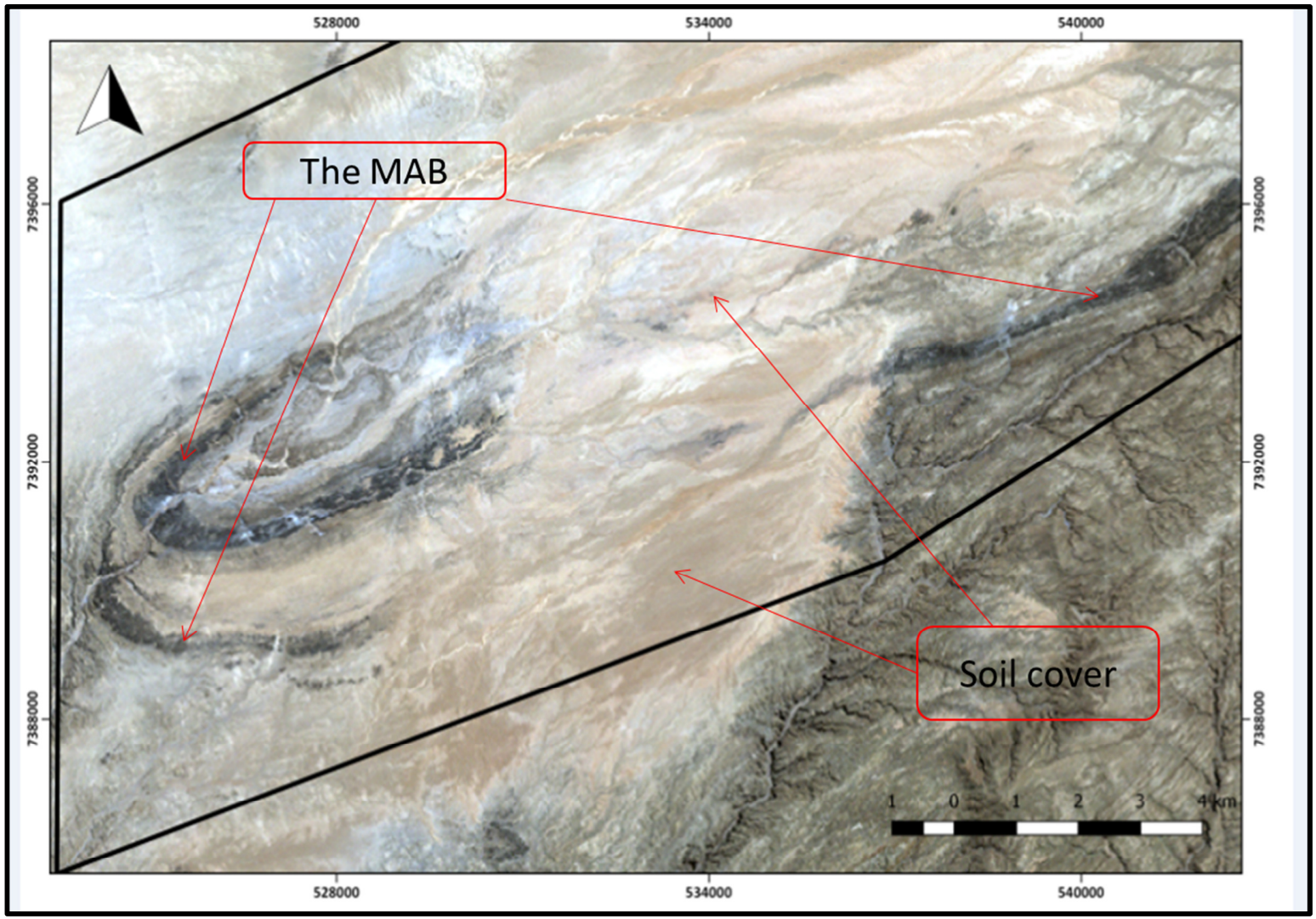

Figure 4.9: A map of Gorob-Hope area that was produced from a true colour composite image (RGB) 321.

Landsat False colour composite (RGB) 457

A false colour composite with band combination (RGB) 457 was used to display differences in rock types of the Gorob-Hope area. All the band combinations were created using ENVI software package and the different band combinations are shown in Table 4.2.

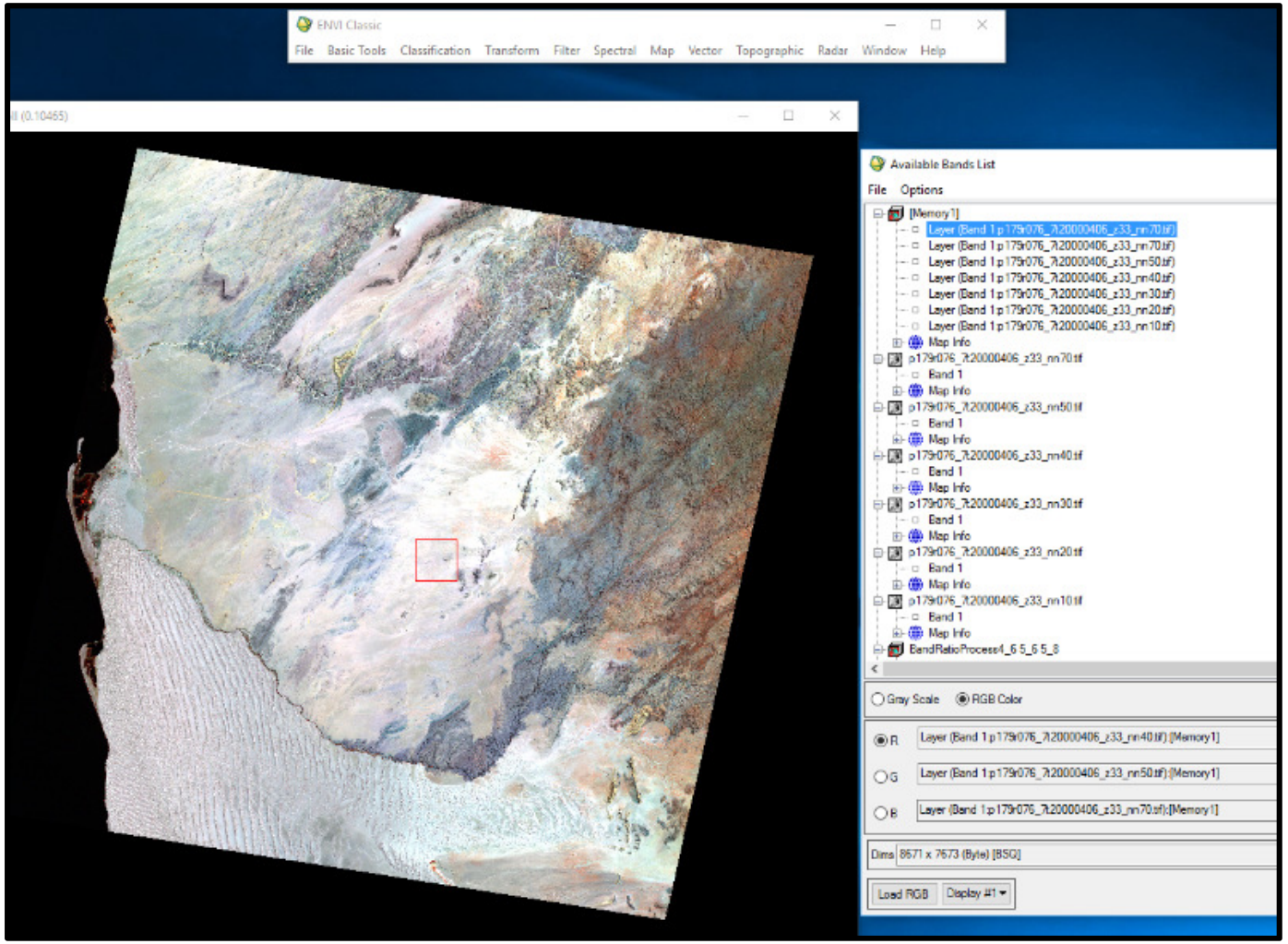

Figure 4.10: A screen shot of a Landsat 7 ETM+ showing the process of false colour composite (RGB) 457

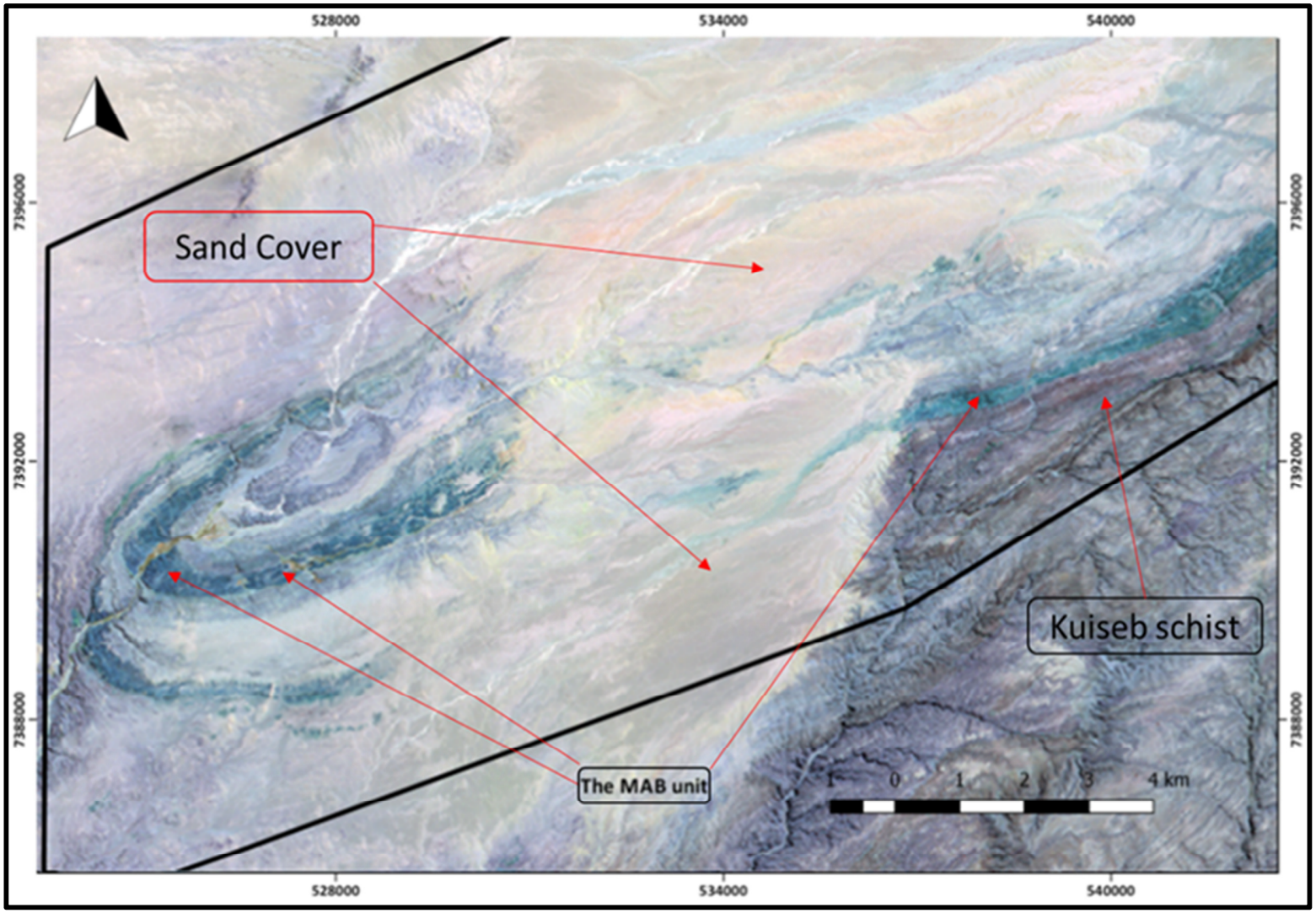

Figure 4.11: A map of Gorob-Hope area that was produced from a false colour composite 457 showing the MAB in blueish, sand and soils in yellow-whitish and Kuiseb schist in greyish colour.

Landsat False colour composite (RGB) 751

The false colour composite 751 in an RGB was exercised in order to enhance the interpretation and visual analysis of geological structures of Gorob-Hope area. The false colour composite 751 has the benefit of preserving morphological features as well as exhibiting different lithological units in different colours because of the use of near and mid infrared portion of the electromagnetic spectral.

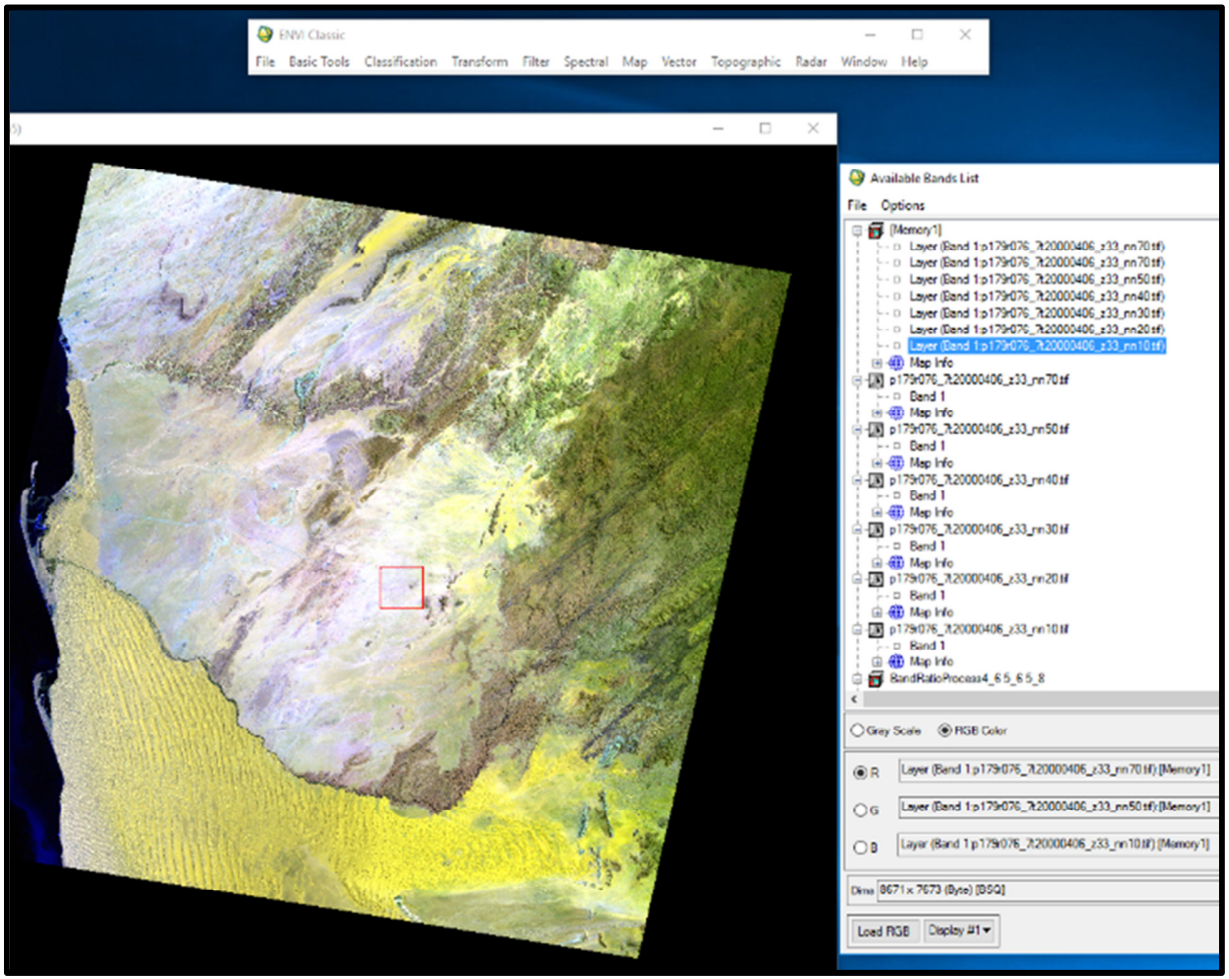

Figure 4.12: A screen shot of a Landsat 7 ETM+ showing the process of false colour composite (RGB) 751

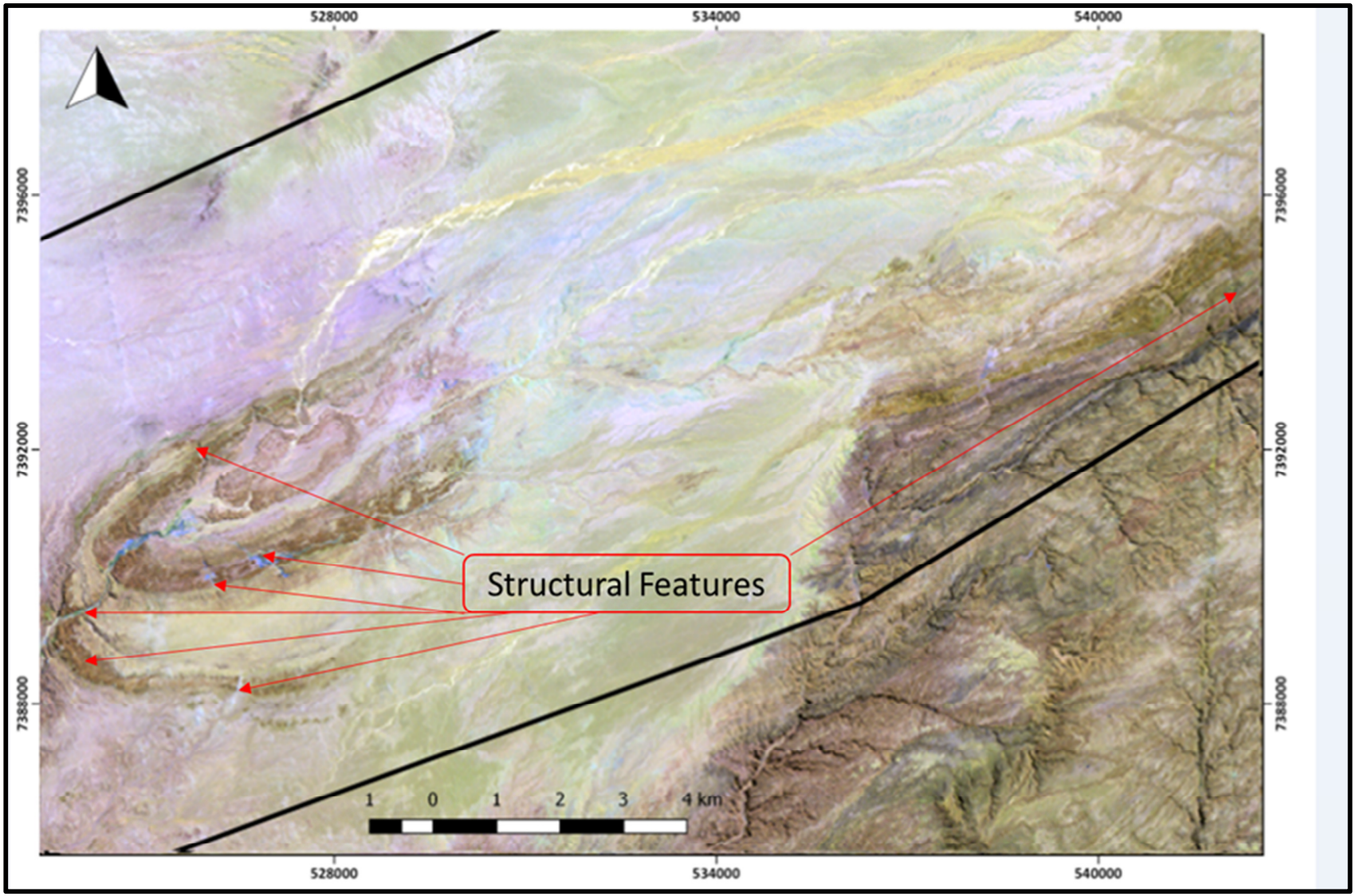

Figure 4.13: A map of Gorob-Hope area that was produced from false colour composite 751 showing linear structures of the MAB.

ASTER_2314_2316

An ASTER_2314_2316 image of Gorob-Hope was processed to show a band combination of 321 that represents natural colour and enhances iron content in the rock units and a band combination of 468 that enhances lithological units and the alteration within the area. Band ratio2 of 4/6, 5/6, and 5/8 was also done for this image to obtain the detailed hydrothermal alterations in the area.

Table 4.5 showing the characteristics of the 3ASTER sensor systems (after Williams, 2009)

Subsystem	Band Number	Spectral Range (µm)	Spatial Resolution (m)	Quantization Levels
VNIR	1	0.52 - 0.60	15	8 bits
	2	0.63 - 0.69		
	3N	0.78 - 0.86		
	3B	0.78 - 0.86		
SWIR	4	1.60 - 1.70	30	8 bits
	5	2.145 - 2.185		
	6	2.185 - 2.225		
	7	2.235 - 2.285		
	8	2.295 - 2.365		
	9	2.360 - 2.430		
TIR	10	8.125 - 8.475	90	12 bits
	11	8.475 - 8.825		
	12	8.925 - 9.257		
	13	10.25 - 10.95		
	14	10.95 - 11.65		

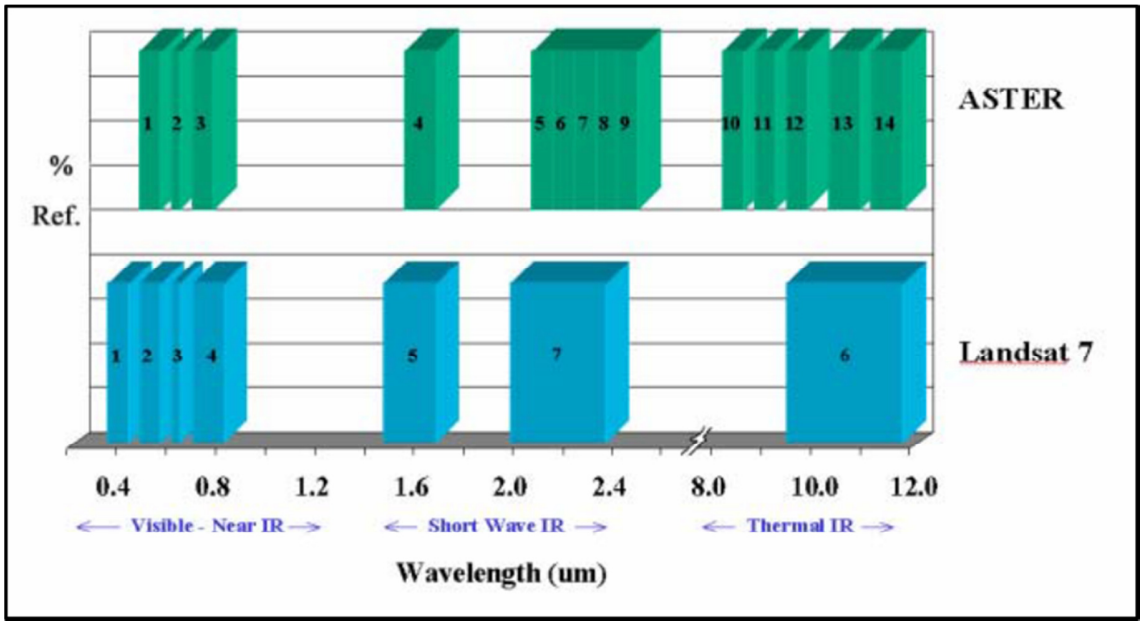

Figure 4.14: Showing the comparison of spectral Bands between ASTER and Landsat (% ref is reflectance percentage) (Williams, 2009).

ASTER_2314_2316 Combination of Bands

The following ASTER image bands of ASTER VNIR Band 1 (0.5560), 2 (0.6610), 3N (0.8070), 4(1.6560), 5 (2.1670), 6 (2.2090), 8 (2.3360) were used for band combinations. The selection of RGB colour combination images using ASTER data were mainly done based on the reflectance spectra of main rock types. The original image bands were shown in an RGB colour composite in order to distinguish the best combination that shows more information of geological features of the study area.

ASTER True colour composite (RGB) 321

The image below is showing the process that was taken in ENVI to do the true colour composite(RGB) 321 on the ASTER _2314_2316 image of the Gorob-Hope area. This particular band combination gives the natural colour and enhances the iron alteration appearance in rocks.

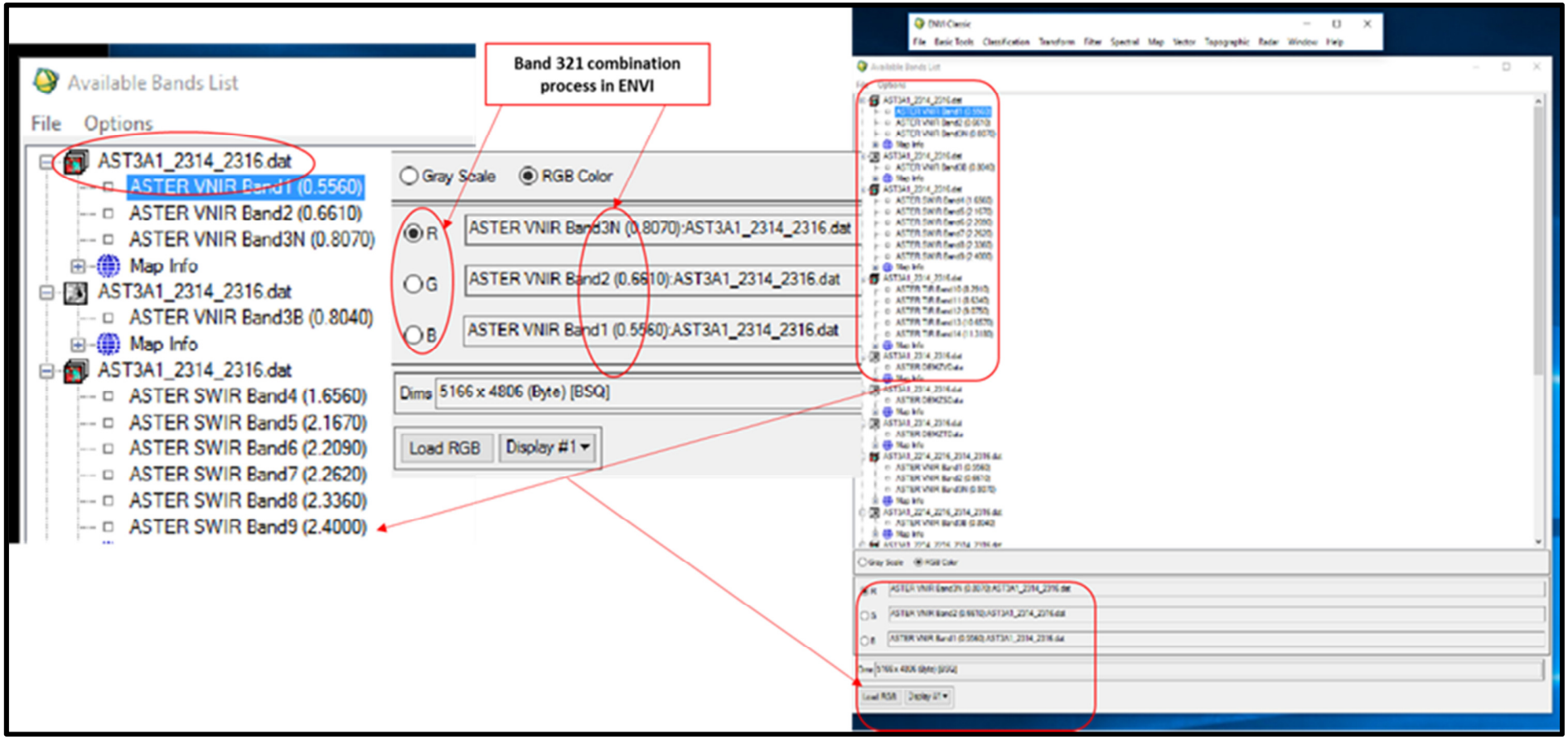

Figure 4.15: A screen shot of the ASTER_2314_2316 (RGB) 321 band combination process

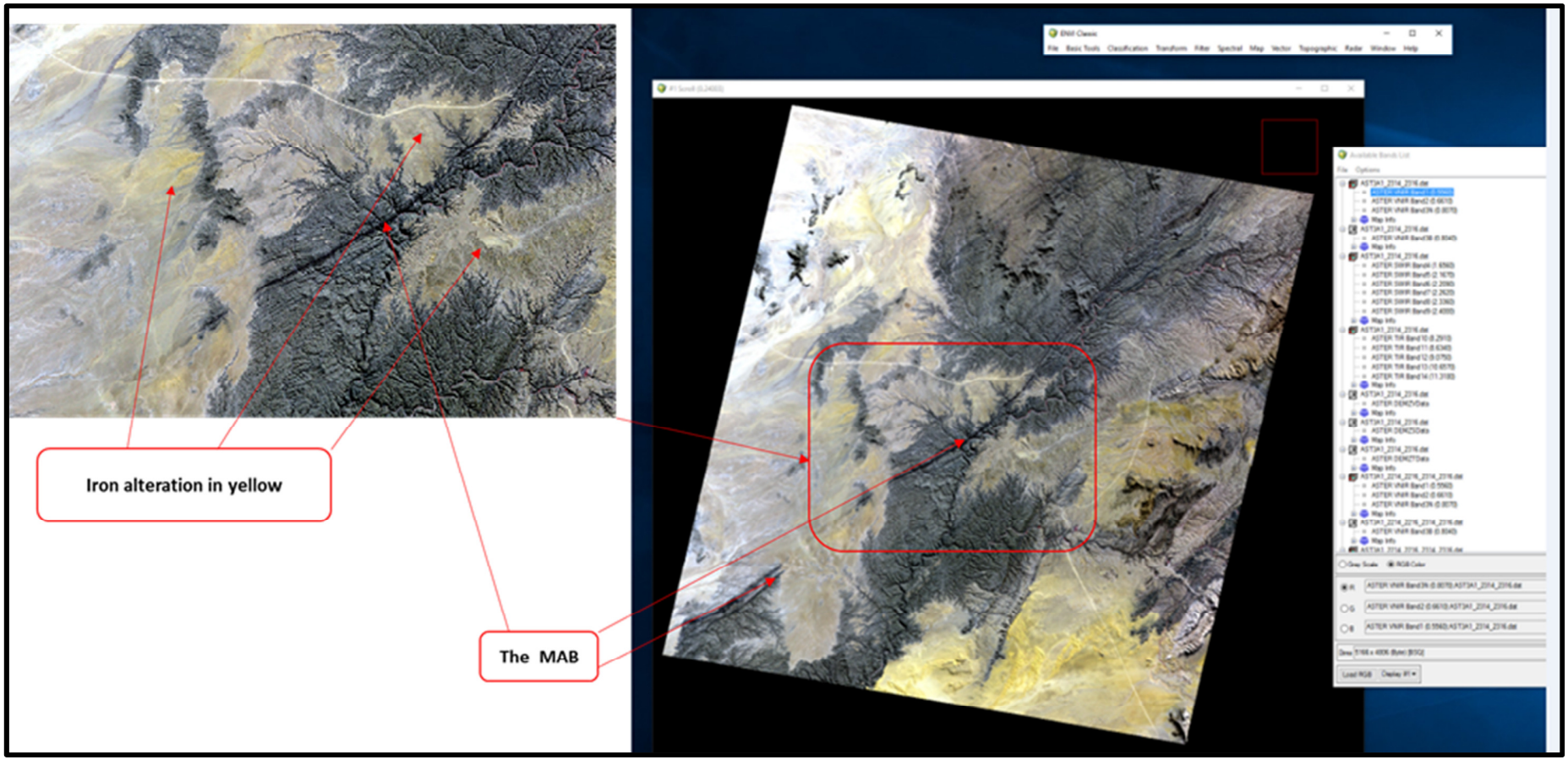

Figure 4.16: A screen shot of ASTER_2314_2316 image showing the process of true colour composite (RGB) 321

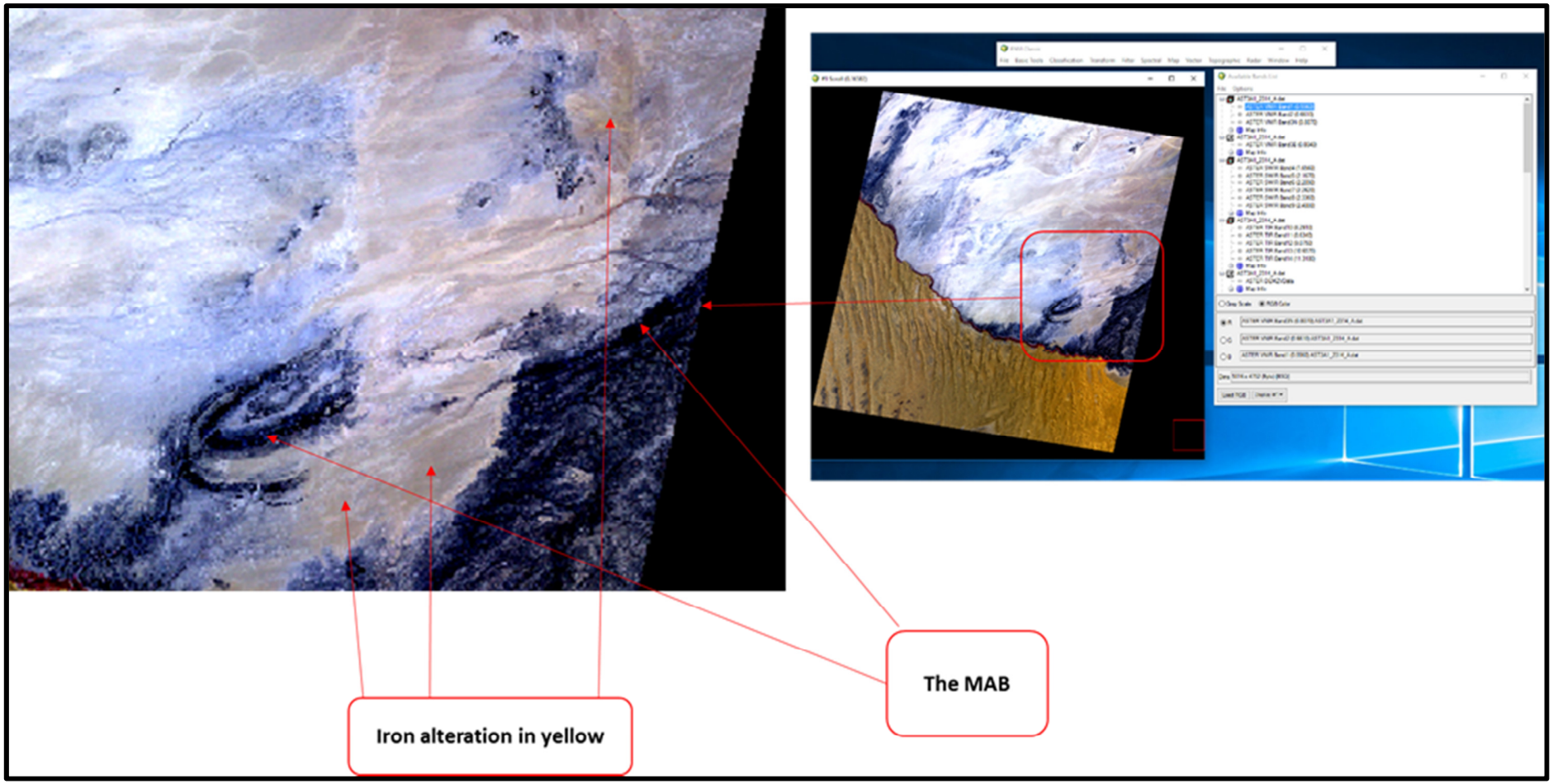

Figure 4.17: A screen shot of ASTER_2314_2316 image showing the process of true colour composite (RGB) 321.

ASTER False colour composite (RGB) 468

The false colour composite 468 in an RGB was exercised in order to enhance the interpretation and visual analysis of hydrothermal alterations of Gorob-Hope area. The false colour composite 468 has the advantage of preserving hydrothermal alterations however it does not give much detail in terms of different types of alterations

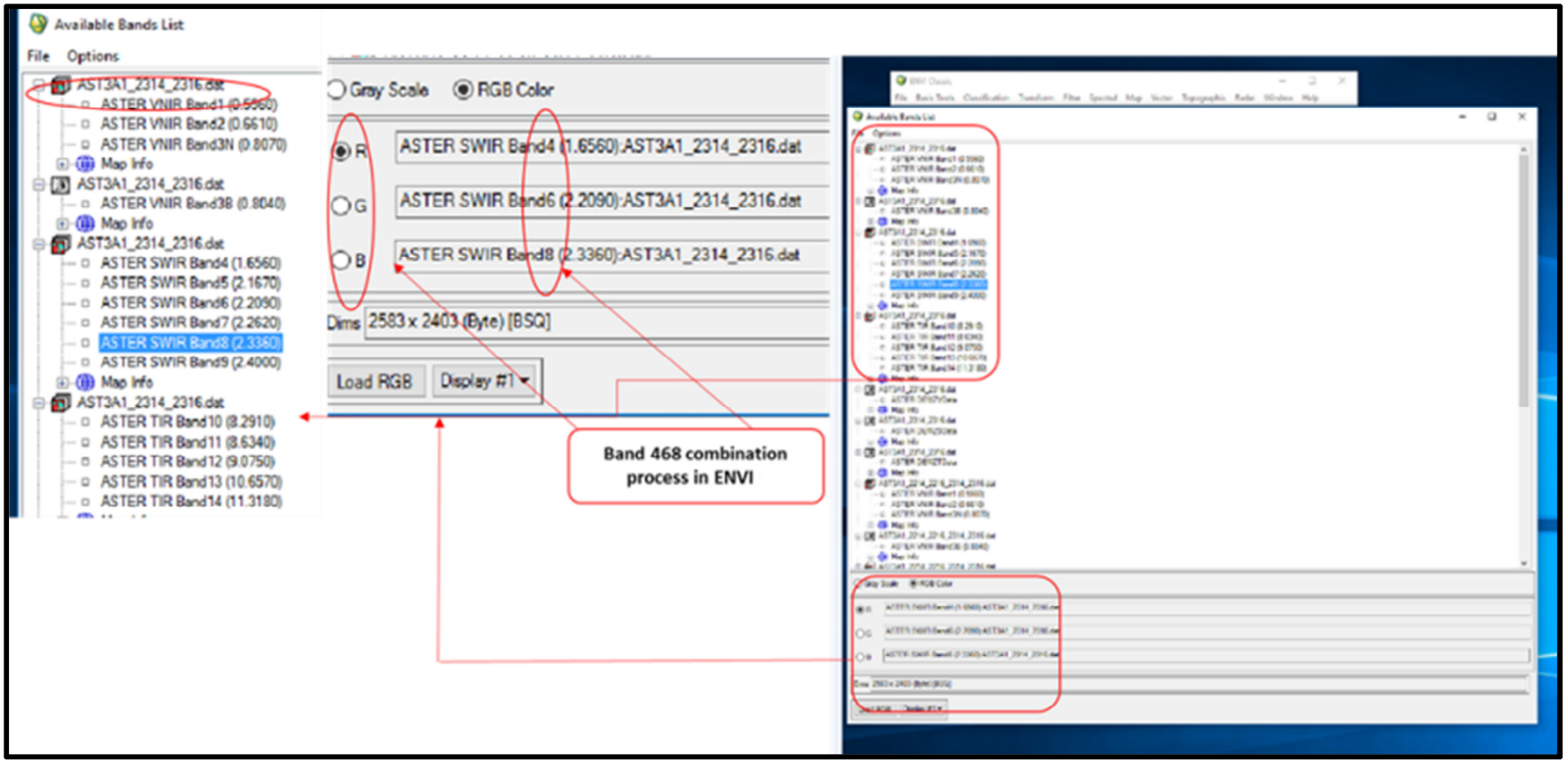

Figure 4.18: A screen shot of the ASTER_2314_2316 (RGB) 468 band combination.

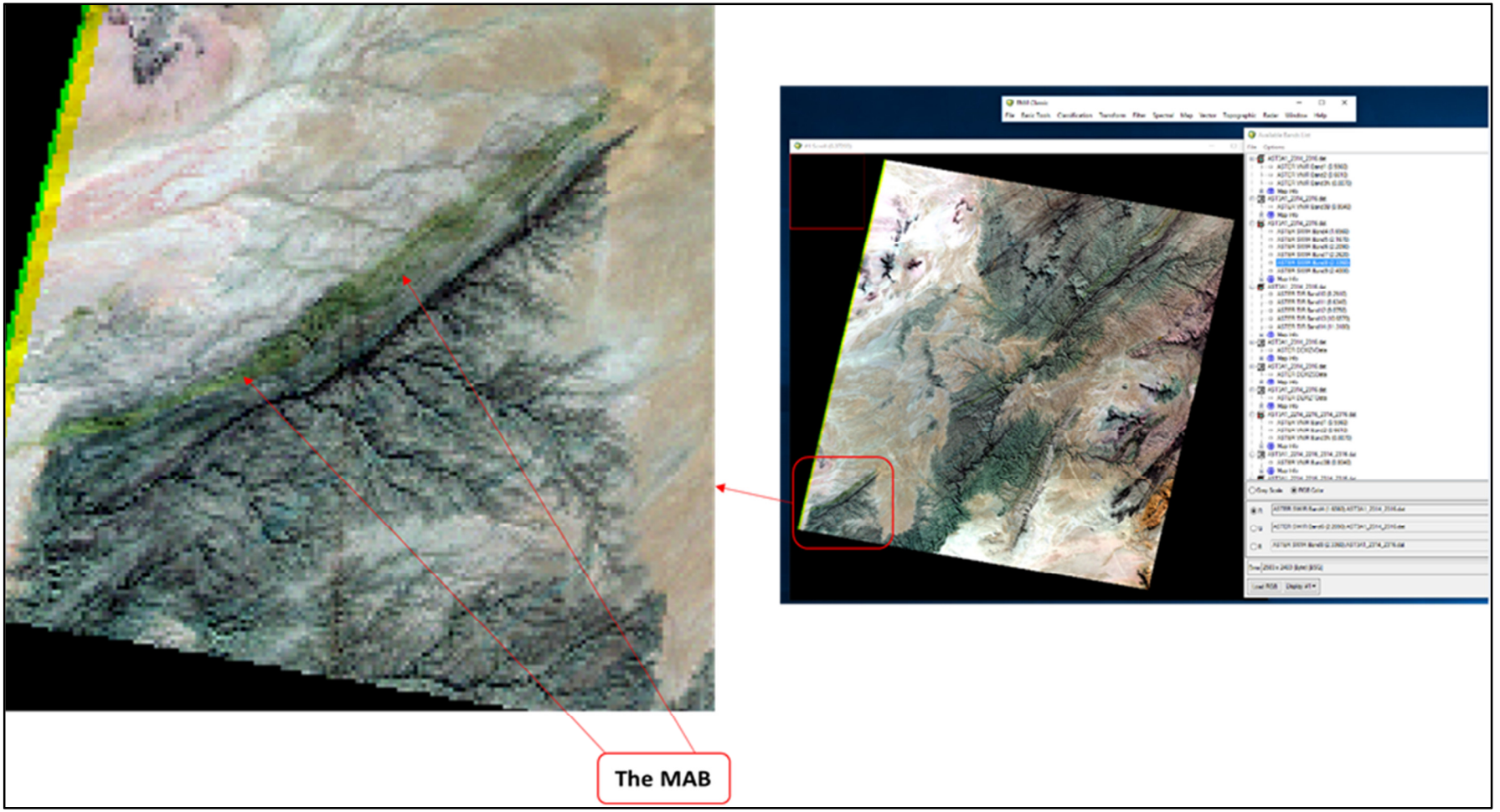

Figure 4.19: A screen shot of ASTER_2314_2316 image showing the process of false colour composite (RGB) 468.

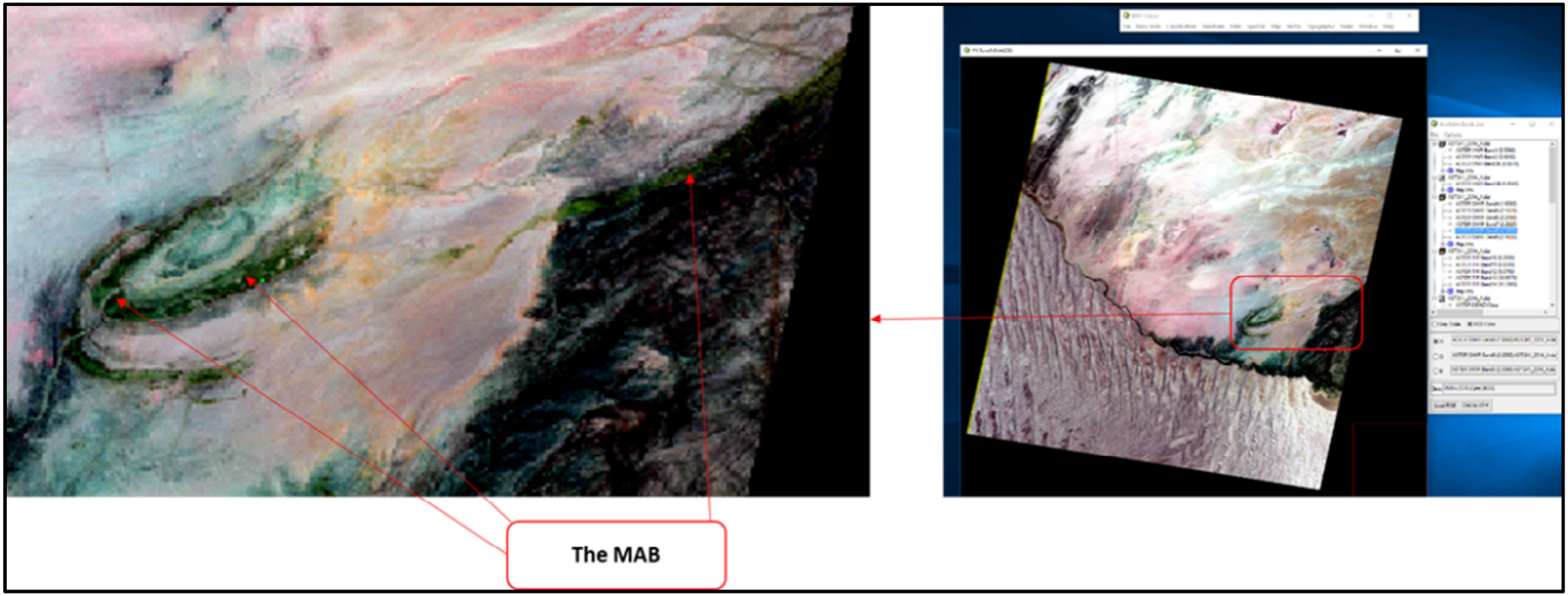

Figure 4.20: A screen shot of ASTER_2314_2316 image showing the process of false colour composite (RGB) 468

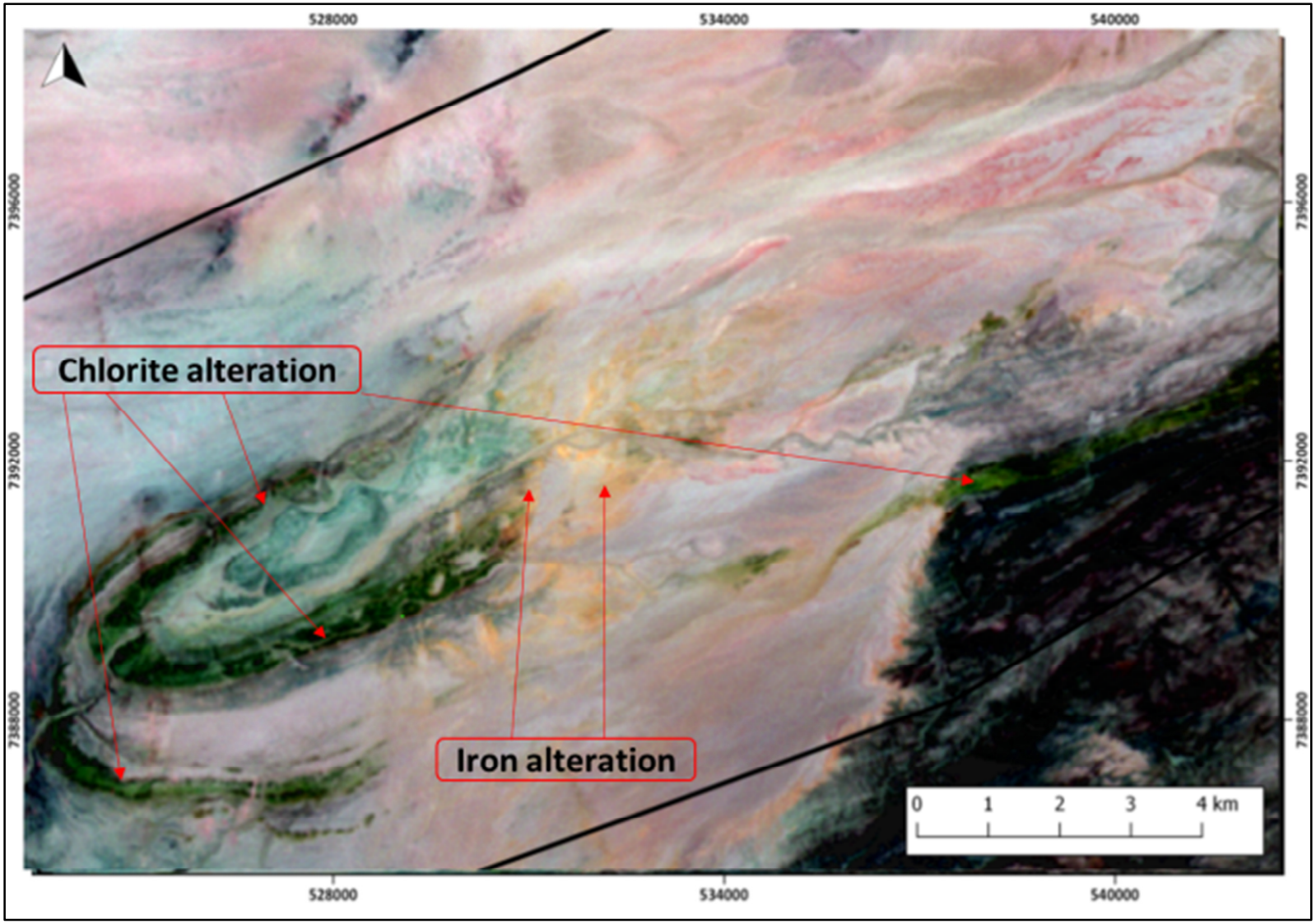

Figure 4.21: A map of Gorob-Hope area that was produced from ASTER_2314_2316 False colour composite (RGB) 468

Spectra signatures

To help identify the presence of Fe, Mg (OH) and Al (OH) in minerals their spectra characteristics can be used (Fig 4.22). For example, the electron transition absorptions at about 0.9 µm vary in wavelength and the intensity of these absorptions is based on the crystal structures and the bonds around the Fe cations. The hydrothermal alteration of minerals is recognized by absorption characteristic structures in the SWIR (Table 4.5). These structures are caused by the vibration of molecules and they are demonstrated as narrow and rather strong absorptions. Illite has absorption minimum around 2.21 µm due to the change in the aluminium content (Clark, 1999).

Hence, the understanding of the features of absorption of minerals in relation to the positions of their wavelengths may be useful in the identification of the minerals of interest. Minerals such as micas and chlorite may be recognised due to of host rocks alteration by hydrothermal fluids which used structures such as faults as migration path ways.

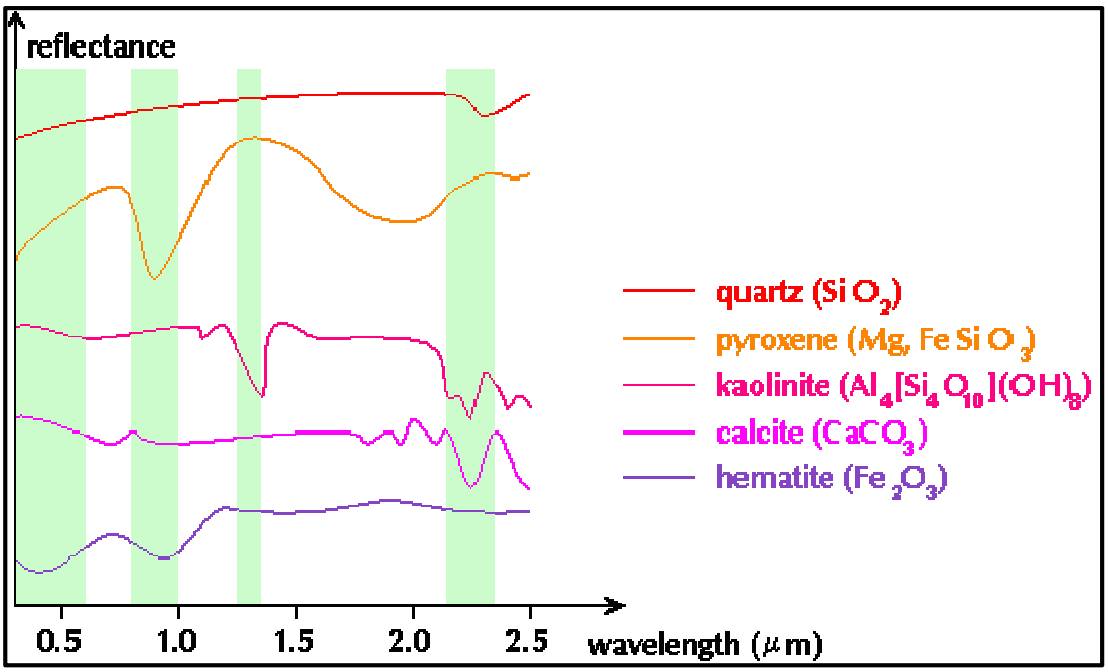

Figure 4.22: A graph showing the characteristic spectra of iron and clay minerals (after Williams, 2009)

Band ratios

Band ratios intensify the spectral dissimilarities between bands and lessen the effects of topography. Division of one spectral band by another assist in producing an image that provides relative band intensities. Band ratios of 4/6, 5/6, and 5/8 were exercised for ASTER_2314_2316 image to get the detailed hydrothermal alteration in the area.

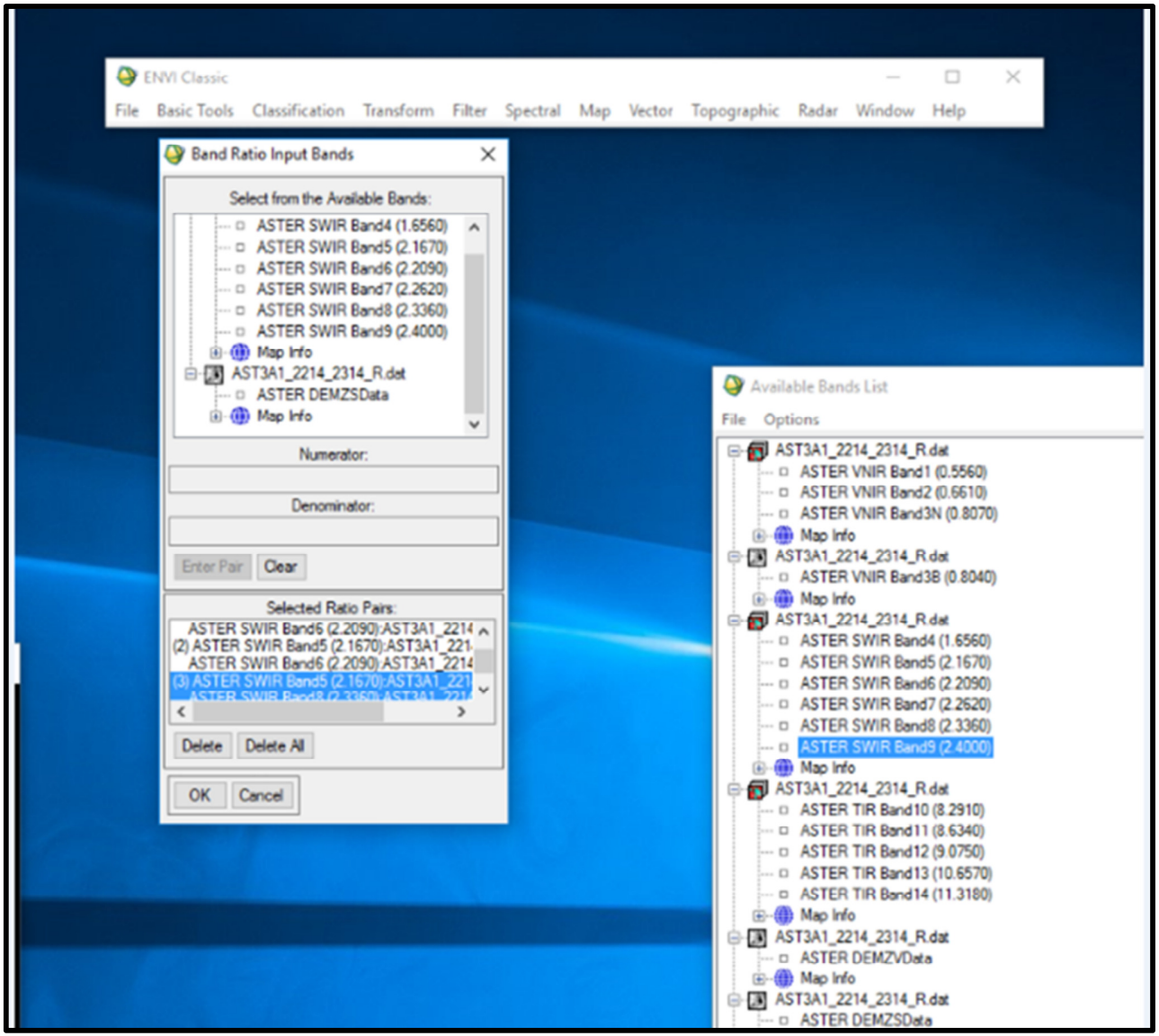

Figure 4.23: A screen shot of the ASTER_2314_2316 showing Band ratios 4/6, 5/6, and 5/8 process

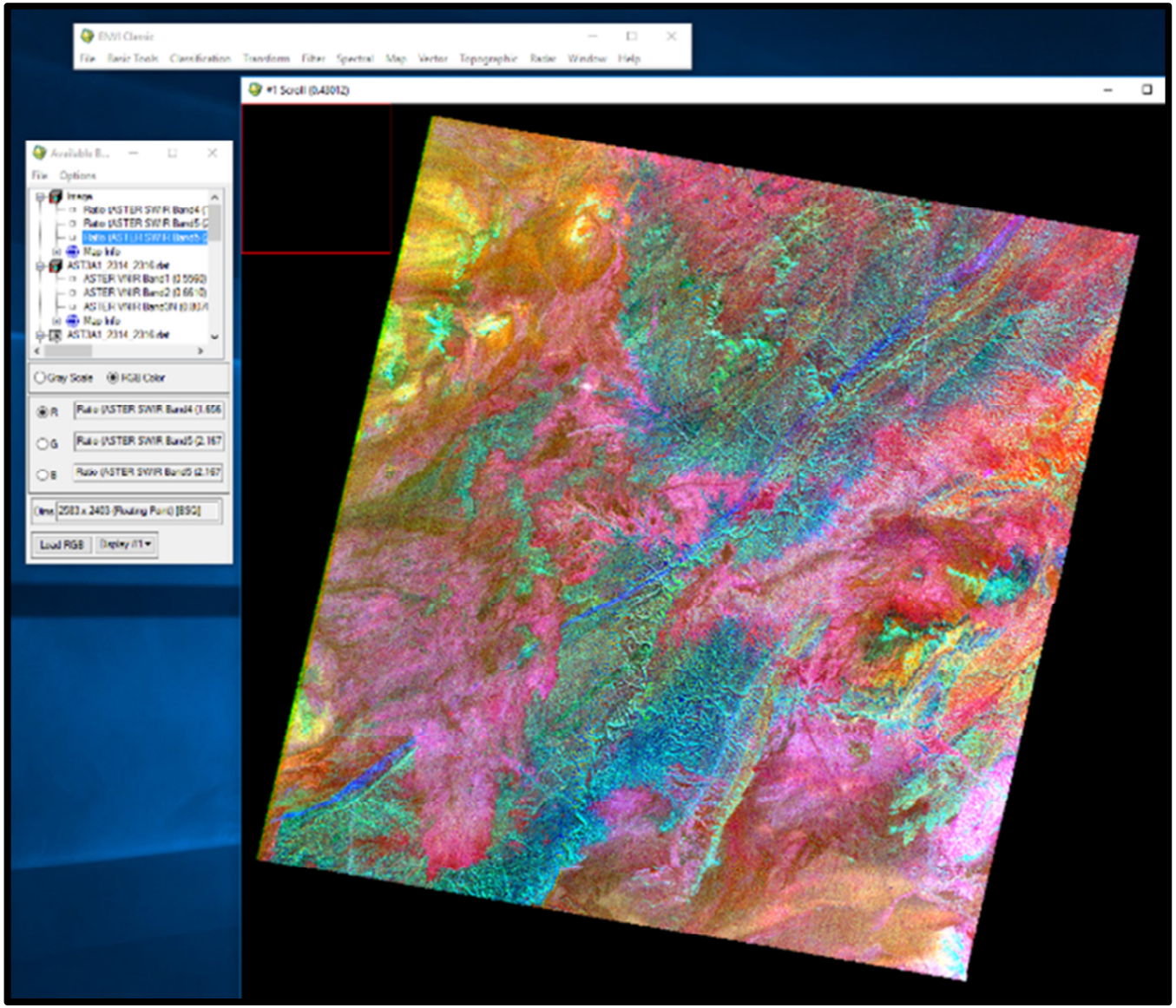

Figure 4.24: A screen shot of the ASTER_2314_2316 showing the process of band ratios of 4/6, 5/6, and 5/8

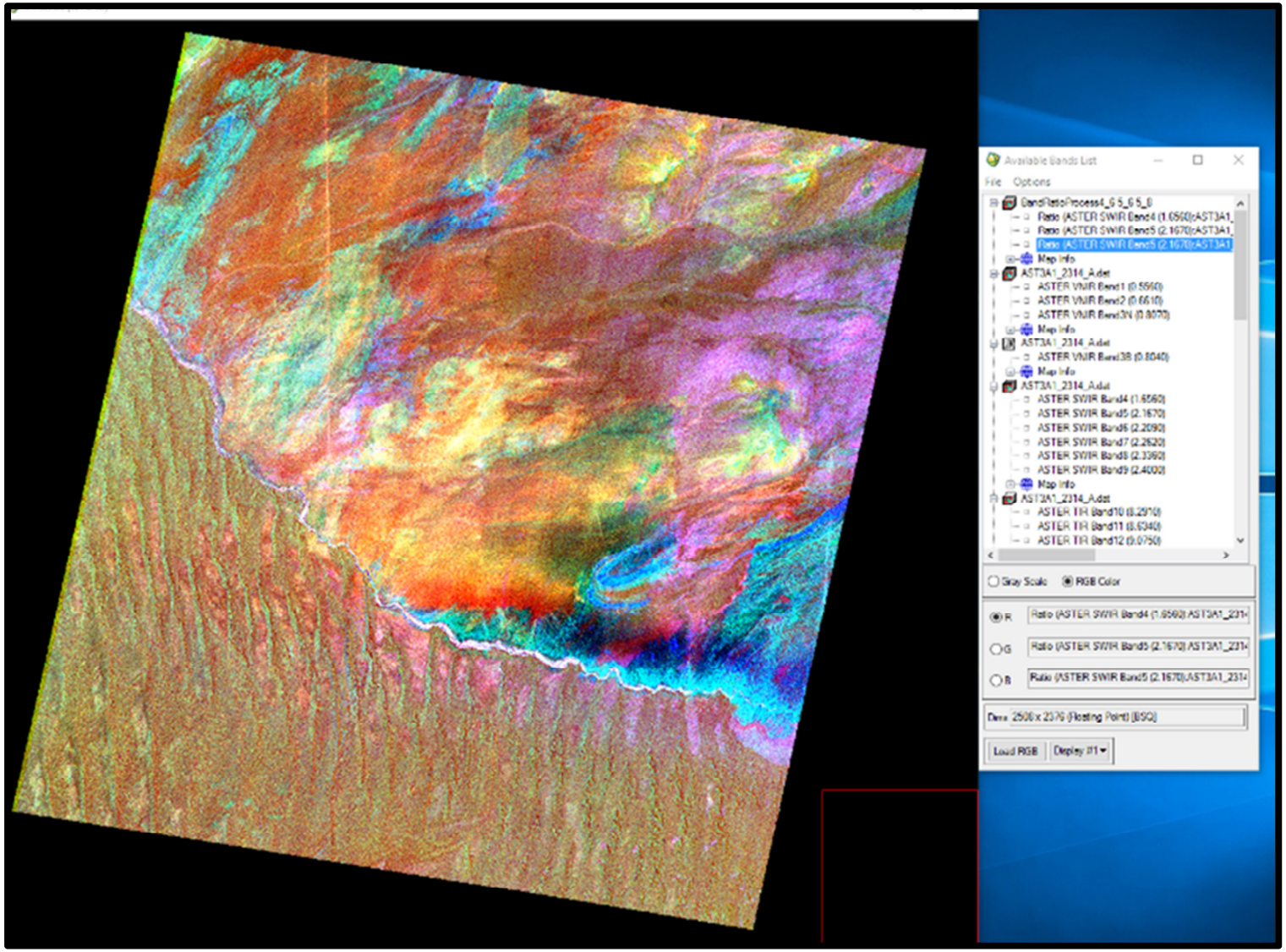

Figure 4.25: showing the output of ASTER band ratio of 4/6, 5/6, and 5/8

Hydrothermally altered units associated with the VMS deposits of the Gorob-Hope area were identified using the ASTER image below (Fig4.26). The Fe, Mg (OH)-bearing mineral units are found in the regions where the magnetite-quartzite bodies are found, whereas Al (OH)-bearing minerals are mostly found in the eroded part of the area.

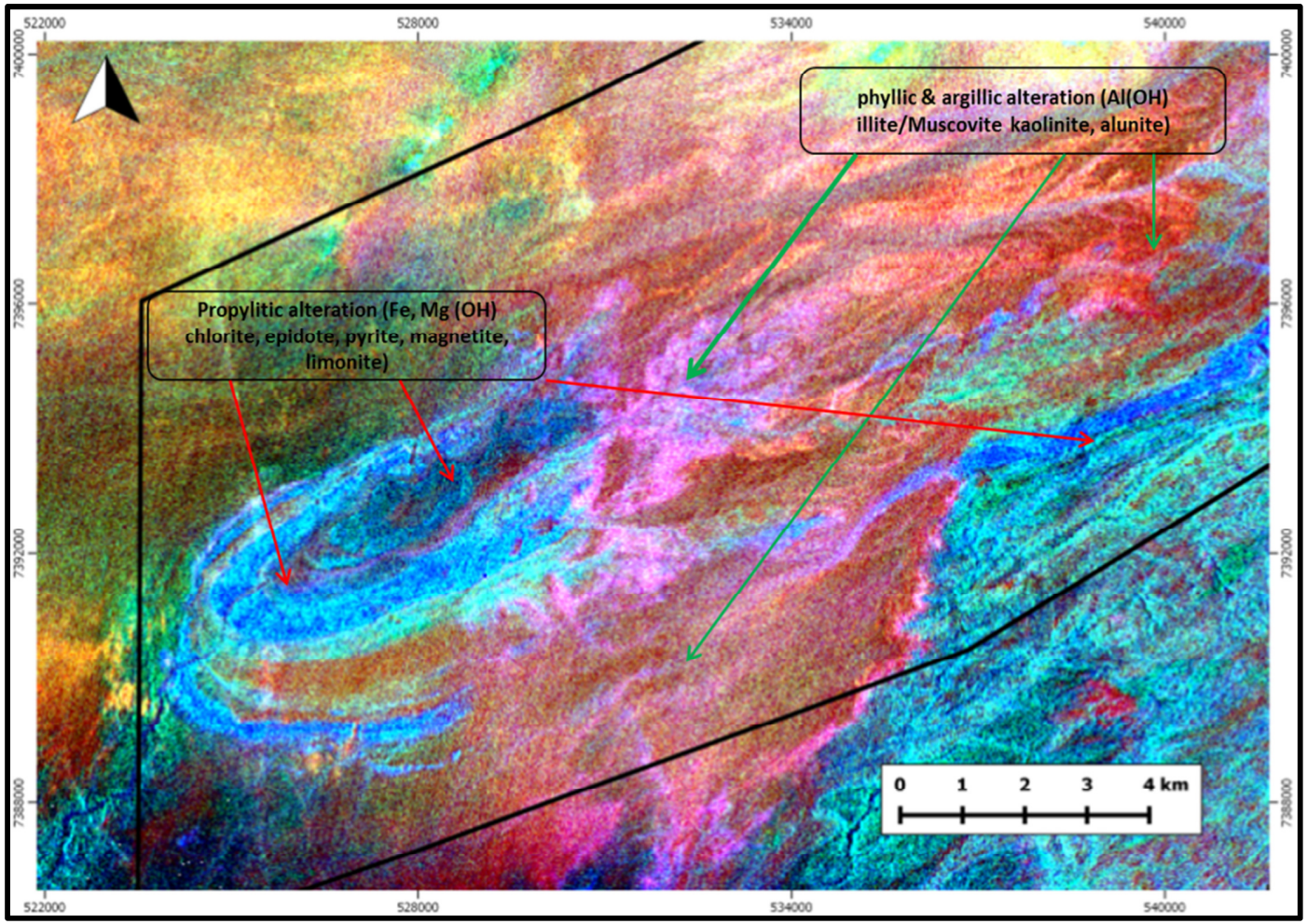

Figure 4.26: A map of Gorob-Hope area that was produced from band ratios of 4/6, 5/6, and 5/8

Chapter 5

5. Data interpretation

5.1. Geological Data

Lithologies

A lithological map was produced from historic geological maps (appendices) showing mainly lithologies that were integrated in ArcGIS (Fig 5.1). As the labels show, the area has well exposed rocks. The lithology in a dark-green colour is amphibolite. It is a coarse-grained metamorphic outcrop that is constitute of mainly green and brown amphibole minerals such as hornblende and riebeckite. The amphiboles are generally members of the hornblende group. It also comprises minor amounts of biotite, epidote, garnet as well as quartz and magnetite. Amphibolite is a rock that is formed at the boundaries of converging plates where regional metamorphism is cause by pressure and heat. Metamorphism of mafic igneous rocks such as basalts and gabbros, or metamorphism of clay-rich sedimentary rocks such as marl or greywacke produces the amphibolite rocks. Elongation and flattening of the mineral grains produced a schistose texture.

Next to the amphibolite outcrop are quartzite and basalt rock units in pink and red respectively. Quartzites are non-foliated metamorphic rocks constitute of almost entirely quartz. They form when quartz-rich sandstones are transformed by pressure, heat, and chemical activities of metamorphism. Due to these conditions sand grains and silica cement that binds them together are recrystallised

Basalts are dark in colour, fine-grained igneous rocks consisting generally of plagioclase and pyroxene minerals. It most normally forms as an extrusive rock, such as a lava flow, but can also form in small intrusive bodies, such as thin sill or dike of igneous rocks. Basalts are formed at divergent plate boundaries on the mid-ocean ridge systems. Here convection currents bring hot rocks from deep in the mantle. This hot rock melts as the divergent boundaries pull apart and the molten rock erupts onto the seafloor, producing basalts.

The quartzite bodies are consistently found along with the basalt bodies. Even though the basalt bodies appear to be bigger in size then the quartzite bodies, they all appear parallel to each other and elongated in one direction.

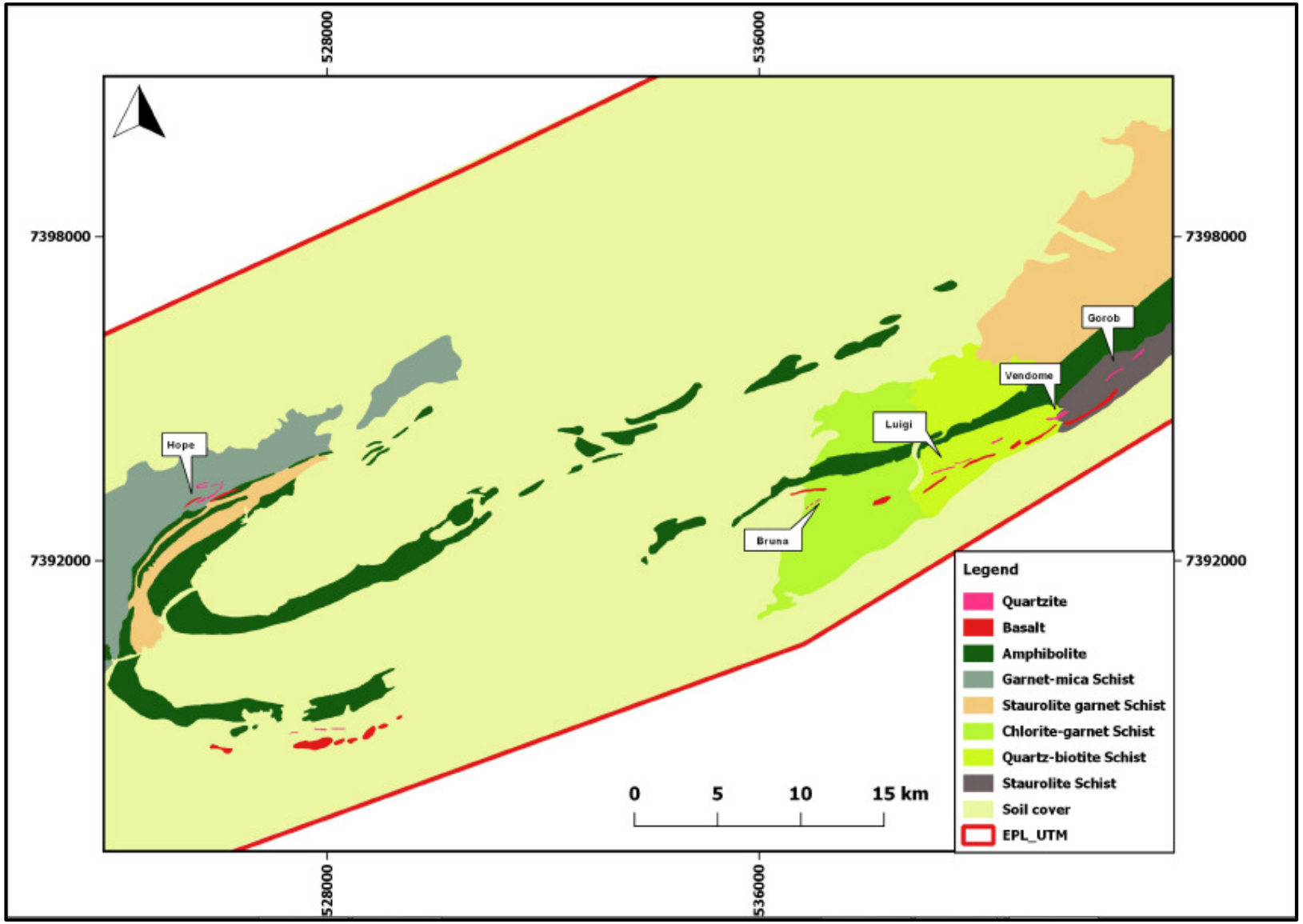

Figure 5.1: A lithological map of Gorob-Hope produced from historic geological data (Table 4.1)

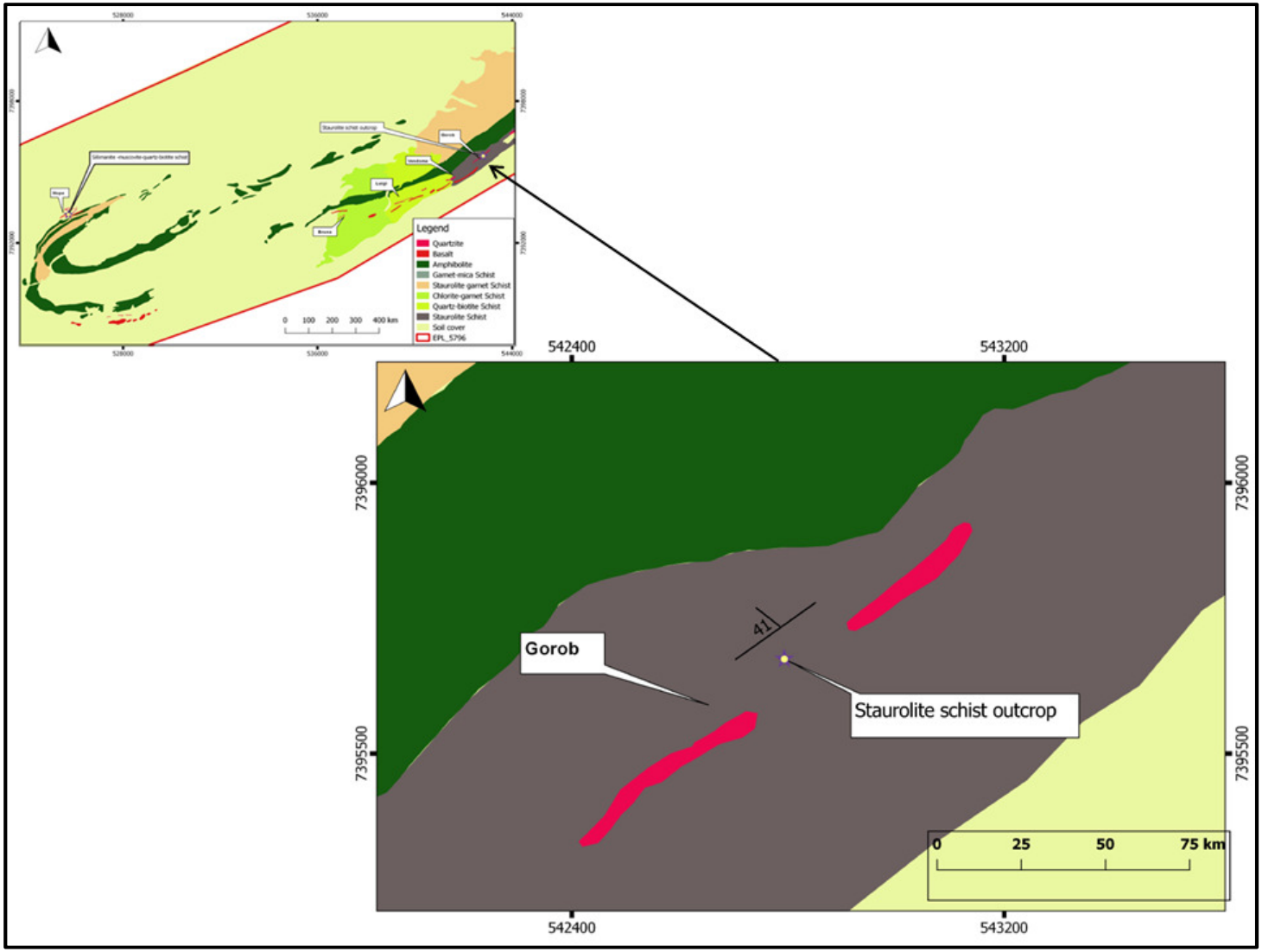

Figure 5.2: A lithological map of the Gorob-hope area produced from historical data (Table 4.1) showing the dip and strike of the staurolite schist outcrop that was found during the traverse (Fig 4.2).

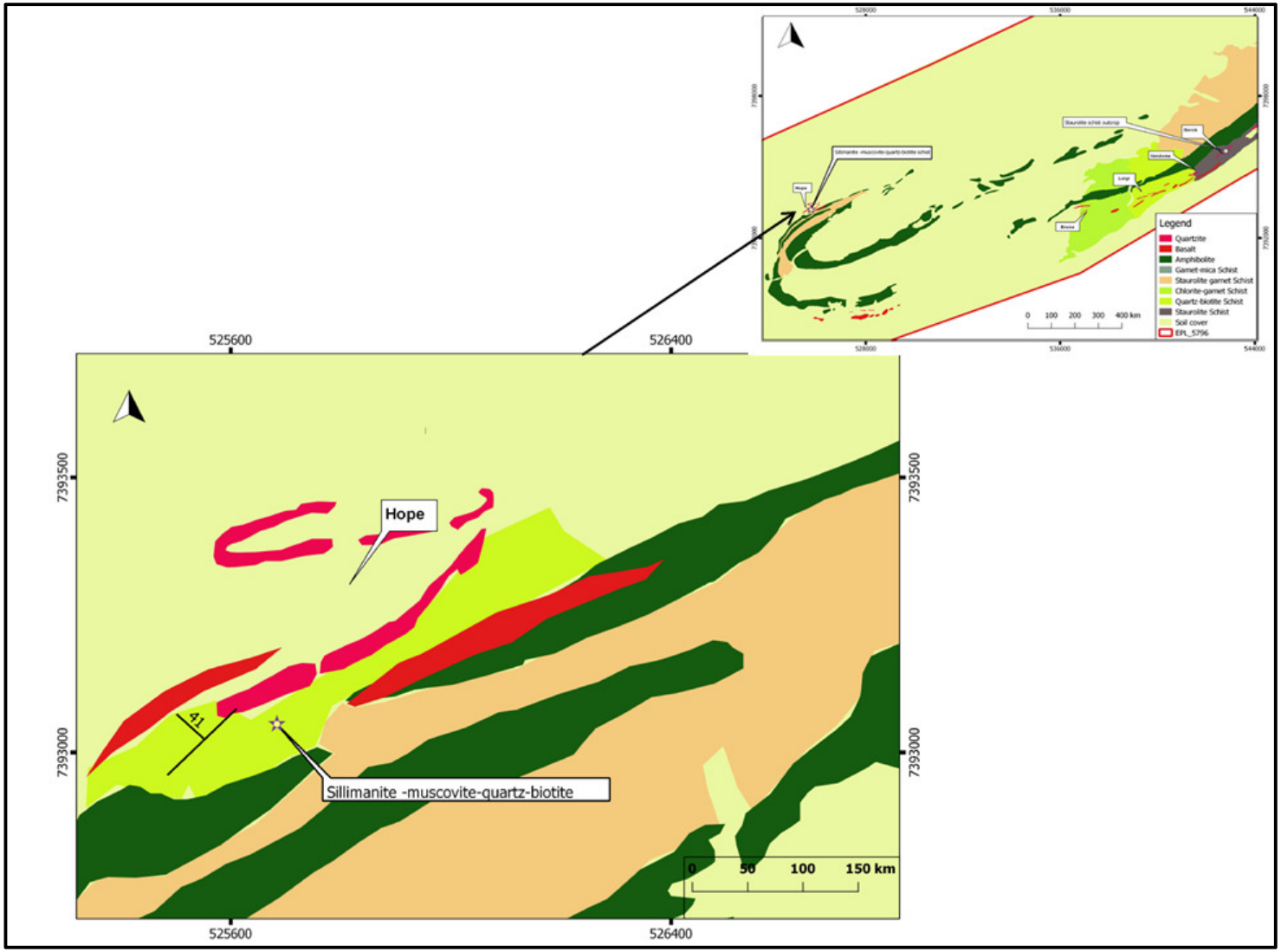

Figure 5.3: A lithological map of the Gorob-Hope produced from historic geological data (Table 4.1) showing the dip and strike of the sillimanite-muscovite-quartz-biotite schist outcrop that was found during the traverse (Fig 4.3)

5.2 Remote sensing Data

Structures

A structural map was produced from a Landsat ETM+ image (appendices) showing mainly structures that were enhanced after the image was processed (Fig 5.4). The area consists of structures such as faults as well as folds that form a synformal feature.

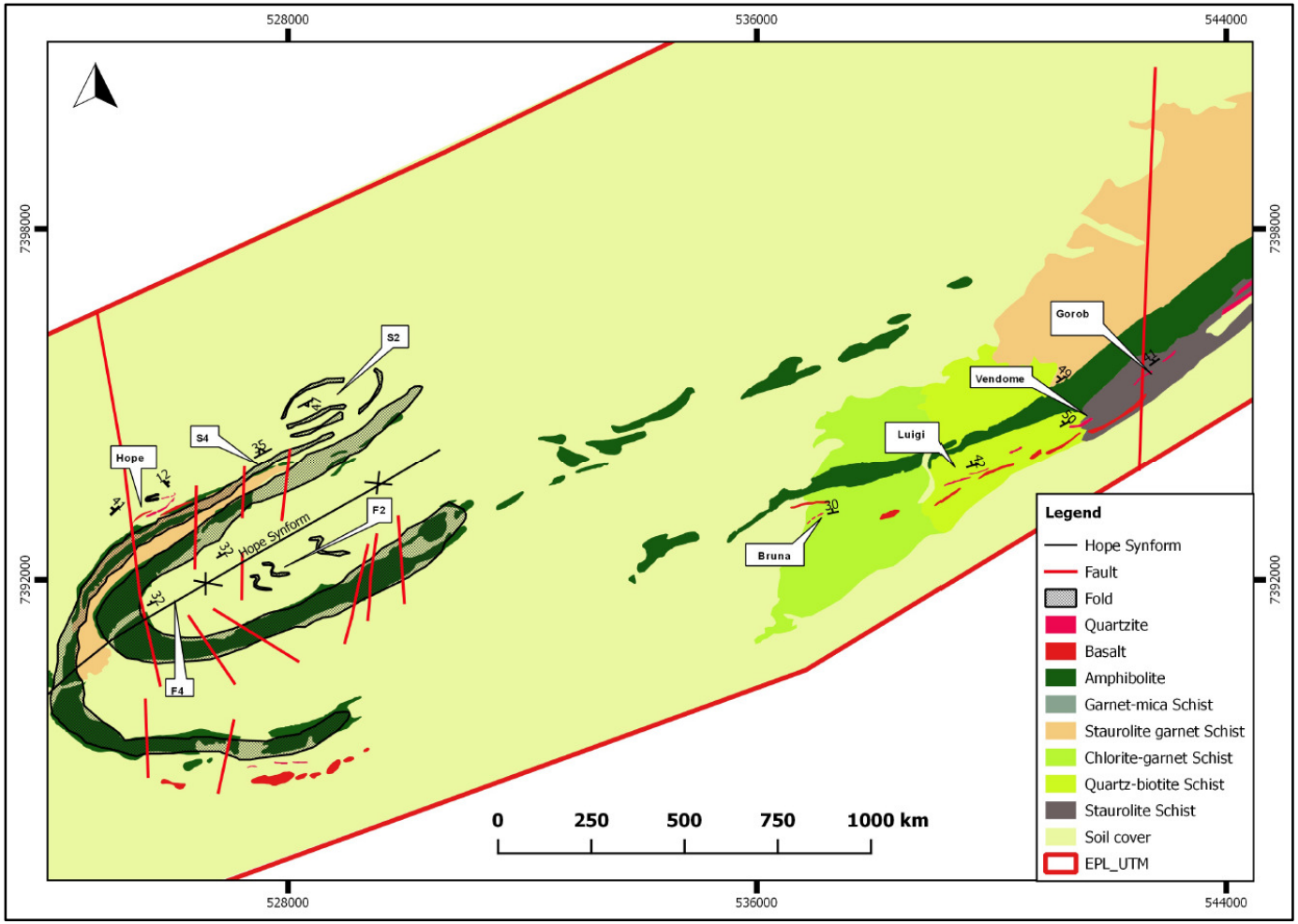

Figure 5.4: A Structural map of Gorob-Hope produced from Landsat 7 ETM+ image, Historic geological maps and field visit structural measurements.

Alterations

The ASTER_2314_2316 image was processed to enhance hydrothermal alteration zones in the area. Band 4 of the ASTER image covers the spectral region where hydrothermal alteration minerals reflect strongly. Band 5 and 6 are major absorption by Al (OH)-bearing minerals such as kaolinite, montmorillonite as well as illite. Band 8 is the major absorption by Fe (OH)-bearing minerals such as jarosite. Band 8 and 9 are major absorptions by Mg (OH)-bearing minerals such as chlorite, talc and carbonate minerals such as calcite and dolomite.

Band ratio of 4/6 enhances argillic alteration which is a hydrothermal alteration of wall rock which introduces clay minerals including kaolinite, smectite and illite. The process normally happens at low temperature and may arise in atmospheric conditions. During argillic alterations kaolinite replaces plagioclase and montmorillonite replaces amphibole and plagioclase.

Band ratios 5/6 enhances phyllic alteration which is a hydrothermal alteration zone in a permeable rock that has been affected by circulation of hydrothermal fluids. It is categorized by the assemblage of quartz+sericite+pyrite which happens at high temperatures and moderately acidic (low PH) situations. Band ratios 5/8 enhances propylitic alteration which is initiated by iron and magnesium bearing hydrothermal fluids altering biotite or amphibole within the rock groundmass, typically resulting in epidote-chlorite-albite alteration.

The propylitic alterations which are the Fe-Mg (OH) bearing mineral units are distributed close to the magnetite quartzite and the basalts, whereas the argillic - phyllic alterations which are the Al (OH) bearing mineral units are spread in the central parts of the study area where the area is mostly eroded (Fig 5.5).

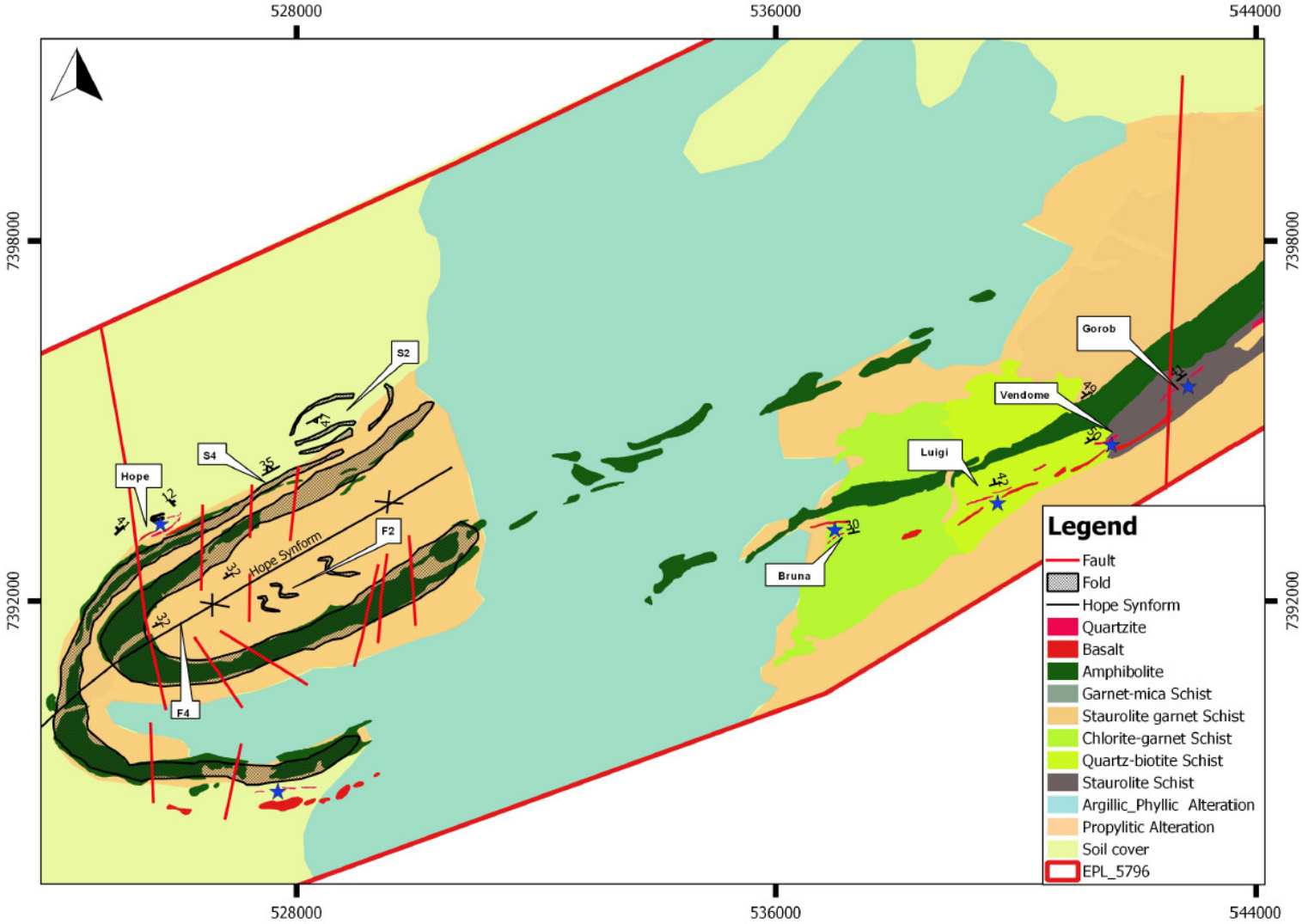

Figure 5.5: A geological map of Gorob-Hope area showing hydrothermal alterations that was produced from ASTER_2314_2316 image.

Chapter 6

6. Discussion and Conclusion

6.1 Discussion

From the historic geological maps, Landsat 7 and ASTER imagery data, features such as lithological units, lineaments and hydrothermal alterations were extracted. The MAB studied in literature could be extracted clearly from both the Landsat 7 and ASTER imagery. The Landsat with (RGB) 457 and 751 used for geological features extraction was helpful since the band combination has an advantage of differentiating different rock types and structures respectively. Structures such as faults, folds and the syncline were clearly seen in the Landsat with (RGB) 751. The ASTER with (RGB) 468 and band ratio (4/6, 5/6, 5/8) was helpful in distinguishing hydrothermal alteration The MAB had a blueish colour; Kuiseb schist had a greyish colour and sand had a yellowish colour.

The geological map (Fig.6.1) is a product of historic geological and remote sensing data integration. As the map shows, the geology of the study area mainly comprises mafic units, such as amphibolites and metabasalts which are originally basalts that have been highly deformed and metamorphosed up to amphibolites facies. The area also contains quartzites which appear to be associated with the volcanic units.

These units are mainly located at the south east, where they appear to be folded, and south west sides of the study area. There are also Kuiseb schists, such as biotite-quartz-garnet schist, and Chlorite-biotite-amphibole schist. These schists were originally mudstones which have been metamorphosed into greenschist to amphibolite facies. It is noted that the magnetite quartzites appear parallel to the basalts, and are generally associated with the mineralisation.

The presence of chlorite biotite-amphibole schist indicates that the schist must have been formed through intense hydrothermal alteration of the mudstones, as well as due to a possibility of retrograde metamorphism. The association of quartz in the mafic volcanic units is due to silica crystallization along foliations during deformation (Klemd et al., 1989). The magnetite quartzites of the area are believed to be of the Auas Formation. This means that the quartzites are older than the amphibolite and basalts followed by the schist being the youngest in the area.

The structures that are found within the area are faults and folds, mainly on the south east side and towards the north west of the EPL. Another notable structure that is found in the area is a syncline that is found on the south east side of the study area.

The historic geological results and the remote sensing images indicate the presence of amphibolites, basalts, and quartzites as well as the Kuiseb schist within Gorob-Hope area. All these units have undergone at least three deformational episodes. The first deformation (F_2) is a regional metamorphic event that is characterised by tight to isoclinal, moderately inclined, gently plunging folds with regional foliation S_2 axial-planar, transposition of bedding parallel to S_2 and boudinage. The second deformation (F_4) is also a regional metamorphic event that is characterised by close, moderately inclined gently

plunging folds (Hope synform) with weak axial-planar foliation. The third deformation episode (Fş) is characterised by local cross-folding, (affected the northern limb of the synform), faulting, intrusion of pegmatites, quartz veins and granite veins parallel to axes. The presence of hydrothermal alteration and a peak metamorphism at amphibolite facies and a later retrograde metamorphism is indicated by the presence of chlorite. The remote sensing data also pinpoints structural features such as faults and folds that are found on the south eastern and south western sides of the area, respectively.

The massive nature of the Gorob-hope sulphides are attributed to post-tectonic renucleation and mobilisation related to the intrusion of the nearby Donkerhoek granitoids. Sulphides are more finely disseminated within the magnetite-quartzites, but in zones of highly remobilised magnetite-quartzite there is a corresponding increase in blebby and more massive sulphides.

Gorob-Hope high ductility contrasts between the magnetite quartzites and the schists have resulted in extremely complex deformation styles. Two deformation phases are responsible for the configuration of the Gorob-hope area. The second deformation phase of the Damaran orogeny folded the Gorob-Hope magnetite-quartzite into a near isoclinal synform shape. The subsequent third phase of deformation, refolded the synform.

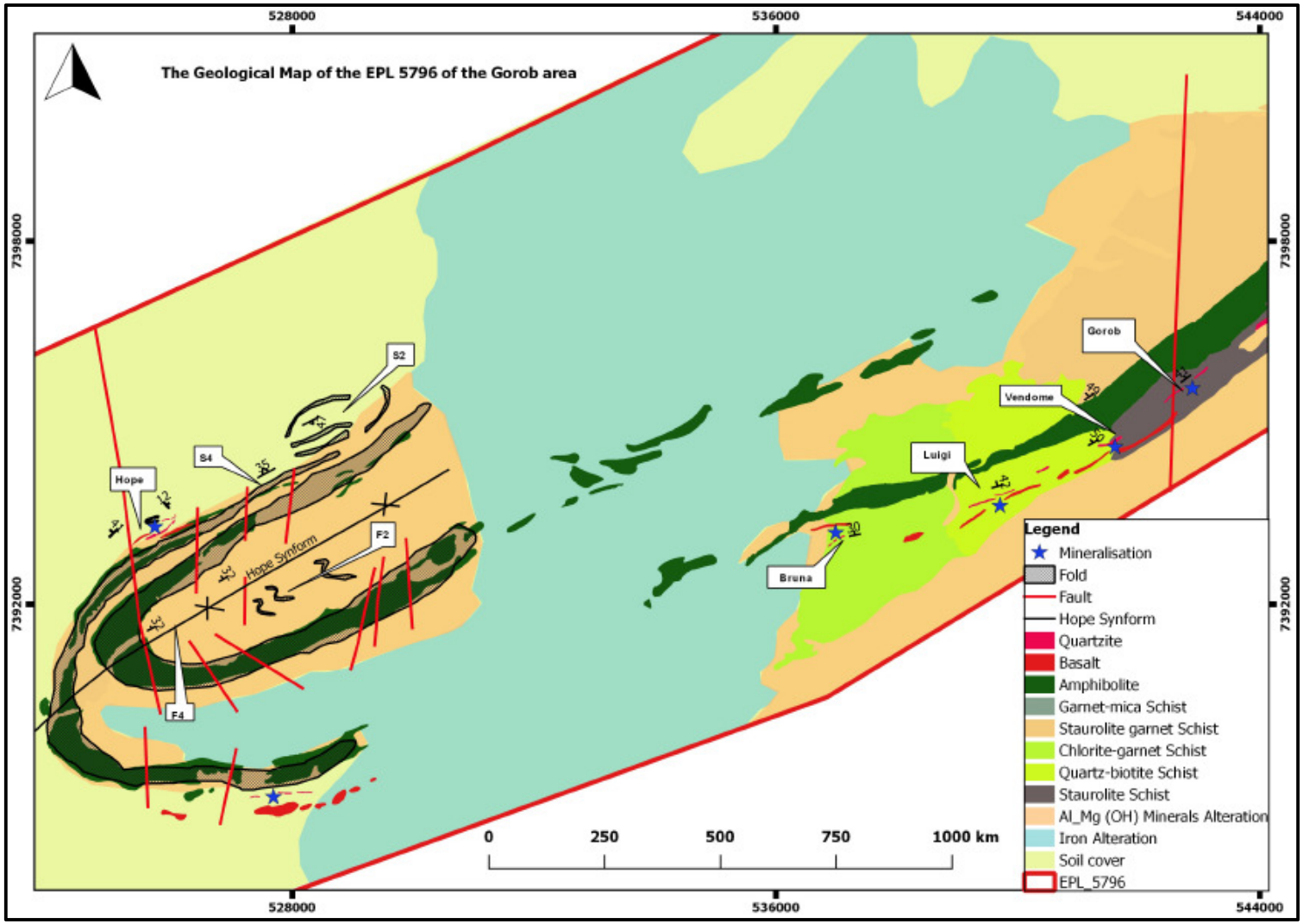

Figure 6.1: A Geological map of Gorob-Hope area with main lithologies, structures alterations and the mineralisation based on historic geological maps and remote sensing data

6.2 Conclusion

Geological mapping by means of remote sensing images is vital and helpful for pre-field geological mapping of a certain area, particularly in areas that are not easily reachable. The accurate enhancement of remote sensing images results in distinctive surface mattes and may make the field mapping planning easier since it will be clear of where to give full attention before the commencement of the field mapping exercise. Drawing of traverse lines as well as recoding of point locations of where variations are found in the images is possible before the field mapping exercise.

The magnetite-quartzite bodies of Gorob-Hope area appear together, consistent and parallel to the mafic volcanic rock units. Hence, there is a spatial relationship between these units. The mineralisation of Gorob-Hope area appears within or around the magnetite-quartzite, therefore these units are associated with the mineralisation in the area.

The mineralisation of Gorob-Hope area occurs within folded magnetite quartzites, therefore these structures are related to the deposits and can be possible guides to ore. The identification and delineation of hydrothermal alteration zones with the use of band ratios of the ASTER image in the study area was possible. The alteration is widely distributed around the ore deposits and could be recognised from Remote Sensing images.

In conclusion, the ore mineralization around Gorob-Hope area is associated with the MAB since it is only found around and/or within the MAB rock types. This is a VMS type deposit where the ore mineralization is brought up to the surface by hydrothermal fluids through the syn-sedimentary faults and is deposited on the surface, hence the ore mineralization in the Gorob-Hope area is structurally controlled. The application of remote sensing data sets and GIS in this research was successful because it aided in answering the questions of the study.

6.3 Recommendations

The application of Remote sensing images and GIS applications to understand how ore deposits are related to the Matchless Amphibole Belt using historic geological maps and multispectral images to identify the features of interest is a most convenient, cheap and time effective exploration technique. For better results, all the data from all exploration techniques should be available in order to capture all the possible existing features.

References

Abrams, M.J., 1984. Landsat 4, Thematic Mapper and Thematic Mapper Simulator data for a Porphyry Copper Deposit. *Photogrammetric Engineering and Remote Sensing,* 50, 1171- 1173.

Aiken, C. L. V., Balde, M., Xu X., Abdel-Salam M., Fuente M. and Mena M. 1997. Integrated studies of Mexico with gravity, magnetic, and GIS database. *The Leading Edge.* Dec. p. 1779-1785.

Akcay, M. and Charles, J., 2004. The environmental impact of mining in the Pontides, Turkey: Reconnaissance sampling and GIS-based analysis. *Geochemistry: Exploration, Environment, Analysis.* v. 4, p. 317-328.

Aly, M. H., Giardino, J. R. and Klein, A. G., 2005. Suitability Assessment for New Minia City, Egypt: A GIS Approach to Engineering Geology. *Environmental & Engineering Geoscience.* v. XI, p. 259-269.

Amera, S. A., 2007. Spectral remote sensing of hydrothermal alteration associated with volcanogenic massive sulphide deposits, Gorob-Hope area, Namibia. MSc thesis (unpbl.), *International Institute for Geo-information Science and Earth Observation*. Enschede, The Netherlands.

Adamson, R. G and Teichmann, R. F. H., 1986. The Matchless cupreous pyrite deposits, South West Africa/Namibia, 1755-1760. In: Anhaeusser, C. R. and Maske, S. (eds) *mineral deposits of Southern Africa*, 2, Geol. soc. s. Afr, 2335pp.

Belt, K. and Stanely, T. Paxton 2005. GIS as an Aid to Visualizing and Mapping Geology and Rock Properties in Regions of Subtle Topography. GSA Bulletin. v. 117, p. 149-160.

Breitkopf, J. H. and Maiden, K. J., 1988. Tectonic settings of the Matchless belt pyritic copper deposits, Namibia. *Economic Geology*, 83, 710-723.

Brew, G., Barazangi, M., Sawa, f T. and Al-Maleh, K., 2000. Tectonic Map and Geologic Evolution of Syria: The Role of GIS. *The Leading Edge*. Feb. p. 176-182.

Clark, R. N., 1999. Spectroscopy of Rocks and Minerals, and Principles of Spectroscopy, in Manual of Remote Sensing, Volume 3, *Remote Sensing for the Earth Sciences*, (A.N. Rencz, ed.) John Wiley and Sons, New York, p 3 - 58.

Cook N.J., Klemd, R. and Okrusch M., 1994. Sulphide mineralogy, Metamorphism and deformation in the Matchless massive sulphide deposit, Namibia. Mineral Deposits 29, 1-15.

Comline, S. R., 1986. Final Report for a prospecting grant M46/3/226, situated in the Namib-Naukluft Park, Swakopmund District, Namibia, p 3 – 30.

Coulter, D. W., 2006. Remote Sensing Analysis of Alteration Mineralogy Associated with Natural Acid Drainage in the Grizzly Peak Caldera, Sawatch Range, Colorado, PhD. Thesis, *Colorado School of Mines*, Colorado, USA.

Cowey, A., 1981. A report on underground exploration at the Hope prospect shaft, Grant M46/3/226, Namib-Naukluft Park, Namibia, p 6 – 25.

Crippen, R.E. and Blom, R.G., 2001. Unveiling the lithology of vegetated terrains in remotely sensed imagery. *Photogrammetric Engineering and Remote Sensing*, 67(8), 935-946.

Dill, H. G., Pollmann, H., Bosecker, K., Hahn, L. and Mwiya, S., 2002. Supergene mineralisation in mining residues of the Matchless cupreous pyrite deposit (Namibia) – a clue to the origin of modern

and fossil duricrusts in semiarid climates. *Journal of Geochemical Exploration*, 75: 43 – 70.

Downing, K. N. and Coward, M. P., 1981. The Okahandja Lineament and its significant for the Damara Tectonics in Namibia. 70(3): 972-1000.

Drury, S. A., 2001. Image Interpretation in geology. Nelson Thrones Blackwell Science, Cheltenham Malden, 290 p. pp.

Farina, P., Catan, F., Colombo, D., Fumagalli, A., Kukavicic, M., Marks F. and Moretti, S., 2005. Remote sensing: a tool for landslide investigations at a basin scale. *Geophysical Research Abstracts*, vol. 7, 10157-10168.

Geological Survey of Namibia. Summary of Namibia's geology, [Online]. Available from: http://www.mme.gov.na/gsn/namibiageology.html [Accessed 23 August 2016].

Gold fields prospecting company. The Geological Map of Gorob area 1:250. 1976 & 1987. Available from: http://www.mme.gov.na/gsn/namibiageology.dbs [Accessed 25 September 2016].

Haussinger, H., Okrusch, M. and Scheepers, D., 1993. Geochemistry of Premetamorphic Hydrothermal Alteration of Metasedimentary rocks Associated with Gorob Massive Sulfide Prospect, Damara Orogeny, Namibia. *Economic Geology, 88: 72-90.*

Kanehira, K. and Tatsumi, T., 1970. Bedded Cupriferous iron sulphide deposits in Japan, a review. In: Tatsumi T. (Ed) "Volcanism and Ore genesis" Tokyo Univ. Press, 55-76.

Killick, A. M., 2000. The Matchless Belt and associated sulphide mineral deposits, Damara Orogen, Namibia. *Communications of the Geological Survey of Namibia*, V.12, pp.73-80.

Kirkham, G. D., Falck, H and Siddorn, J. 2003. An Integrated 3D GIS Model of the Yellowknife Camp: A Tool for Efficient Development. *Explor. Mining Geol*. v. 12, p. 49-59.

Klemd, R., Maiden, K.L., Okrusch M. and Richter, P., 1989. Geochemistry of the Matchless metamorphosed massive sulphide deposit, South West Africa/Namibia: Wall-rock alteration during submarine ore-forming processes. Economic Geology, 84, 603-617

Mahmood, G., and Easson, T., 2006. Comparing ASTER and Landsat 7 ETM+ for change Detection. *ASPRS 2006 Annual conference Reno, Nevada, p.12*.

Miller R. M., 1983. Tectonic Implications of the contrasting geochemistry of Damaran mafic volcanic rocks, South West Africa/Namibia. In: Evolution of the Damara orogeny of SWA/Namibia, *Spec.Publ.geol.soc*.S.Afr.11:115-138.

Miller, R. M., 2008. The geology of Namibia. Geological Survey of Namibia, Ministry of Mines and Energy, Windhoek, pp.1-1-28-13.

Orange, D. L. and Michael, A., 1999. Applications of multibeam mapping to exploration and production: Detecting seeps, mapping geohazards, and managing data overload with GIS. *The Leading Edge*. Apr. p. 495-501.

Pawlowski, R., 2000. GIS applied to exploration: Caserta Block, Central Apennines, southern Italy. *The Leading Edge.* Feb. p. 193-196.

Pirajno, F. and Jacob, R. E., 1991. Gold mineralisation in the intracontinental branch of the Damara Orogen, Namibia: a preliminary survey. *Journal of African earth sciences*, 13(3/4): 305 – 311.

Preussinger, H., 1990. Host-rock geology of the metamorphosed massive sulphide deposits at Gorob in the Pan-African Damara Orogen, Namibia. *Journal of African Earth Science*, 10(4): 717-732.

Rees, W.G., 1990. Physical principles of remote sensing: Cambridge *University Press*, Cambridge, England.

Rokos, D., Mavrantza, R., Vamvoukakis, C., St-Seymour, K., Kouli, M., Karfakis, I., Denes, G., 2000. Localisation of alteration zoning for the detection of epithermal gold by integration of remote sensing and geochemical techniques. Lesvos Island, Aegean Sea, Hellas. *Proceeding of the fourteenth International conference on Applied geologic remote sensing*, Las Vegas Nevada. 161-168.

Sabins, F. F., 1999. Remote sensing for mineral exploration. *Ore Geology Reviews.* 14(3-4): 157-183.

Schneider, G.I.C and Lauenstein, H. J., 1992. A new occurrence of vesignieite from the Gorob-hope copper deposit, Namibia. *Mineralogical Magazine*, 56:67-69.

Seber, D., Steer, D., Sandvol, E., Sandvol, C., Brindisi, C. and Barazangi, M., 2000. Design and Development of Information Systems for the Geosciences: An Application to the Middle East. *GeoArabia*, v. 5, p. 269-296.

Van der Meer, F. and Bakker, W., 1998. Validated surface mineralogy from high-spectral resolution remote sensing: *a review and a novel approach applied to god exploration using AVIRIS dat*. Terra Nova, 10(2):112-119.

Vane, G. R., Green, O., Chrien, T.G., Enmark, H.T., Hansen, E.G., and Porter, W.M., 1993. The Airborne Visible/Infrared Imaging Spectrometer (AVIRIS): *Remote Sensing of Environment*, v.44, p.127-143.

Williams, D., 2009. Landsat 7 Science Data user's handbook NASA website, http://landsathandbook.gsfc. .nasa.org. Last update August 4 2015.

Washington, D.C. and Drury, S.A., 1987. Image Interpretation in Geology. Chapman and Hall, London, 283 p.

Appendices

Appendix	Title	Type	Description	Location	Date acquired	Uses
I	3281-EPL226-Geo-Map6-GO-B-1	Geological map	➢ Scale: 1:36 000 ➢ Showing lithological units (amphibolites, quartzites, granites and pegmatites).	Gorob –Hope	27/05/1970	➢ Georeference ➢ digitise
II	2887-EPL507-GLG-map-Area	Geological map	➢ Showing lithological units (quartzites, schist and the MAB).	Gorob –Hope	Not recorded	➢ Georeference ➢ digitise
III	2931-EPL507-Geology-GOR 83	Geological map	➢ Scale: 1:50 000 ➢ Showing lithological units (quartz-schist, marble and the MAB)	Gorob-Hope	04/10/1976	➢ Georeference digitise
IV	2887-EPL507-GLG-Plan-Map	Geological map			27/04/1970	➢ Georeference ➢ digitise
V	Landsat 7 ETM+	Satellite image	UTM -Zone 33S	Gorob-Hope	06/04/2000	321 colour composites
VI	Landsat 7 ETM+	Satellite image	UTM -Zone 33S	Gorob-Hope	06/04/2000	475 colour composite
VII	Landsat 7 ETM+	Satellite image	UTM -Zone 33S	Gorob-Hope	06/04/2000	751 colour composite
VIII	ASTER-2314-2316	Satellite image	UTM -Zone 33S	Gorob-Hope	09/04/1999	321 colour composites
IX	ASTER-2314-2316	Satellite image	UTM -Zone 33S	Gorob-Hope	09/04/1999	464 colour composite & 4/6, 5/6, 5/8 band ratios

Appendix I

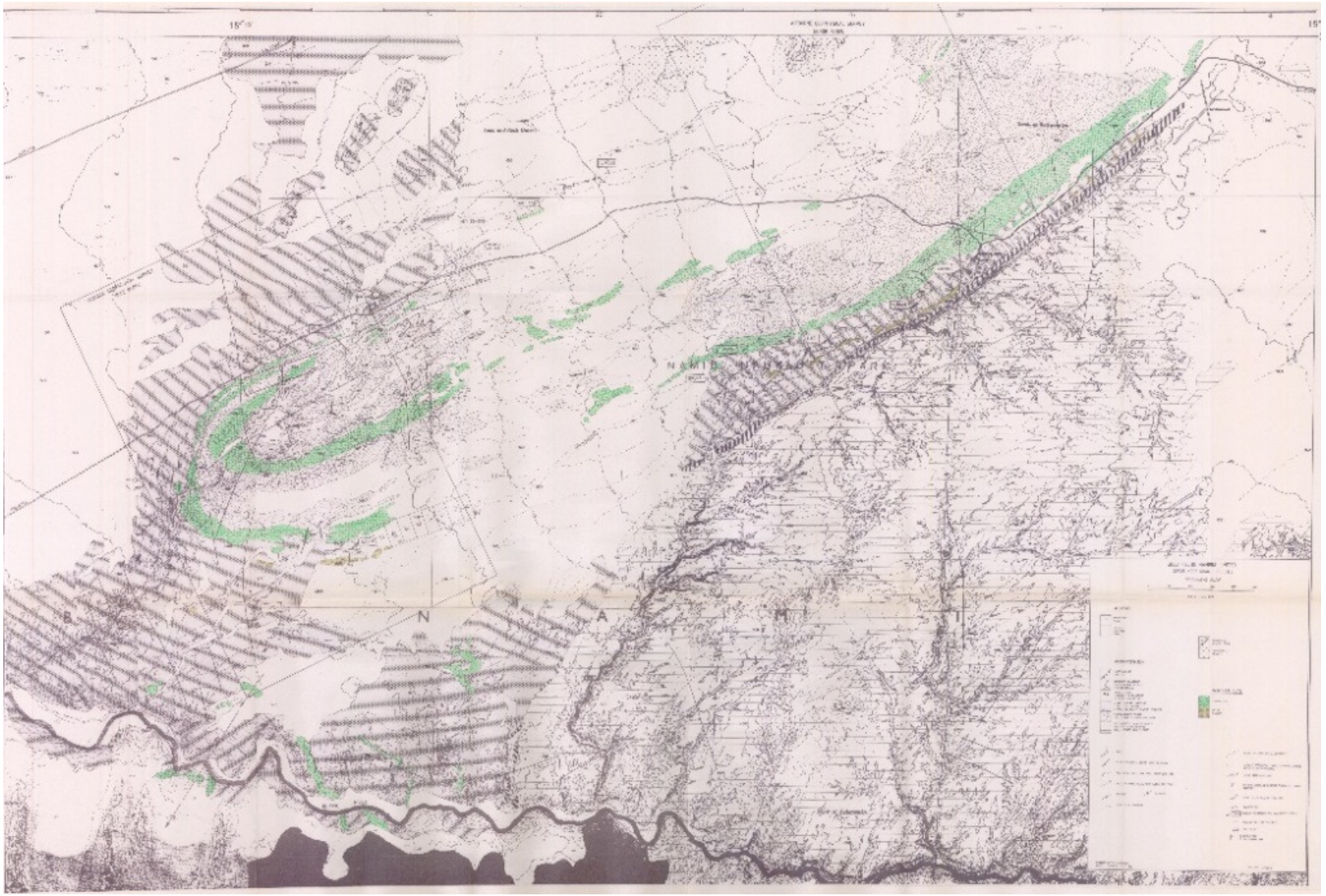

Appendix II

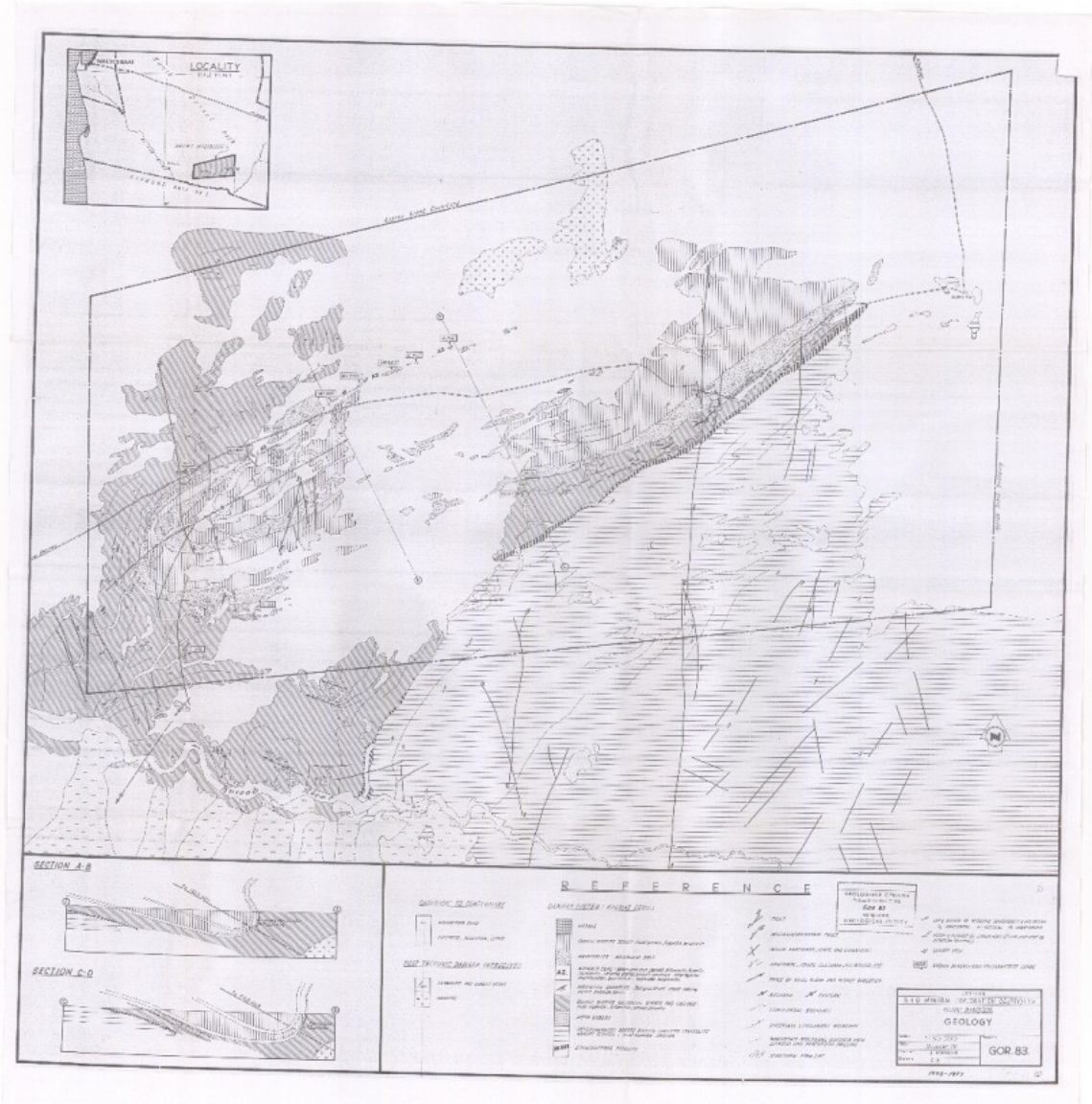

Appendix III

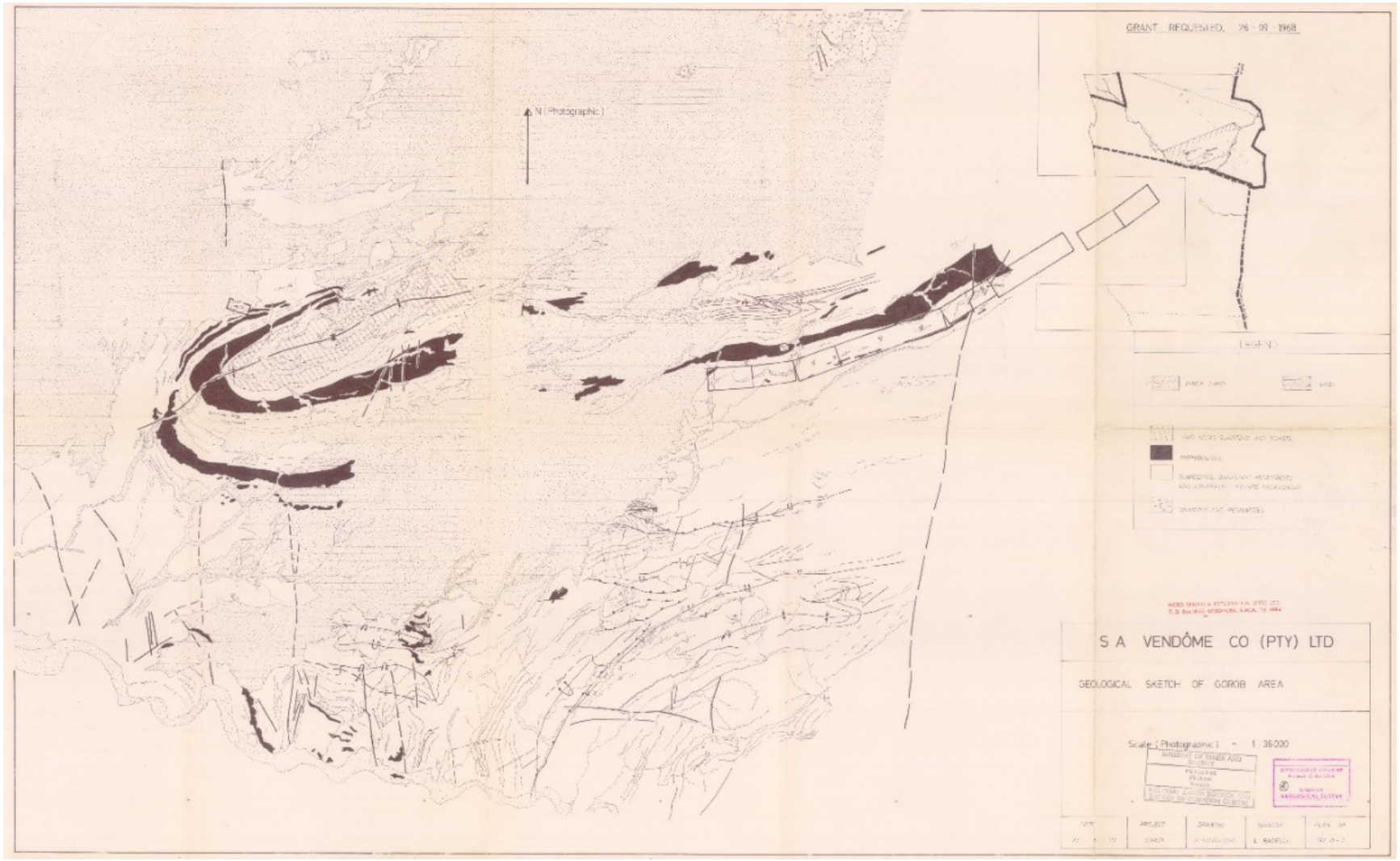

Appendix IV

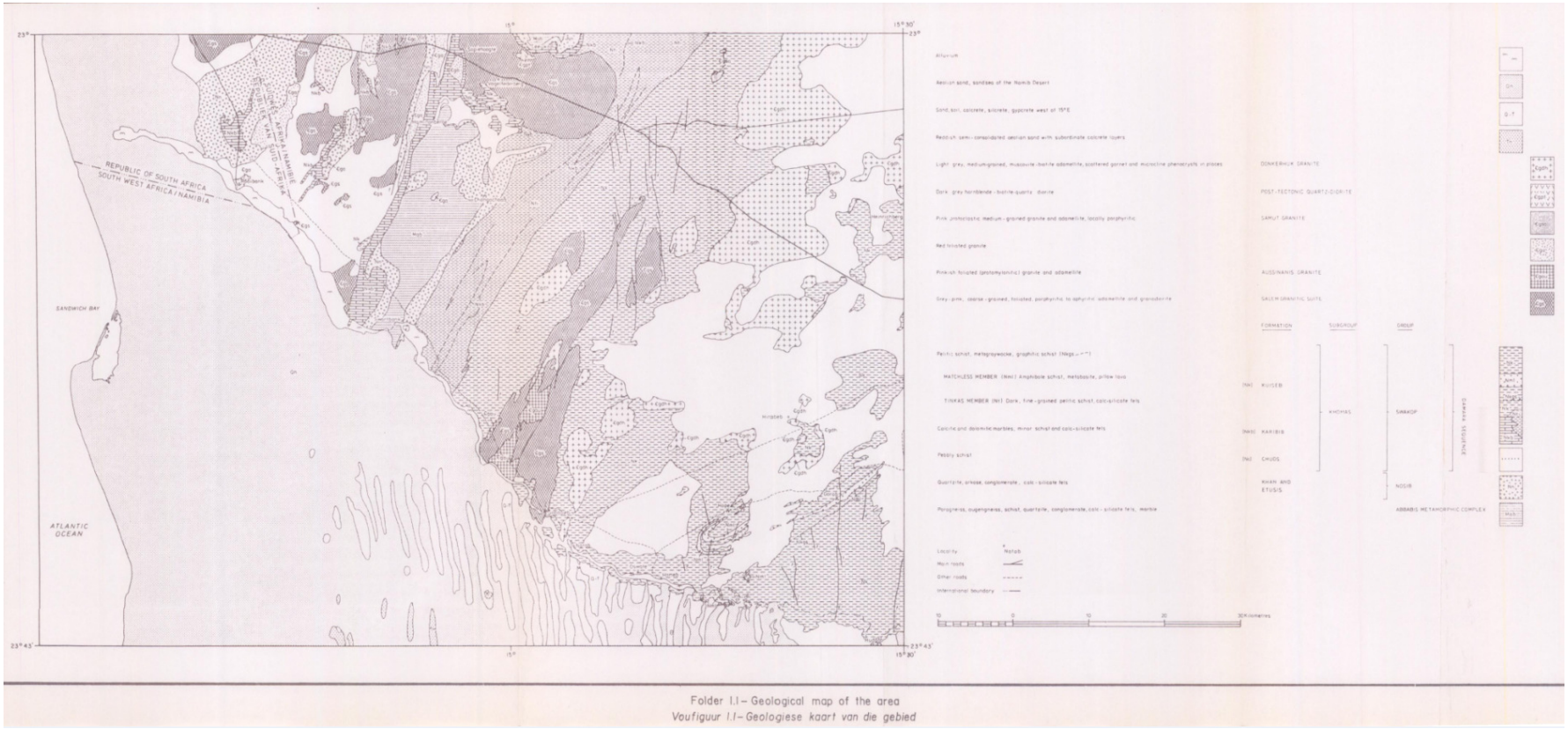

Folder I.I – Geological map of the area
Voufiguur I.I – Geologiese kaart van die gebied

Appendix V

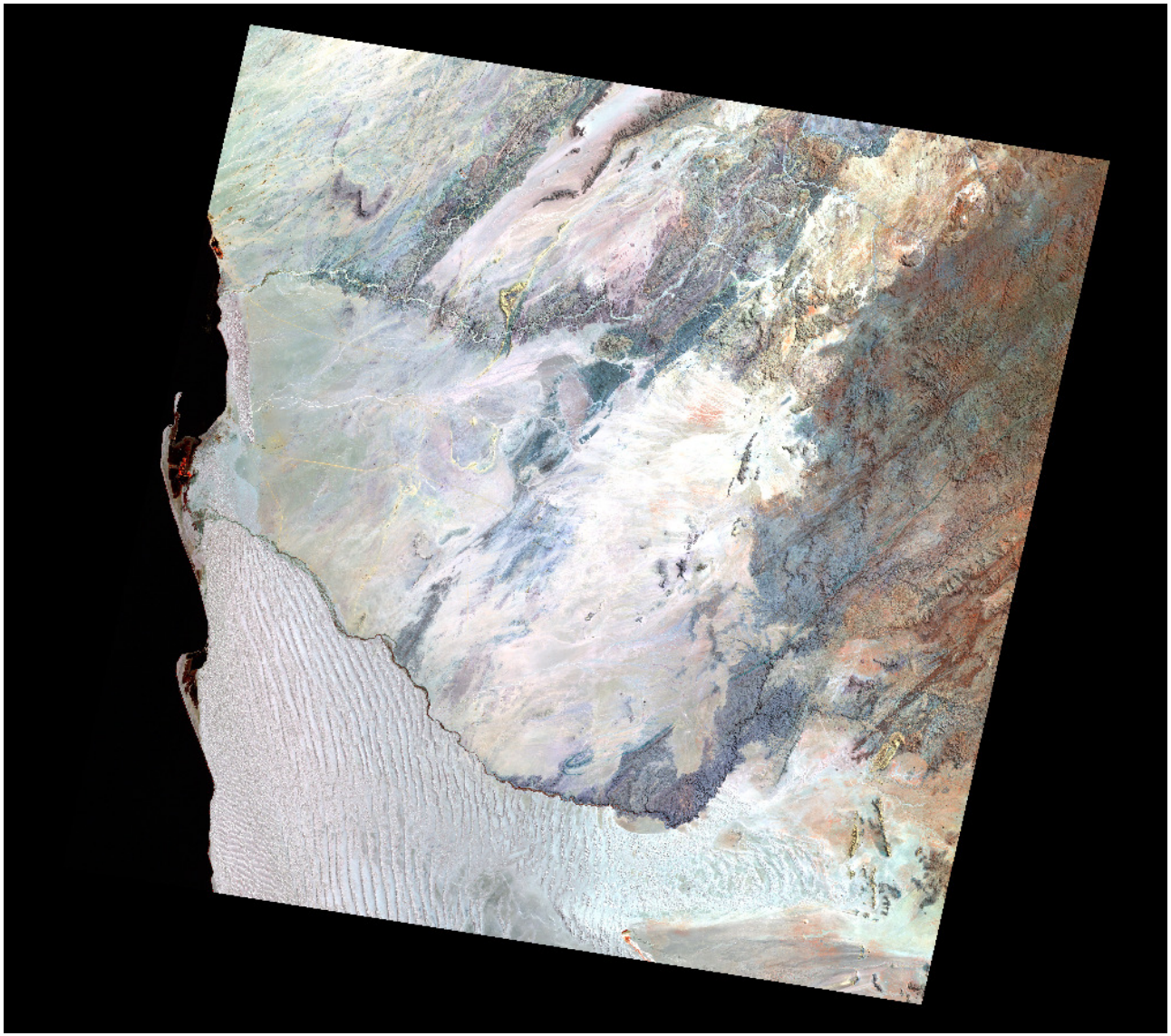

Appendix VI

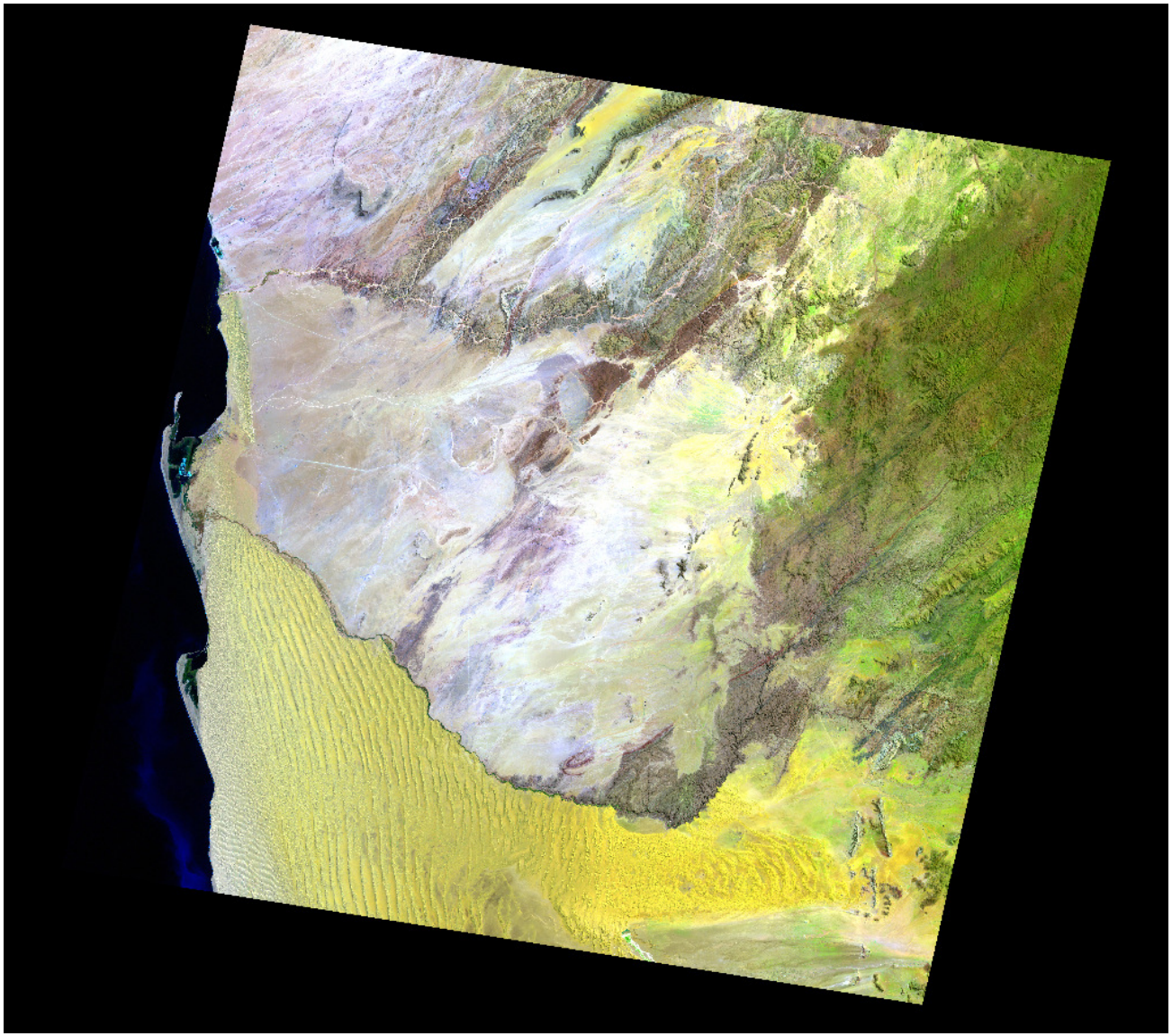

Appendix VII

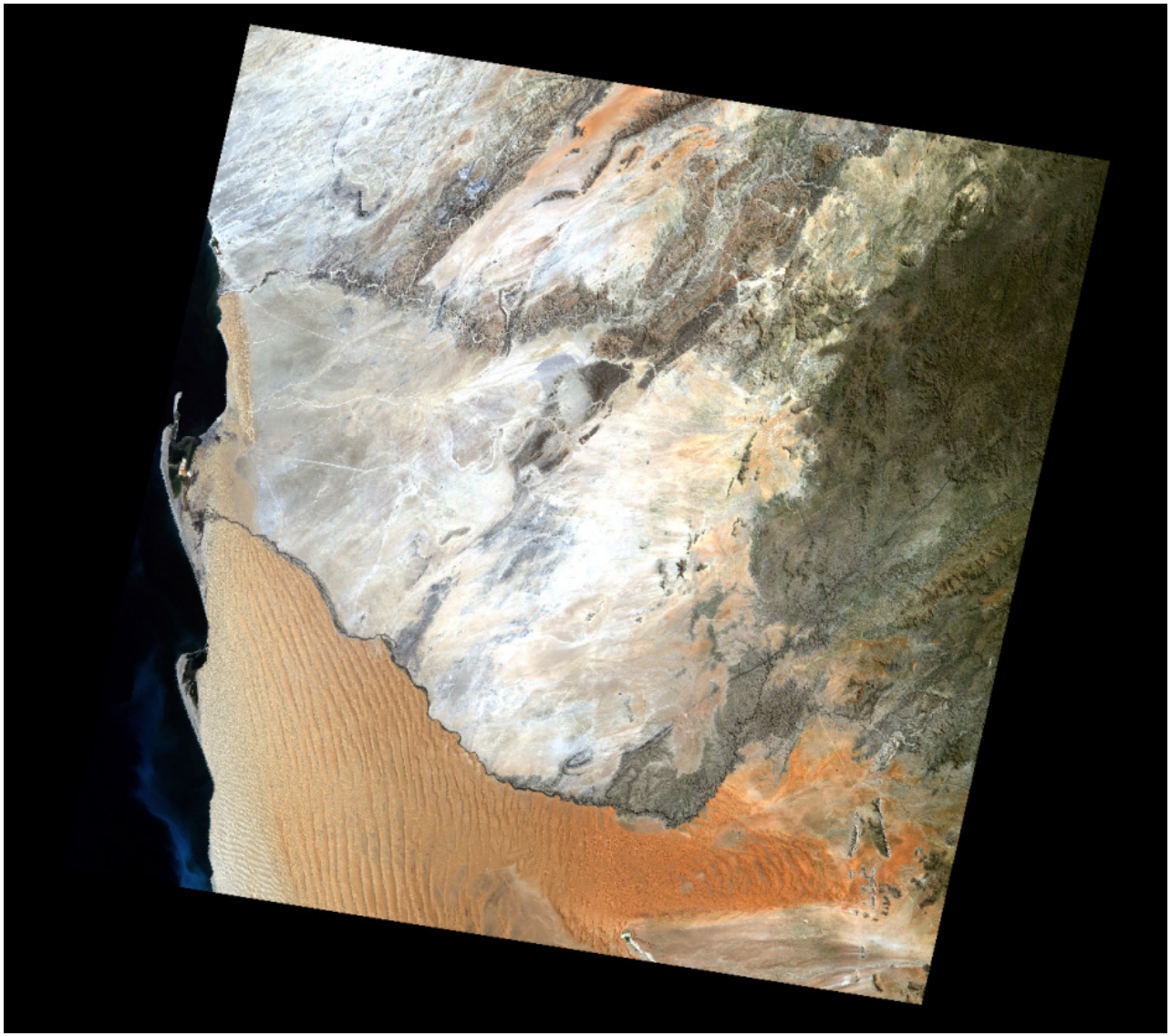

AppendixVIII

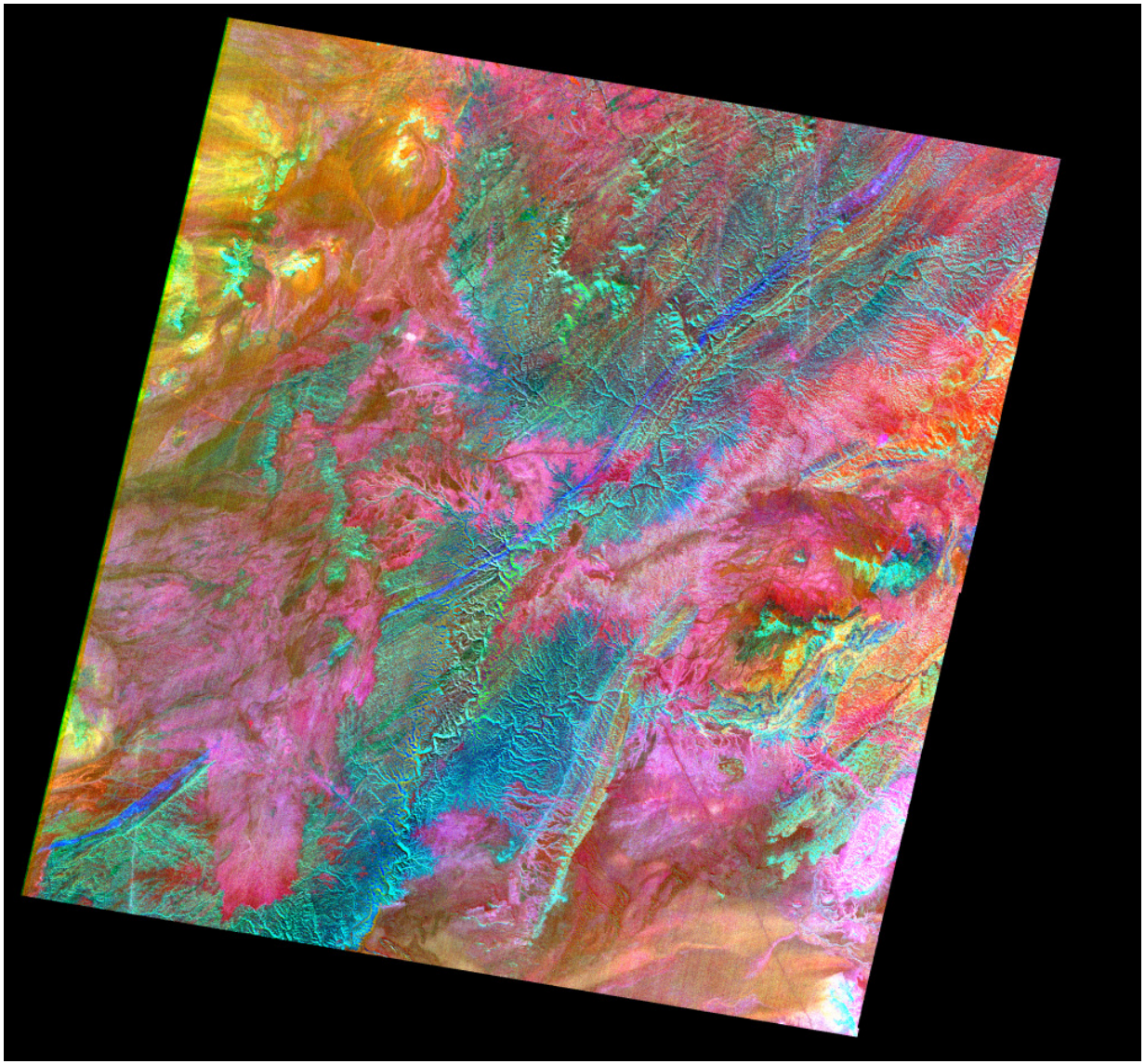

Appendix IX

